Convergent selection of a WD40 protein that enhances grain yield in maize and rice

Wenkang Chen[1,3]*, Lu Chen[2]*‡, Xuan Zhang[1,3]*, Ning Yang[2,4]*, Jianghua Guo[1], Min Wang[1], Shenghui Ji[1], Xiangyu Zhao[1], Pengfei Yin[1], Lichun Cai[1], Jing Xu[1], Lili Zhang[1], Yingjia Han[1], Yingni Xiao[1], Gen Xu[1], Yuebin Wang[2], Shuhui Wang[1], Sheng Wu[1], Fang Yang[2], David Jackson[2,5], Jinkui Cheng[1,3], Saihua Chen[6], Chuanqing Sun[1], Feng Qin[1,3], Feng Tian[1,3], Alisdair R. Fernie[7], Jiansheng Li[1,3]†, Jianbing Yan[2,4]†, Xiaohong Yang[1,3]†

[1]State Key Laboratory of Plant Physiology and Biochemistry and National Maize Improvement Center of China, China Agricultural University, Beijing 100193, China

[2]National Key Laboratory of Crop Genetic Improvement, Huazhong Agricultural University, Wuhan 430070, China

[3]Center for Crop Functional Genomics and Molecular Breeding, China Agricultural University, Beijing 100193, China

[4]Hubei Hongshan Laboratory, Wuhan 430070, China

[5]Cold Spring Harbor Laboratory, Cold Spring Harbor, New York 11724, USA

[6]Key Laboratory of Plant Functional Genomics of the Ministry of Education, Yangzhou University, Yangzhou, Jiangsu 225009, China

[7]Department of Molecular Physiology, Max-Planck-Institute of Molecular Plant Physiology, Am Mühlenberg 1, 14476 Potsdam-Golm, Germany

*These authors contributed equally to this work.

‡Present address: State Key Laboratory of Plant Genomics and National Center for Plant Gene Research, Institute of Genetics and Developmental Biology, Chinese Academy of Sciences, Beijing 100101, China.

†Corresponding authors. Email: yxiaohong@cau.edu.cn (X.Y.); yjianbing@mail.hzau.edu.cn (J.Y.); lijiansheng@cau.edu.cn (J.L.).

Abstract

A better understanding of the extent of convergent selection among crops could greatly improve breeding programs. Here we show that the quantitative trait locus *KRN2* in maize and its rice ortholog, *OsKRN2*, experienced convergent selection. These orthologs encode WD40 proteins and interact with a gene of unknown function, DUF1644, to negatively regulate grain number in both crops. Knockout of *KRN2* in maize or *OsKRN2* in rice increased grain yield by ~10% and ~8%, respectively, with no apparent trade-offs in other agronomic traits. Furthermore, genome-wide scans identified 490 pairs of orthologous genes that underwent convergent selection during maize and rice evolution, and these were enriched for two shared molecular pathways. *KRN2*, together with other convergently selected genes, provides an excellent target for future crop improvement.

One-sentence Summary

KRN2, together with other convergently selected genes identified in maize and rice, provides insights for knowledge-driven crop breeding.

Main Text

The major cereals, including maize, rice, wheat, barley and sorghum, were domesticated independently ~10,000 years ago and represent a primary source of human calories (*1*). Genome-wide analyses indicate that domestication and improvement in the cereals were complex and involved numerous genes associated with

various biological traits (*2–5*). Although the cereals underwent independent domestication and improvement, many morphological and physiological or biochemical traits appear to have been under convergent selection resulting in an ease of cultivation, high yield, and nutrient richness (*1*). Given the close phylogenetic relationships among cereals, a key question is whether convergent phenotypic selection in distinct lineages was driven by conserved molecular changes. In some cases, selection in independent lineages appears to have acted on conserved genetic loci that control convergent phenotypes (*6–8*), whereas in other cases the convergent phenotypic changes appear to have arisen by diverse genetic routes due to homoplasy (*9–11*).

Two of the most economically important crops, maize (*Zea mays* L. ssp. *mays*) and rice (*Oryza sativa* L.), diverged >50 million years ago (*12*). Although the collinearity of cereal genomes has long been recognized (*12–14*), only a few genes—such as those involved in shattering resistance—have been identified as having been convergently selected during the evolution of maize and rice (*7*, *15*). Hence, a genome-wide identification of the genes that have undergone convergent selection in maize and rice could help understand the evolution of crop species as well as accelerate breeding programs.

KRN2 is a selected gene underlying kernel row number variation

We mapped eight quantitative trait loci (QTLs) for kernel row number (KRN) in a maize recombinant inbred line (RIL) population developed from a cross between an inbred line, B73, and an introgression line, MT-6, of which ~25% of its genome is derived

from that of teosinte, the wild ancestor of maize (*16*) (**Fig. 1A and table S1**). *qKRN2*, the QTL with the largest effect, was located within a selective sweep on the short arm of chromosome 2 (*2*), and the maize allele increased KRN relative to the teosinte allele. To identify the gene(s) underlying *qKRN2*, we performed positional cloning using nine markers and 7,056 individuals derived from a backcross of MT-6/B73 F_1 plants with B73 (**fig. S1**). We delimited this QTL to a 5,799-bp region that contained only one candidate gene (*Zm00001d002641*), which we named *KRN2* (**Fig. 1, B and C**). Comparisons of the maize and teosinte alleles indicated that the maize (B73) allele increased KRN by ~1.4 rows relative to teosinte (**Fig. 1, D and E**). To confirm the function of *KRN2*, we identified a loss-of-function allele carrying a *Mutator* (*Mu*) transposon insertion in exon 1. Ears from plants homozygous for the *Mu* insertion produced ~1.8 more rows than wild-type segregants (**fig. S2**). These results suggest that *KRN2* is the causal gene for KRN variation in *qKRN2* and that loss-of-function alleles can increase KRN in maize.

Genomic sequencing identified 63 single-nucleotide polymorphisms (SNPs) and 37 insertions or deletions (InDels) in the promoter and 5' untranslated region (UTR) of *KRN2*, as well as seven synonymous and seven nonsynonymous SNPs in coding exons between the B73 and teosinte alleles (**Fig. 1C and fig. S3)**. Real-time quantitative PCR (qPCR) showed that *KRN2* expression was lower in NIL-$KRN2^{B73}$ relative to NIL-$KRN2^{teosinte}$ in the early stage of maize inflorescence meristem (IM) development (**Fig. 1F and fig. S4**). To test if the sequence polymorphisms in the promoter or 5'UTR might underlie these different expression levels, we performed transient expression assays in

maize protoplasts, in which two fragments (~1.2 kb or ~2.0 kb) upstream of the start codon of *KRN2* from maize or teosinte were fused upstream of the luciferase (LUC) gene (**Fig. 1G**). Both teosinte fragments exhibited higher LUC activity than the maize fragments (**Fig. 1H**), suggesting that polymorphisms within the ~1.2-kb region of *KRN2* accounts for expression differences between maize and teosinte alleles. Furthermore, we overexpressed the coding sequences of $KRN2^{B73}$ and of $KRN2^{teosinte}$ alleles in a maize inbred line, and confirmed enhanced expression of *KRN2* by qPCR (**fig. S5, A to C**). Compared with wild-type plants, all six independent overexpression lines consistently decreased KRN by ~2.0 rows, with no difference between *Ubi*::$KRN2^{B73}$ and *Ubi*::$KRN2^{teosinte}$ transgenic plants (**fig. S5D**). These findings indicate that KRN changes are mediated through changes in *KRN2* expression, most likely caused by polymorphisms within the ~1.2-kb promoter and 5'UTR region.

To ascertain if *KRN2* underwent selection during maize evolution, we calculated nucleotide diversity across its promoter and coding region. Similar diversity was observed between maize landraces and inbred lines (**Fig. 1I**). We observed a reduction in nucleotide diversity in maize relative to its ancestor, *Zea mays* ssp. *parviglumis* (hereafter, *parviglumis*; $\pi_{parviglumis} = 2.6 \times 10^{-2}$, $\pi_{landrace} = 6.1 \times 10^{-3}$, $\pi_{inbred} = 2.1 \times 10^{-3}$), and a negative Tajima's D-statistic in maize inbred lines and landraces for an ~700-bp region containing the 5'UTR of *KRN2* (**Fig. 1I and fig. S6**), suggesting that this region underwent selection. This result was further supported by a coalescence simulation (**fig. S6**). This severe loss of diversity could not be explained by domestication bottleneck or modern improvement in maize alone. Our selection analyses seem to suggest that

human selection was likely involved in the evolution of *KRN2* between initial domestication and modern improvement. Taken together, both our transgenic studies and surveys of nucleotide diversity suggest that selection in the non-coding upstream regions resulted in a reduction in *KRN2* expression and, in turn, an increased KRN in maize.

KRN2 negatively regulates KRN by interacting with DUF1644, a protein of unknown function

Sequence analysis of *KRN2* predicted that it encodes a cytoplasmic WD40 protein containing seven WD40 repeats (**figs. S7 and S8, A and B**). Members of the WD40 family act as scaffolds for protein-protein interactions (*17*, *18*) and have diverse functions in plants, including in development, metabolite biosynthesis and immune responses (*19–21*). To understand the molecular mechanism of KRN2, we identified six potential interaction partners using a yeast two-hybrid (Y2H) screen (**table S2**). Among them, we focused on the gene *DUF1644*, which encodes a DUF1644-containing protein that localized to both the cytoplasm and the nucleus (**fig. S8, A and C**). We confirmed a direct interaction between KRN2 and DUF1644 by Y2H assays as well as split firefly LUC complementation assays (**Fig. 2, A and B**). Next, to further elucidate the relationship between *KRN2* and *DUF1644*, we generated *krn2* and *duf1644* null mutants by CRISPR-Cas9 technology as well as a *krn2 duf1644* double mutant (**fig. S9**). Neither *duf1644* single mutants had an obvious phenotype, but the *krn2 duf1644* double mutant had a significantly higher KRN as compared with the *krn2* single mutant (16.3 ± 1.2 compared with 15.9 ± 1.1; unpaired *t* test, t = 2.0, df = 124, $P = 4.6 \times 10^{-2}$;

Fig. 2C and fig. S9). This result suggests that DUF1644 acts with KRN2, although it remains unknown how this affects KRN and the underlying molecular function of DUF1644.

To better understand the cause of the increase in KRN, we measured IM size. The NIL-*KRN2*^{B73} IMs (345.5 ± 25.2 μm) were wider than those of NIL-*KRN2*^{teosinte} (313.0 ± 19.6 μm), and *KRN2* overexpression decreased IM diameter by ~56 μm (**fig. S10**). Consistently, both the *krn2* single mutant and *krn2 duf1644* double mutant significantly increased their IM size as compared with the wild-type plants (unpaired *t* test; 446.3 ± 33.0 μm compared with 422.4 ± 23.8 μm, t = 3.3, df = 61, $P = 1.7 \times 10^{-3}$ for the single mutant; 465.9 ± 27.4 μm compared with 422.4 ± 23.8 μm, t = 6.5, df = 56, $P = 2.6 \times 10^{-8}$ for the double mutant; **Fig. 2, D and E**). We hypothesize that these increases in IM size provided additional space for initiation of spikelet pair meristems and, hence, a higher KRN (**Fig. 2F)**.

Convergent selection of the *KRN2* ortholog in rice

A single ortholog of *KRN2* containing conserved WD40 domains was identified in most major cereal crops (**Fig. 3A and fig. S7**). The rice *KRN2* ortholog, *Os04g0568400* (hereafter, *OsKRN2*), mapped to a region that underwent a selective sweep (27.5–29.0 Mb) on rice chromosome 4 (*3*) that is syntenic with the short arm of chromosome 2 in maize (**Fig. 3B**) and is within a QTL for rice grain number (*22*, *23*). These observations suggest that *OsKRN2* may have also experienced selection on rice grain number. Consistent with this, nucleotide diversity was reduced in an ~1,100-bp region upstream

of the *OsKRN2* start codon in cultivated rice (**fig. S11**). As expected, a minimum-spanning tree of 27 haplotypes in the ~1,100-bp region separated wild rice *Oryza rufipogon* (hereafter, *rufipogon*; 59 accessions) from cultivated rice (109 accessions) based on the sequenced accessions (**Fig. 3C**).

OsKRN2 was expressed in all rice tissues, with high levels in panicle primordia (**fig. S12**), which was similar to the *KRN2* expression profile in maize. Rice panicle branches are initiated by branch meristems, which are analogous to spikelet pair meristems in maize (*24*). We made *OsKRN2* null mutants using CRISPR-Cas9 technology, and, similar to the results in maize, we observed an increase in secondary branches from an average of 16.0 (± 2.5) branches in wild type to up to 18.9 (± 3.5) in the null mutants (**Fig. 3, D and E, and fig. S13**). Consequently, an increase in grain number in the mutant panicles (up to 118.1 ± 11.9 grains) was observed as compared with wild-type panicles (107.7 ± 9.5 grains) (**Fig. 3F**). In contrast, lines overexpressing *OsKRN2* had fewer secondary branches with fewer grains (**Fig. 3, G to I, and fig. S13**). These findings indicate that *OsKRN2* likely controls grain production in rice by affecting the number of secondary branches. In addition, Y2H and split firefly LUC complementation assays confirmed a direct interaction between OsKRN2 and OsDUF1644 (**fig. S14**), suggesting that a conserved protein interaction controls KRN in maize and the number of secondary branches in rice.

Gene editing of *KRN2* and *OsKRN2* enhances grain yield in maize and rice field trials

We next asked if gene editing of *KRN2*/*OsKRN2* could increase yield in the field, as an indicator of applicability in breeding programs. Thus, we planted maize *KRN2* and rice *OsKRN2* gene-edited lines in multiple environments for yield testing (**Fig. 4**). For maize, field tests across three environments showed that two *KRN2*-edited lines (*CR-krn2-1* and *CR-krn2-2*) stably increased KRN by ~1.6–2.0 rows and kernel numbers per ear by ~27–53 kernels, resulting in an increase in grain yield of 9.0–10.5% (**Fig. 4B, figs. S9B and S15, and table S3**). Remarkably, these *krn2* knockouts did not alter plant architecture, flowering time, or ear length, although kernel width was slightly reduced (**Fig. 4A and table S3**). In rice, *OsKRN2*-edited lines (*CR-oskrn2-1* and *CR-oskrn2-2*) showed a similar increase in the number of grains per panicle (average increase of 9.8–10.3 grains per panicle) and grain yield per plant (7.9–8.2%), again with no obvious changes in other agronomic traits (**Fig. 4, C and D, and fig. S16**). These findings indicate that a complete loss-of-function allele of *KRN2/OsKRN2* increased grain yield without an apparent negative impact on other agronomic traits in tested environments. Yet, whether the performance is consistent in diverse environments remains to be resolved. We neither identified any natural loss-of-function mutations of *KRN2/OsKRN2* nor detected association signals for grain number–related traits in natural populations, including hundreds of diverse lines in maize (**table S4**) and rice (*25*), suggesting that gene editing of *KRN2*/*OsKRN2* could provide a unique way to modify grain number in breeding lines.

Genome-wide convergent selection between maize and rice

Morphologically, cultivated maize and rice differ substantially from their ancestors and

display a 'domestication syndrome' known as a common suite of traits that have changed in domesticated crops (*26*). These include the loss of seed dispersal, decreased seed dormancy, and increased grain number, size, and weight (**Fig. 5A**) (*1*). In addition to *KRN2/OsKRN2* for grain number, two additional orthologous gene pairs—*ZmSh1*/*OsSh1* for seed shattering (*7*) and *ZmSWEET4c*/*OsSWEET4* for grain filling (*27*)—have also experienced convergent selection during maize and rice evolution. Hence, it is worth exploring the extent of molecular convergence on a genome-wide scale between maize and rice to ask how often selection acts on orthologous gene pairs. We therefore re-analyzed selected genes using two large new datasets, including ~65 million SNPs in 507 maize inbred lines and 70 *parviglumis* accessions and ~71 million SNPs in 461 cultivated rice and 257 wild rice accessions (**fig. S17 and table S5**). Utilizing phylogenetic information (*3*, *28*), we estimated cross-population composite likelihood ratios (XP-CLR) (*29*) followed by cross-validation on the basis of permutation tests for nucleotide diversity in the regions with the top 10% XP-CLR scores (*2*). By comparing maize and *parviglumis*, we identified a total of 69.6 Mb selected genomic regions that covered 3.3% of the maize B73 reference genome (*30*) and contained 3,163 genes (**Fig. 5B, tables S6 to S8**). In this analysis, we identified two canonical domestication genes: *tb1*, which controls branching (*31*), and *tga1*, which controls the formation of the stony fruitcase (*32*) (**Fig. 5B and table S7**). In rice, we identified a total of 27.6, 25.8, and 26.3 Mb selected genomic regions, including 7,709, 10,196, and 7,864 genes, respectively, by comparing *rufipogon* with *Oryza sativa* subsp. *japonica*, *Oryza sativa* subsp. *indica*, and *Oryza sativa*, respectively (hereafter,

japonica, *indica*, and *sativa*; **Fig. 5C, fig. S18, tables S6 to S8**). Collectively, these selected regions covered 17.2% (64.0 Mb) of the Nipponbare reference genome (*33*) and encompassed 18,755 genes (**tables S6 to S8**). Notably, 16 genes that are known to have undergone selection were detected, such as *PROG1* for growth habit (*34*, *35*) and *OsLG1* for inflorescence architecture (*36*, *37*) (**Fig. 5C, fig. S18 and table S7**).

By comparing these datasets, we identified 490 pairs of orthologous genes that had an apparent history of convergent selection in maize and rice (**Fig. 5D and table S7**), which is significantly greater than that expected by chance (permutation test, $P < 0.001$; **Fig. 5E**), indicating that we observed an excess of shared selected genes in maize and rice based on comparative genomics results. However, given the time period during which traits of common interest to humans were selected is far less than that for the evolutionary divergence between maize and rice (*12*), it is not surprising that only a limited number of selected genes in maize (15.5%) and rice (2.6%) experienced convergent selection during evolution. Of the 490 orthologous gene pairs, 67.8% were localized to syntenic blocks between the maize and rice genomes (**Fig. 5D and table S7**). In addition to the three known orthologous gene pairs that have undergone convergent selection mentioned above, the functions of an additional 13 orthologous gene pairs have been experimentally verified. These include *KN1*/*OSH1*, regulators of shoot meristem development (*38*, *39*), and *SBE1*, which controls starch biosynthesis (*40*, *41*) (**table S7**). The prevalence of shared selected genes with conserved functions supports the idea that common phenotypic shifts during maize and rice evolution acting on conserved genes are driven at least in part by convergent selection, which in maize

and rice likely occurred both during and post domestication. Further characterization of these orthologs could provide insights into the processes driving human selection on cereal traits and, in turn, enhance knowledge-driven crop breeding.

Interestingly, the convergently selected orthologous genes appear to be significantly enriched in specific pathways in maize and rice (multiple-testing correction via the g:Profiler g:SCS algorithm, adjusted $P < 0.05$) including two commonly enriched pathways (starch and sucrose metabolism, and biosynthesis of cofactors; **Fig. 5F**). Starch is the main component of cereal seeds and contributes substantially to grain yield, so it is reasonable that starch and sucrose metabolism is a primary pathway of convergent selection when human selection targeted high cereal productivity. Of 25 maize and 93 rice selected genes that are known contributors to the starch metabolic pathway (*42*, *43*), we found that 11 orthologous gene pairs showed convergence at the genic level (**Fig. 5G and table S9**). The types and functions of starch synthesis–related enzymes are highly conserved, although, their copy number and isoenzyme number differ between maize and rice (*43*). Hence, different functionally redundant paralogs could be differentially selected. For example, *UGP1* was selected in maize, whereas its homolog, *UGP2*, was selected in rice (**Fig. 5G**). In addition to whether a gene contributes to selected traits, whether a gene is selected is also affected by the levels of genetic diversity and the frequency of the pre-existing desirable alleles in the ancestral population (*1*, *10*, *44*). For example, *TPS4* was selected in maize but not in rice (**Fig. 5G**). The various levels of genetic diversity in wild ancestors (e.g., there is less nucleotide diversity in maize than in its *parviglumis* ancestor, but there is

more in cultivated rice than in its *rufipogon* ancestor; **fig. S19**) indicate that it may be difficult to target *TPS4* for selection in rice. These findings suggest that some orthologous genes function in the same metabolic or regulatory pathway for the same selected traits but have distinct selection routes among crops. Indeed, the degree of genetic convergence via convergent selection is related to the conservation and complexity of the gene network for a given selection (*11*).

Discussion

Collectively, we found a set of 490 orthologous genes that underwent convergent selection during maize and rice evolution, including *KRN2/OsKRN2*, which affect grain number. As grain number is a common domestication syndrome trait as well as a key grain yield component in cereal crops, exploring the role of *KRN2/OsKRN2* across the cereals could provide new opportunities for enhancing production of other global crops, such as wheat. These findings suggest that the identification of genes that have undergone convergent selection could further inform breeding efforts of cereals. A deep understanding of the conservation of selection-driven genetic elements will not only enable more rapid innovation of the maize and rice germplasm but also inform knowledge-driven *de novo* domestication of new crops to meet the diverse needs of food production worldwide (*45*).

Methods Summary

QTL mapping for KRN in the MT-6/B73 RIL population was performed using composite interval mapping (*46*). *qKRN2* was positionally cloned using a recombinant-

derived progeny testing strategy (*47*). The functions of *KRN2*, *DUF1644*, and *OsKRN2* were investigated via mutant analysis, transgenic overexpression or CRIPSR-Cas9 gene editing. The constructed overexpression and gene-editing vectors were transformed into maize inbred line LH244 or rice cultivar Nipponbare through an *Agrobacterium*-mediated transformation system. *KRN2*-based association mapping was performed using a mixed linear model (*48*) in a subset of 379 maize inbred lines (*49*). The yield tests of *KRN2*/*OsKRN2* gene-edited lines were carried out in a randomized block design with three replicates.

The expression levels of *KRN2* and *OsKRN2* in tested samples were detected via qPCR. The expression differences caused by the sequence polymorphisms in *KRN2* promoter or 5'UTR were tested by transient expression assays in maize protoplasts (*50*). The candidate interaction partners of KRN2 were identified using a Y2H screen by Hybrigenics Services. The interaction between KRN2/OsKRN2 and DUF1644/OsDUF1644 was validated by Y2H assays and split firefly LUC complementation assays in tobacco (*51*). The fresh IM was imaged with a scanning electron microscope, and then the IM diameter was measured with an EZ4 HD stereo microscope and corresponding LAS EZ software.

To determine whether the *KRN2* or *OsKRN2* locus has undergone molecular evolution in maize or rice, we sequenced their target regions in a set of cultivar, landrace, and wild relatives. Nucleotide diversity (π) and Tajima's D were calculated using DnaSP software (*52*). Coalescent simulations were performed for *KRN2* using the MS program (*53*). Minimum spanning tree was constructed for *OsKRN2* using Arlequin

software (*54*).

To explore the extent of molecular convergence on a genome-wide scale between maize and rice, we collected or generated two high-depth SNP datasets in 507 maize inbred lines and 70 *parviglumis* accessions, and 461 cultivated rice and 257 wild rice accessions. The genetic relationship of rice accessions was estimated using ADMIXTURE software (*55*), and confirmed by PCA using GCTA software (*56*). The SNP alignment (*57*) and phylogenetic tree construction in maize and rice were performed using SNPhylo software (*58*). The genome-wide scans for selection signals were performed via an XP-CLR method (*29*) followed by cross-validation on the basis of permutation tests for the nucleotide diversity ratio between wild and cultivar accessions (*2*, *57*). The genes that are located within the selected regions were regarded as having undergone selection. The maize and rice orthologs were identified utilizing reciprocal blastp with the protein sequence coverage ≥ 0.7. Collinearity was analyzed using MCScanX software (*59*). Permutation test was performed for the enrichment of the orthologous genes under convergent selection (*57*). Finally, g:Profiler program (*60*) was used for KEGG pathway enrichment analysis of genes under convergent selection.

All details of the materials and methods, including those summarized above, are provided in the supplementary materials.

References and Notes

1. J. F. Doebley, B. S. Gaut, B. D. Smith, The molecular genetics of crop domestication. *Cell* **127**, 1309–1321 (2006). doi: 10.1016/j.cell.2006.12.006

2. M. B. Hufford *et al.*, Comparative population genomics of maize domestication and improvement. *Nat. Genet.* **44**, 808–811 (2012). doi: 10.1038/ng.2309

3. X. Huang *et al.*, A map of rice genome variation reveals the origin of cultivated rice. *Nature* **490**, 497–501 (2012). doi: 10.1038/nature11532

4. A. Pankin, M. von Korff, Co-evolution of methods and thoughts in cereal domestication studies: a tale of barley (*Hordeum vulgare*). *Curr. Opin. Plant Biol.* **36**, 15–21 (2017). doi: 10.1016/j.pbi.2016.12.001

5. Y. Liang, H. Liu, J. Yan, F. Tian, Natural variation in crops: realized understanding, continuing promise. *Annu. Rev. Plant Biol.* **72**, 357–385 (2021). doi: 10.1146/annurev-arplant-080720-090632

6. A. H. Paterson *et al.*, Convergent domestication of cereal crops by independent mutations at corresponding genetic loci. *Science* **269**, 1714–1718 (1995). doi: 10.1126/science.269.5231.1714

7. Z. Lin *et al.*, Parallel domestication of the *Shattering 1* genes in cereals. *Nat. Genet.* **44**, 720–724 (2012). doi: 10.1038/ng.2281

8. M. Wang *et al.*, Parallel selection on a dormancy gene during domestication of crops from multiple families. *Nat. Genet.* **50**, 1435–1441 (2018). doi: 10.1038/ng.3352

9. H. Tang *et al.*, Seed shattering in a wild sorghum is conferred by a locus unrelated to domestication. *Proc. Natl. Acad. Sci. USA* **110**, 15824–15829 (2013). doi: 10.1073/pnas.1305213110

10. B. S. Gaut, Evolution is an experiment: assessing parallelism in crop

domestication and experimental evolution. *Mol. Biol. Evol.* **32**, 1661–1671 (2015). doi: 10.1093/molbev/msv105

11. Q. Chen, W. Li, L. Tan, F. Tian, Harnessing knowledge from maize and rice domestication for new crop breeding. *Mol. Plant* **14**, 9–26 (2021). doi: 10.1016/j.molp.2020.12.006
12. B. S. Gaut, Evolutionary dynamics of grass genomes. *New Phytol*. **154**, 15–28 (2002). doi: 10.1046/j.1469-8137.2002.00352.x
13. M. D. Gale, K. M. Devos, Comparative genetics in the grasses. *Proc. Natl. Acad. Sci. U.S.A.* **95**, 1971–1974 (1998). doi: 10.1073/pnas.95.5.1971
14. A. H. Paterson, J. E. Bowers, B. A. Chapman, Ancient polyploidization predating divergence of the cereals, and its consequences for comparative genomics. *Proc. Natl. Acad. Sci. U.S.A.* **101**, 9903–9908 (2004). doi: 10.1073/pnas.95.5.1971
15. M. R. Woodhouse, M. B. Hufford, Parallelism and convergence in post-domestication adaptation in cereal grasses. *Phil. Trans. R. Soc. B* **374**, 20180245 (2019). doi: 10.1098/rstb.2018.0245
16. L. Cai, K. Li, X. Yang, J. Li, Identification of large-effect QTL for kernel row number has potential for maize yield improvement. *Mol. Breed.* **34**, 1087–1096 (2014). doi: 10.1007/s11032-014-0101-8
17. C. U. Stirnimann, E. Petsalaki, R. B. Russell, C. W. Müller, WD40 proteins propel cellular networks. *Trends Biochem. Sci*. **35**, 565–574 (2010). doi: 10.1016/j.tibs.2010.04.003
18. B. P. Jain, S. Pandey, WD40 repeat proteins: signalling scaffold with diverse

functions. *Protein J.* **37**, 391–406 (2018). doi: 10.1007/s10930-018-9785-7

19. K. A. Lease *et al.*, A mutant Arabidopsis heterotrimeric G-protein β subunit affects leaf, flower, and fruit development. *Plant Cell* **13**, 2631–2641 (2001). doi: 10.1105/tpc.010315

20. Y. Wu *et al.*, Presence of tannins in sorghum grains is conditioned by different natural alleles of *Tannin1*. *Proc. Natl. Acad. Sci. U.S.A.* **109**, 10281–10286 (2015). doi: 10.1073/pnas.1201700109

21. Q. Wu *et al.*, The maize heterotrimeric G protein β subunit controls shoot meristem development and immune responses. *Proc. Natl. Acad. Sci. U.S.A.* **117**, 1799–1805 (2020). doi: 10.1073/pnas.1917577116

22. M. J. Thomson *et al.*, Mapping quantitative trait loci for yield, yield components and morphological traits in an advanced backcross population between *Oryza rufipogon* and the *Oryza sativa* cultivar Jefferson. *Theor. Appl. Genet.* **107**, 479–493 (2003). doi: 10.1007/s00122-003-1270-8

23. C. Li, A. Zhou, T. Sang, Genetic analysis of rice domestication syndrome with the wild annual species, *Oryza nivara*. *New Phytol*. **170**, 185–194 (2006). doi: 10.1111/j.1469-8137.2005.01647.x

24. P. Bommert, N. Satoh-Nagasawa, D. Jackson, H. Hirano, Genetics and evolution of inflorescence and flower development in grasses. *Plant Cell Physiol*. **46**, 69–78 (2005). doi: 10.1093/pcp/pci504

25. X. Bai *et al*. Genome-wide association analysis reveals different genetic control in panicle architecture between *indica* and *japonica* rice. *Plant Genome* **9**, (2016).

doi: 10.3835/plantgenome2015.11.0115.

26. K. Hammer, Das Domestikationssyndrom. *Kulturpflanze* **32**, 11–34 (1984). doi: 10.1007/BF02098682

27. D. Sosso *et al.*, Seed filling in domesticated maize and rice depends on SWEET-mediated hexose transport. *Nat. Genet.* **47**, 1489–1493 (2015). doi: 10.1038/ng.3422

28. Y. Matsuoka *et al.*, A single domestication for maize shown by multilocus microsatellite genotyping. *Proc. Natl. Acad. Sci. U.S.A.* **99**, 6080–6084 (2002). doi: 10.1073pnas.052125199

29. H. Chen, N. Patterson, D. Reich, Population differentiation as a test for selective sweeps. *Genome Res.* **20**, 393–402 (2010). doi: 10.1101/gr.100545.109

30. Y. Jiao *et al.*, Improved maize reference genome with single-molecule technologies. *Nature* **546**, 524–527 (2017). doi: 10.1038/nature22971

31. A. Studer, Q. Zhao, J. Ross-Ibarra, J. Doebley, Identification of a functional transposon insertion in the maize domestication gene *tb1*. *Nat. Genet.* **43**, 1160–1163 (2011). doi: 10.1038/ng.942

32. H. Wang *et al.*, The origin of the naked grains of maize. *Nature* **436**, 714–719 (2005). doi: 10.1038/nature03863

33. S. A. Goff *et al.*, A draft sequence of the rice genome (*Oryza sativa* L. ssp. *japonica*). *Science* **296**, 92–100 (2002). doi: 10.1126/science.1068275

34. L. Tan *et al.*, Control of a key transition from prostrate to erect growth in rice domestication. *Nat. Genet.* **40**, 1360–1364 (2008). doi: 10.1038/ng.197

35. J. Jin *et al.*, Genetic control of rice plant architecture under domestication. *Nat. Genet.* **40**, 1365–1369 (2008). doi: 10.1038/ng.247

36. T. Ishii *et al.*, *OsLG1* regulates a closed panicle trait in domesticated rice. *Nat. Genet.* **45**, 462–465 (2013). doi: 10.1038/ng.2567

37. Z. Zhu *et al.*, Genetic control of inflorescence architecture during rice domestication. *Nat. Commun.* **4**, 2200 (2013). doi: 10.1038/ncomms3200

38. R. A. Kerstetter, D. Laudencia-Chingcuanco, L. G. Smith, S. Hake, Loss of function mutations in the maize homeobox gene, *knotted1*, are defective in shoot meristem maintenance. *Development* **124**, 3045–3054 (1997). PMID: 9272946

39. K. Tsuda, Y. Ito, Y. Sato, N. Kurata, Positive autoregulation of a *KNOX* gene is essential for shoot apical meristem maintenance in rice. *Plant Cell* **23**, 4368–4381 (2011). doi: 10.1105/tpc.111.090050

40. S. L. Blauth *et al.*, Identification of *Mutator* insertional mutants of starch-branching enzyme 1 (*sbe1*) in *Zea mays* L. *Plant Mol. Biol.* **48**, 287–297 (2002). doi: 10.1023/a:1013335217744

41. H. Satoh *et al.*, Starch-branching enzyme I-deficient mutation specifically affects the structure and properties of starch in rice endosperm. *Plant Physiol.* **133**, 1111–1121 (2003). doi: 10.1104/pp.103.021527

42. F. Fichtner, J. E. Lunn, The role of trehalose 6-phosphate (Tre6P) in plant metabolism and development. *Annu. Rev. Plant Biol.* **72**, 737–760 (2021). doi: 10.1146/annurev-arplant-050718-095929

43. L. Huang, H. Tan, C. Zhang, Q. Li, Q. Liu, Starch biosynthesis in cereal

endosperms: An updated review over the last decade. *Plant Commun.* **2**, 100237 (2021). doi: 10.1016/j.xplc.2021.100237

44. L. Wang *et al.*, Molecular parallelism underlies convergent highland adaptation of maize landraces. *Mol. Biol. Evol.* **38**, 3567–3580 (2021). doi: 10.1093/molbev/msab119

45. A. R. Fernie, J. Yan, *De Novo* Domestication: An alternative route toward new crops for the future. *Mol. Plant* **12**, 615–631 (2019). doi: 10.1016/j.molp.2019.03.016

46. Z. B. Zeng, Precision mapping of quantitative trait loci. *Genetics* **136**, 1457–1468 (1994). doi: 10.1093/genetics/136.4.1457

47. J. Tian, *et al.*, Teosinte ligule allele narrows plant architecture and enhances high-density maize yields. *Science* **365**, 658–664 (2019). doi: 10.1126/science.aax5482

48. J. Yu, *et al.*, A unified mixed-model method for association mapping that accounts for multiple levels of relatedness. *Nat. Genet.* **38**, 203–208 (2006). doi: 10.1038/ng1702

49. X. Yang *et al.*, Characterization of a global germplasm collection and its potential utilization for analysis of complex quantitative traits in maize. *Mol. Breed*. **28**, 511–526 (2011). doi: 10.1007/s11032-010-9500-7

50. C. Huang *et al.*, *ZmCCT9* enhances maize adaptation to higher latitudes. *Proc. Natl. Acad. Sci. USA* **115**, E334–E341 (2018). doi: 10.1073/pnas.1718058115

51. Z. Zhang, J. Yang, Y. Wu, Transcriptional regulation of zein gene expression in maize through the additive and synergistic action of opaque2, prolamine-box

binding factor, and O2 heterodimerizing proteins. *Plant Cell* **27**, 1162–1172 (2015). doi: 10.1105/tpc.15.00035

52. P. Librado, J. Rozas, DnaSP v5: a software for comprehensive analysis of DNA polymorphism data. *Bioinformatics* **25**, 1451–1452 (2009). doi: 10.1093/bioinformatics/btp187

53. R. R. Hudson, Generating samples under a Wright-Fisher neutral model of genetic variation. *Bioinformatics* **18**, 337–338 (2002). doi: 10.1093/bioinformatics/18.2.337

54. L. Excoffier, H. E. Lischer, Arlequin suite ver 3.5: a new series of programs to perform population genetics analyses under Linux and Windows. *Mol. Ecol. Resour.* **10**, 564–567 (2010). doi: 10.1111/j.1755-0998.2010.02847.x

55. D. H. Alexander, J. Novembre, K. Lange, Fast model-based estimation of ancestry in unrelated individuals. *Genome Res.* **19**, 1655–1664 (2009). doi: 10.1101/gr.094052.109

56. J. Yang, S. H. Lee, M. E. Goddard, P. M. Visscher, GCTA: a tool for genome-wide complex trait analysis. *Am. J. Hum. Genet.* **88**, 76–82 (2011). doi: 10.1016/j.ajhg.2010.11.011

57. W. Chen *et al.*, Code and processed data for "Convergent selection of a WD40 protein that enhances grain yield in maize and rice." Figshare (2022). doi: 10.6084/m9.figshare.18104336

58. T. H. Lee, H. Guo, X. Wang, C. Kim, A. H. Paterson, SNPhylo: a pipeline to construct a phylogenetic tree from huge SNP data. *BMC Genomics* **15**, 162 (2014).

doi: 10.1186/1471-2164-15-162

59. Y. Wang *et al.*, *MCScanX*: a toolkit for detection and evolutionary analysis of gene synteny and collinearity. *Nucleic Acids Res.* **40**, e49 (2012). doi: 10.1093/nar/gkr1293

60. U. Raudvere *et al.*, g:Profiler: a web server for functional enrichment analysis and conversions of gene lists (2019 update). *Nucleic Acids Res.* **47**, W191–W198 (2019). doi: 10.1093/nar/gkz369

61. R. J. Elshire *et al.*, A robust, simple Genotyping-by-Sequencing (GBS) approach for high diversity species. *PLoS ONE* **6**, e19379 (2011). doi: 10.1371/journal.pone.0019379

62. P. J. Bradbury *et al.*, TASSEL: software for association mapping of complex traits in diverse samples. *Bioinformatics* **23**, 2633–2635 (2007). doi: 10.1093/bioinformatics/btm308

63. X. Huang *et al.*, High-throughput genotyping by whole-genome resequencing. *Genome Res.* **19**, 1068–1076 (2009). doi: 10.1101/gr.089516.108

64. D. D. Kosambi, The estimation of map distance from recombination values. *Ann Eugen.* **12**, 172–175 (1944). doi.org/10.1111/j.1469-1809.1943.tb02321.x

65. E. Lander, D. Botstein, Mapping mendelian factors underlying quantitative traits using RFLP linkage maps. *Genetics* **121**, 185–199 (1989). PMID: 2563713

66. T. D. Schmittgen, K. J. Livak, Analyzing real-time PCR data by the comparative C_T method. *Nat. Protoc.* **3**, 1101–1108 (2008). doi: 10.1038/nprot.2008.73

67. S. I. Wright *et al.*, The effects of artificial selection on the maize genome. *Science*

308, 1310–1314 (2005). doi: 10.1126/science.1107891

68. F. Tian, N. M. Stevens, E. S. Buckler, Tracking footprints of maize domestication and evidence for a massive selective sweep on chromosome 10. *Proc. Natl. Acad. Sci. USA* **106**, Suppl1: 9979–9986 (2009). doi: 10.1073/pnas.0901122106

69. E. Formstecher *et al.*, Protein interaction mapping: A *Drosophila* case study. *Genome Res.* **15**, 376–384 (2005). doi: 10.1101/gr.2659105

70. K. Tamura, G. Stecher, D. Peterson, A. Filipski, S. Kumar, MEGA6: Molecular Evolutionary Genetics analysis version 6.0. *Mol. Biol. Evol*. **30**, 2725–2729 (2013). doi: 10.1093/molbev/mst197

71. A. G. Teacher, D. J. Griffiths, HapStar: automated haplotype network layout and visualization. *Mol. Ecol. Resour.* **11**, 151–153 (2011). doi: 10.1111/j.1755-0998.2010.02890.x

72. B. Langmead, S. L. Salzberg, Fast gapped-read alignment with Bowtie 2. *Nat. Methods* **9**, 357–359 (2012). doi: 10.1038/nmeth

73. H. Li *et al.*, The Sequence Alignment/Map format and SAMtools. *Bioinformatics* **25**, 2078–2079 (2009). doi: 10.1093/bioinformatics/btp352

74. L. Chen *et al.*, Portrait of a genus: the genetic diversity of *Zea*. *bioRxiv* (2021). doi.org/10.1101/2021.04.07.438828

75. A. M. Bolger, M. Lohse, B. Usadel, Trimmomatic: a flexible trimmer for Illumina sequence data. *Bioinformatics* **30**, 2114–2120 (2014). doi: 10.1093/bioinformatics/btu170

76. W. Wang *et al.*, Genomic variation in 3,010 diverse accessions of Asian cultivated

rice. *Nature* **557**, 43–49 (2018). doi: 10.1038/s41586-018-0063-9

77. X. Zheng *et al.*, Genomic signatures of domestication and adaptation during geographical expansions of rice cultivation. *Plant Biotechnol. J.* **20**, 16–18 (2022). doi:10.1111/pbi.13730

78. H. Li, Aligning sequence reads, clone sequences and assembly contigs with BWA-MEM. arXiv:1303.3997 [q-bio.GN (2013)

79. P. Danecek *et al.*, The variant call format and VCFtools. *Bioinformatics* **27**, 2156–2158 (2011). doi: 10.1093/bioinformatics/btr330

80. S. Purcell *et al.*, PLINK: a tool set for whole-genome association and population-based linkage analyses. *Am. J. Hum. Genet.* **81**, 559–575 (2007). doi: 10.1086/519795

81. I. Letunic, P. Bork, Interactive Tree Of Life (iTOL) v5: an online tool for phylogenetic tree display and annotation. *Nucleic Acids Res.* **49**, W293–W296 (2021). doi: 10.1093/nar/gkab301

82. Z. Liu *et al.*, Expanding maize genetic resources with predomestication alleles: maize-teosinte introgression populations. *Plant Genome* **9**, (2016). doi:10.3835/plantgenome2015.07.0053

83. H. Zhao *et al.*, CrossMap: a versatile tool for coordinate conversion between genome assemblies. *Bioinformatics* **30**, 1006–1007 (2014). doi: 10.1093/bioinformatics/btt730

84. H. Yu *et al.*, Gains in QTL detection using an ultra-high density SNP map based on population sequencing relative to traditional RFLP/SSR markers. *PLoS ONE* **6**,

e17595 (2011). doi: 10.1371/journal.pone.0017595

85. M. Kanehisa, S. Goto, KEGG: kyoto encyclopedia of genes and genomes. *Nucleic Acids Res.* **28**, 27–30 (2000). doi: 10.1093/nar/28.1.27

86. J. Reimand *et al.*, Pathway enrichment analysis and visualization of omics data using g:Profiler, GSEA, Cytoscape and EnrichmentMap. *Nat. Protoc.* **14**, 482–517 (2019). doi: 10.1038/s41596-018-0103-9

Acknowledgments: We thank L. Tan and H. Chen for help growing rice, G. Wang for sharing the wild rice leaves, and J. Ross-Ibarra for constructive suggestions on manuscript revision. **Funding:** This research was supported by the National Natural Science Foundation of China (91935302, 31421005, 31961133002, and 91435205), the National Key Research and Development Program of China (2020YFE0202300), Beijing Outstanding Young Scientist Program (BJJWZYJH01201910019026), Young Elite Scientists Sponsorship Program by CAST (2019QNRC001), and the National Science Foundation (IOS-2129189). **Author contributions:** X.Y., J.Y., and J.L. conceived and designed this study. W.C., X.Z., J.G., S.J., X-Y.Z., L-C.C., J.X., L.Z., Y.H., Y.X., G.X., Y.W., S-H.W., S.W., J.C. and S.C. performed experiments. L.C., X.Z., W.C., N.Y., M.W., and P.Y. analyzed data. F.Y., D.J., C.S., F.Q., F.T., and A.F. contributed valuable suggestions on this study. W.C., L.C., X.Z., N.Y., J.Y., and X.Y. wrote the manuscript. All the authors edited and proofed the manuscript. **Competing interests:** D.J. serves as a consultant for Inari Agriculture, and the authors declare no competing interests. A patent with application No. PCT/CN2018/117844 is pending.

Data and materials availability: All data are available in the main text, Supplementary Materials, public database or referenced permanent online repositories. Sequence data were deposited in NCBI GenBank under accession number MW238854-MW239029 for *KRN2*, MW219821-MW219975 and OK655843-OK655881 for *OsKRN2*, PRJNA771523 for all CRISPR knockouts in maize and rice, and PRJNA771230 for our re-sequenced rice data. The alignments used for phylogenetic tree and all codes are provided online at Figshare (*57*).

Supplementary Materials

Materials and Methods

Figs. S1 to S19

Tables S1 to S12

References (*61–86*)

MDAR Reproducibility Checklist

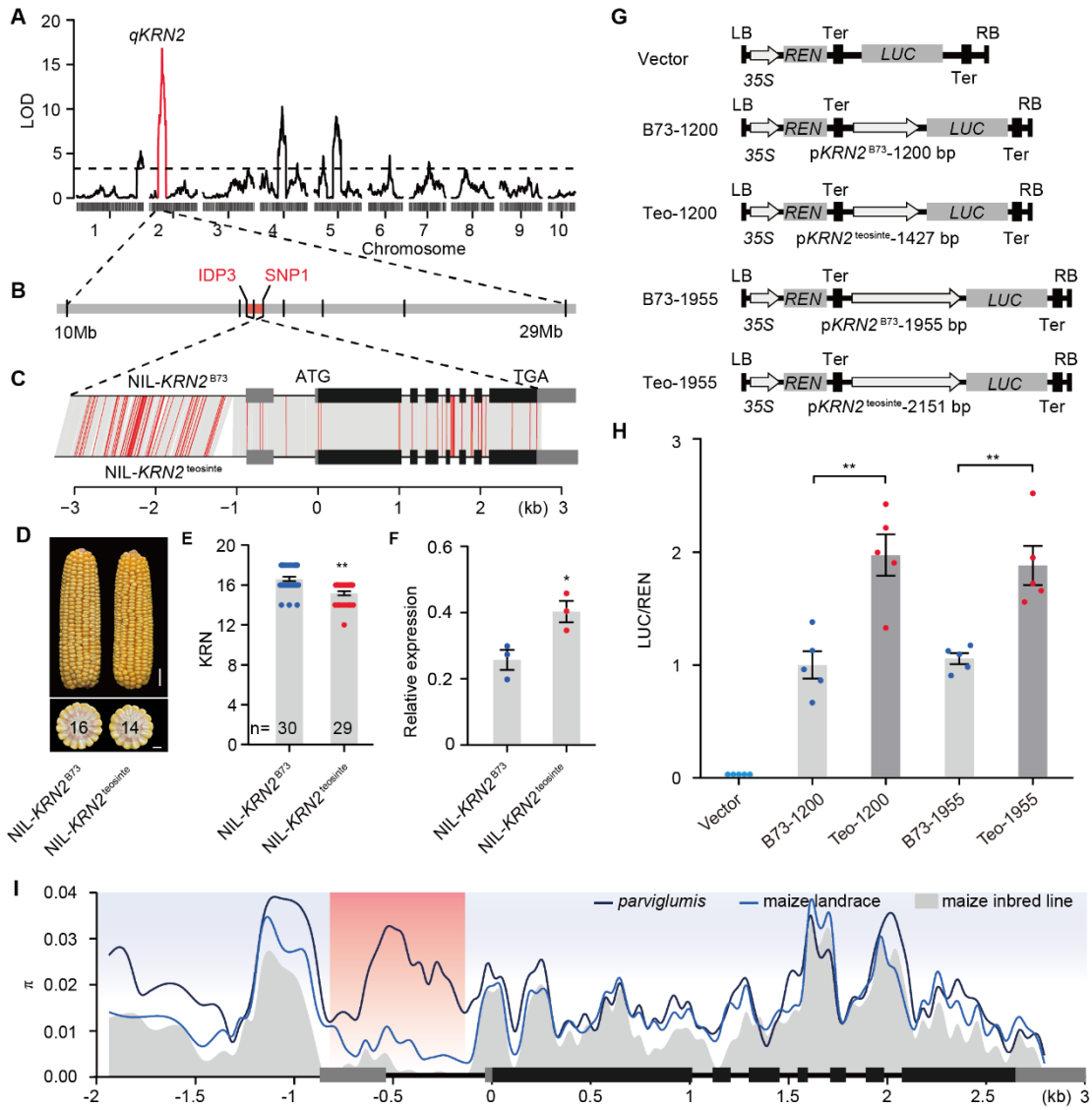

Fig. 1. *KRN2* affects kernel row number and underwent selection during maize domestication. (**A**) Logarithm of odds (LOD) profile of QTLs for KRN in the MT-6/B73 RIL population. The dashed line shows the threshold LOD value (3.3) for putative QTLs. (**B**) *qKRN2* was fine mapped to a 5,799-bp interval (red) flanked by the markers IDP3 and SNP1. (**C**) *KRN2* gene structure and sequence comparison of the target region between NIL-*KRN2*^{B73} and NIL-*KRN2*^{teosinte}. Black shading, exons; gray shading, UTRs. The red lines denote SNPs, and the white spaces show InDels. (**D** to **F**) Ear performance (D), KRN quantification (E), and *KRN2* expression in 0.5-mm IMs (F) of NIL-*KRN2*^{B73} and NIL-*KRN2*^{teosinte}. Scale bars in (D): 2 cm for the ear and 1 cm for

ear transverse sections. The expression levels of *KRN2* in (F) were quantified using qPCR, and normalized to that of maize *ACTIN*. (**G**) Constructs used to test the effect of polymorphisms in the promoter and 5'UTR on *KRN2* expression in transient expression assays in maize leaf protoplasts. B73-1200, Teo-1200, B73-1955, and Teo-1955 constructs harbor the promoter and 5'UTR of different *KRN2* alleles, including 1,200 bp from B73, 1,427 bp from teosinte, 1,955 bp from B73, and 2,151 bp from teosinte. (**H**) The teosinte sequences drive increased LUC activity in comparison with the B73 alleles. The data were normalized with respect to the average values of the B73-1200 construct. (**I**) Nucleotide diversity across the *KRN2* locus. A 150-bp sliding window with a 35-bp step size was used to calculate nucleotide diversity (π). The selected region (–800 to –100 bp) is shaded in red. In (E), (F), and (H), the data represent the mean ± standard error (s.e.m.), n = 3 in (F) and n = 5 in (H); two-tailed Student's *t* test, $^{**}P < 0.01$, $^{*}P < 0.05$.

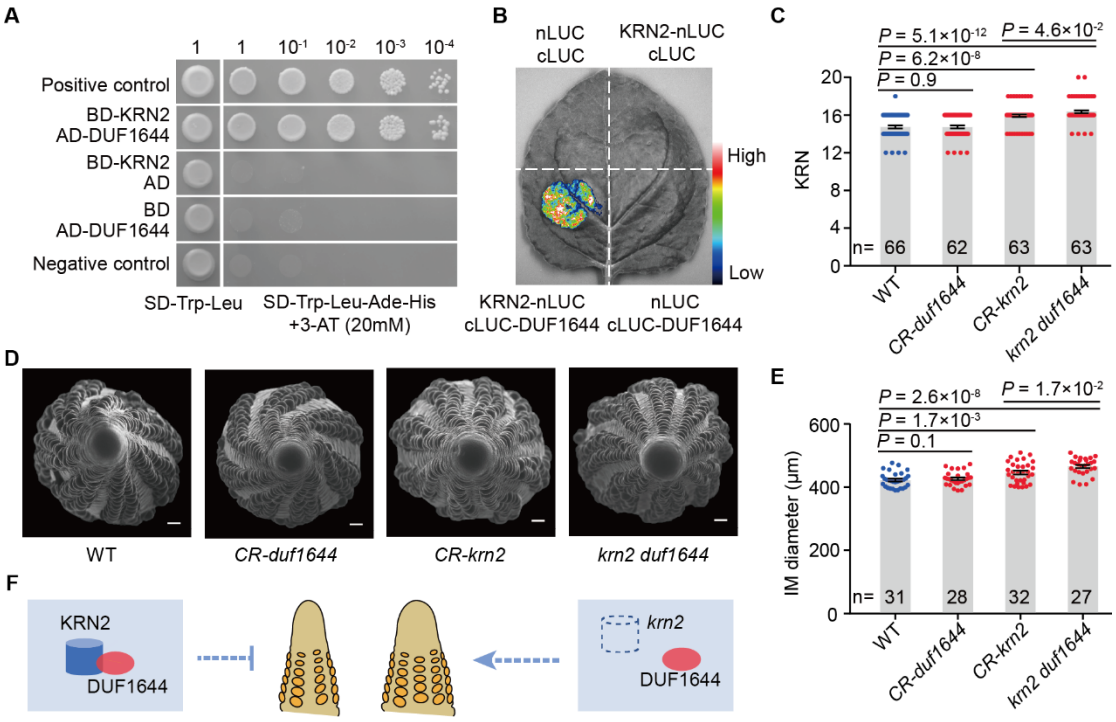

Fig. 2. KRN2 and its interactor, DUF1644, regulate KRN in a synergistic pathway. (**A** and **B**) Interaction between KRN2 and DUF1644 confirmed by Y2H assays (A) and the split firefly LUC complementation assay in tobacco (B). BD, binding domain; AD, activation domain; Trp, tryptophan; Leu, leucine; Ade, adenine; His, histidine; 3-AT, 3-aminotriazole. Fluorescence intensity represents the strength of the interaction. (**C** to **E**) KRN quantification (C), top-down scanning electron microscopy views of ear primordia (D), and IM diameter quantification (E) from wild type (WT) and the single and double mutants of *krn2* and *duf1644*. In (C) and (E), the data represent the mean ± s.e.m. *P*-values were calculated from two-tailed Student's *t* test. Scale bars in (D): 100 μm. (**F**) A hypothetical working model for *KRN2* in controlling KRN in maize. When KRN2 function is lost, DUF1644 cannot interact with it, resulting in an increase in IM diameter and, consequently, KRN. Otherwise, DUF1644 interacts with KRN2 to synergistically and negatively regulate IM diameter and KRN.

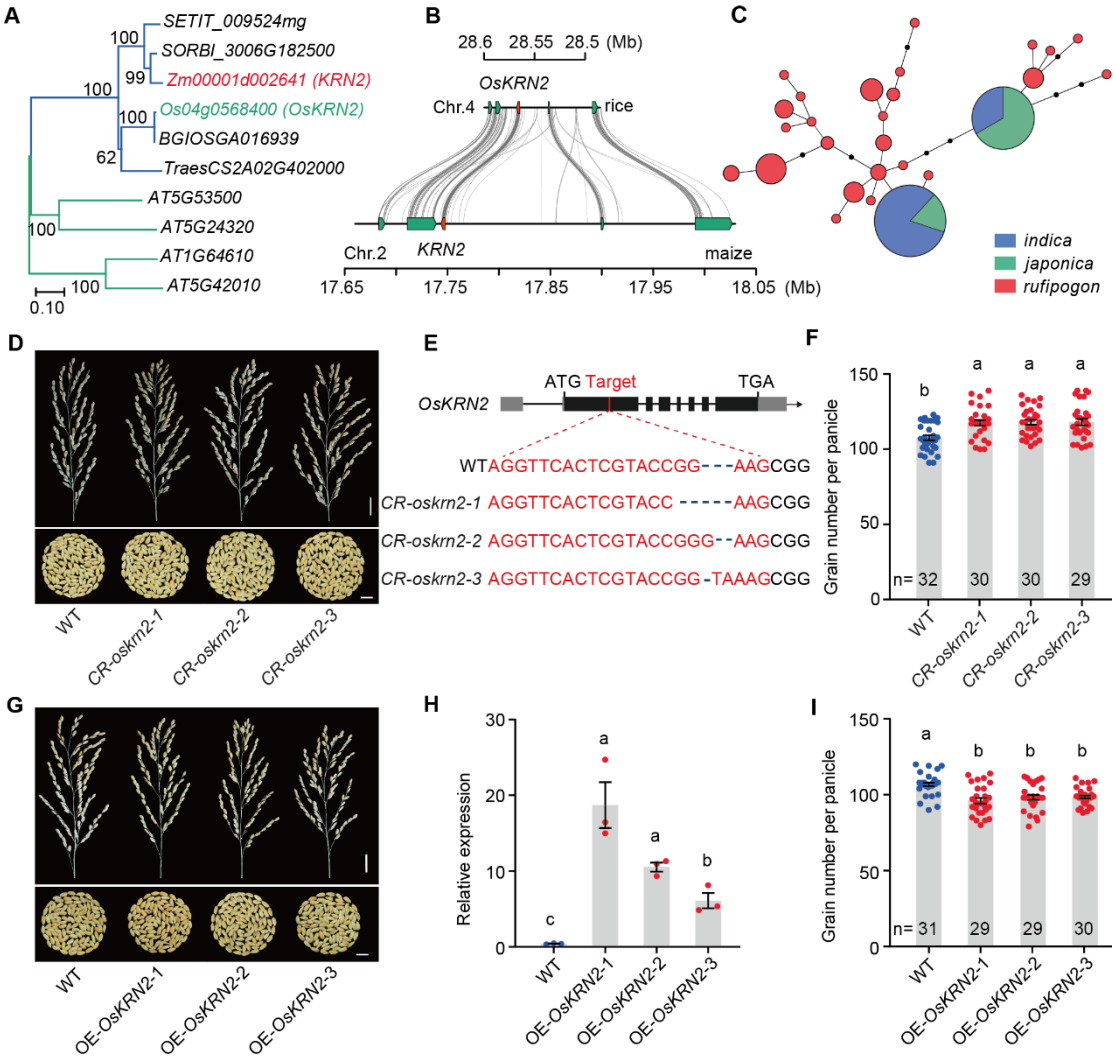

Fig. 3. *OsKRN2* is a selected gene in rice and contributes to grain number. (**A**) The neighbor-joining phylogenetic tree of *KRN2* and its orthologs from major cereal crops and *Arabidopsis*. Bootstrap values from 1,000 replicates are indicated at each node, and the scale represents branch length. (**B**) Comparative genomic analysis of syntenic and conserved sequences in the 0.4/0.1-Mb region around *KRN2*/*OsKRN2* (red) from maize (B73) and rice (Nipponbare). The aligned orthologs from left to right with green color are *Zm00001d002639*, *Zm00001d002640*, *Zm00001d002642*, and *Zm00001d002644* in maize and *Os04g0568900*, *Os04g0568800*, *Os04g0567800*, and *Os04g0566900* in rice. (**C**) A minimum-spanning tree for the ~1,100-bp *OsKRN2* promoter and 5'UTR region.

Each haplotype group is represented by a circle, and the size of the circle is proportional to the accession number within the haplotype. (**D**) *CR-oskrn2* mutants increase panicle branching and grain number. (**E**) Null coding sequences of *CR-oskrn2* mutants. Gene diagram is shown. Black shading, exons; gray shading, UTRs. The red line indicates the gRNA site. (**F**) Quantification of grain number per panicle from wild type (WT) and *CR-oskrn2* mutants. (**G** to **I**) Panicle morphologies and grains per panicle (G), *OsKRN2* expression level (H), and grain number per panicle (I) of WT and *OsKRN2*-overexpressing transgenic lines. The expression levels of *OsKRN2* in (H) were quantified using qPCR, and normalized to that of rice *ACTIN*. Scale bars in (D) and (G): 2 cm for panicle morphologies and 1 cm for grains. In (F), (H), and (I), the data represent the mean ± s.e.m., n = 3 in (H); different letters indicate significant differences at $P < 0.05$ (one-way ANOVA followed by Tukey's multiple comparison test).

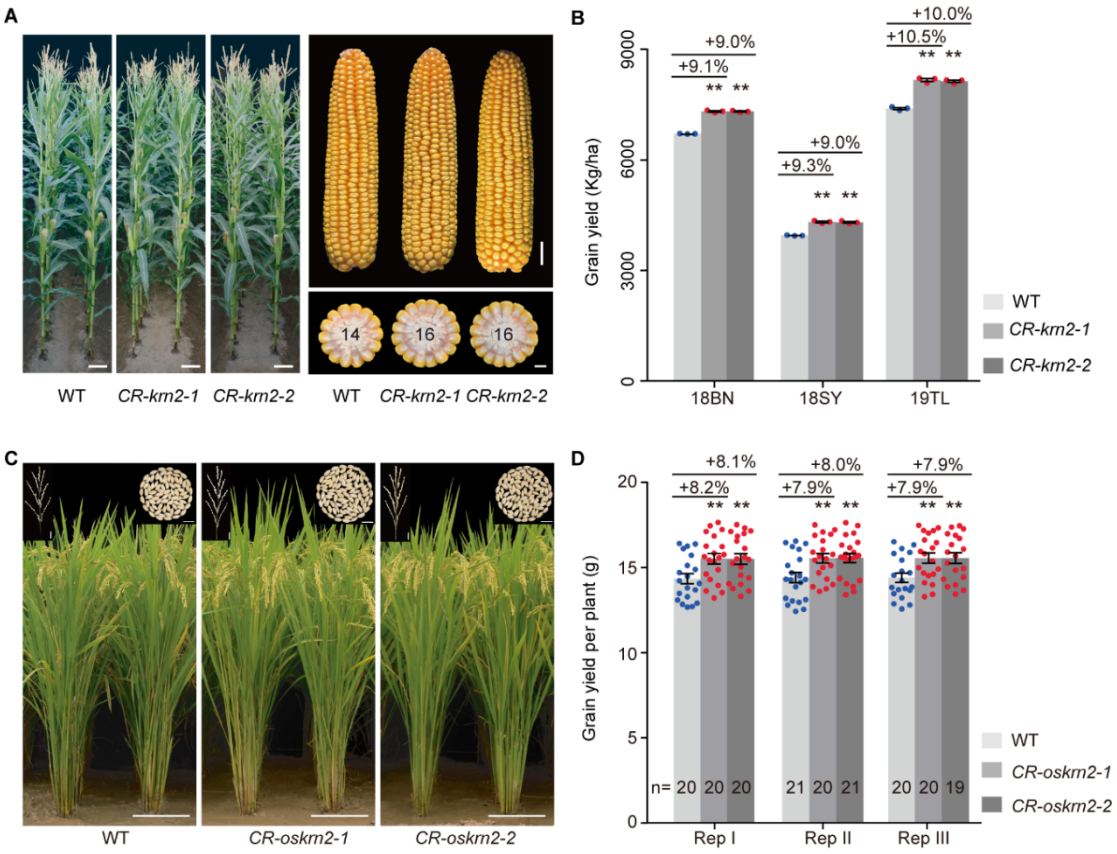

Fig. 4. Yield performance of *KRN2* and *OsKRN2* gene-edited lines under field conditions. (**A**) Plant and ear morphologies of wild type (WT), *CR-krn2-1*, and *CR-krn2-2*. (**B**) Grain yield of WT, *CR-krn2-1*, and *CR-krn2-2* in three locations. At each location, 26–38 ears for each replicate were quantified. The data represent the mean ± s.e.m. from three replicates (shown as dots) in each location. 18BN, 18SY, and 19TL indicates the field trials performed in Bayan Nur in 2018, Sanya in 2018, and Tieling in 2019, respectively. (**C**) Plants, panicle, and grain morphologies of WT, *CR-oskrn2-1*, and *CR-oskrn2-2*. (**D**) Grain yield of WT, *CR-oskrn2-1*, and *CR-oskrn2-2* in one location with three replicates (Rep I to Rep III). For each replicate, 19–21 plants were quantified. The data represent the mean ± s.e.m. Scale bars in (A) and (C): 20 cm for plants, 2 cm for ears and panicles, and 1 cm for ear transections and grains. In (B) and (D), two-tailed Student's *t* test; $^{**}P < 0.01$.

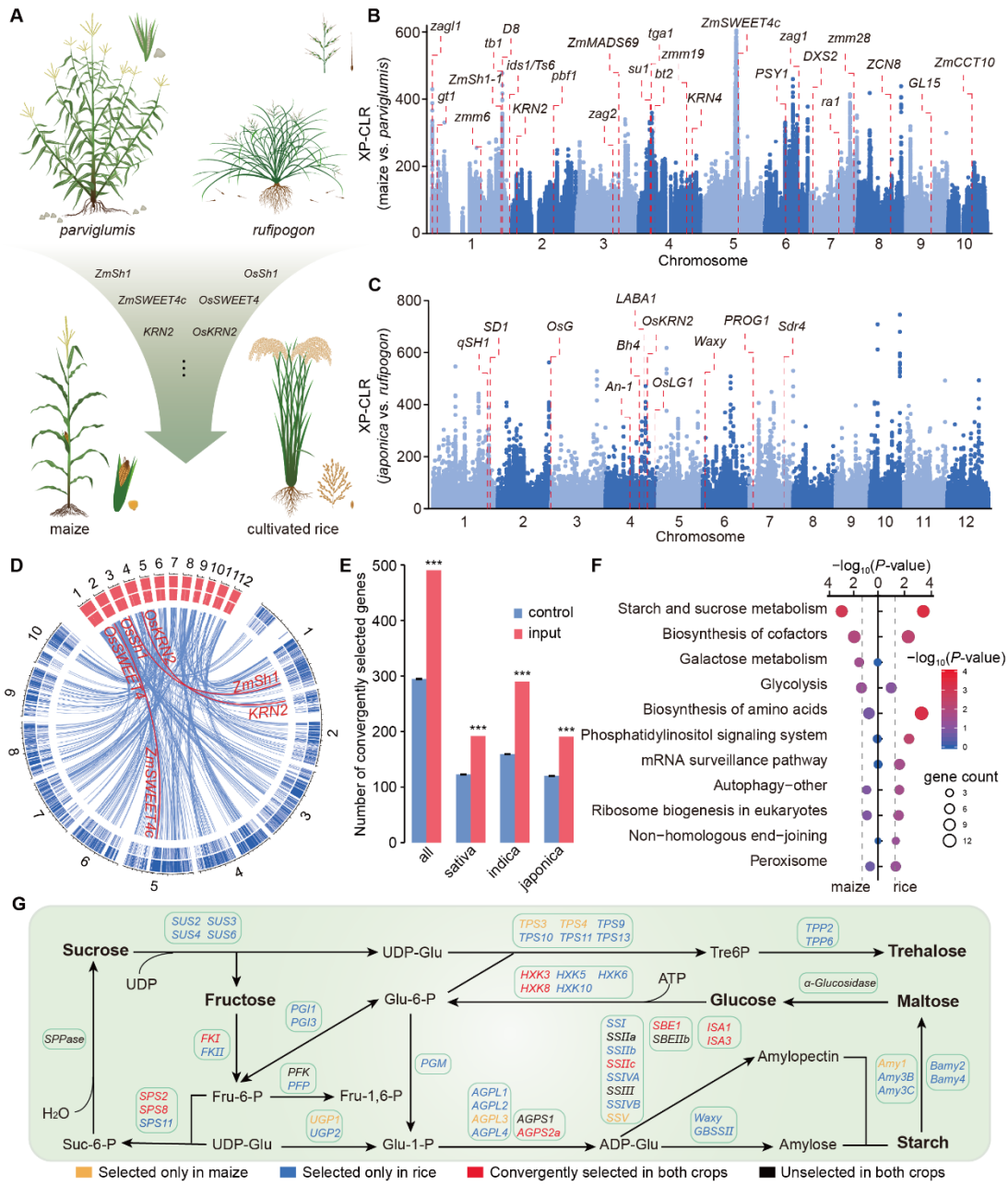

Fig. 5. Overview of convergent selection in maize and rice. (**A**) Convergence of traits in domesticated species vs. wild ancestors, likely driven by genes with conserved functions. Three pairs of known orthologous genes under convergent selection are shown: *ZmSh1*/*OsSh1* for seed shattering (*7*), *ZmSWEET4c*/*OsSWEET4* for grain filling (*27*), and *KRN2/OsKRN2* for grain number. (**B** and **C**) Genome-wide XP-CLR values between maize and *parviglumis* (B) and between *japonica* and *rufipogon* (C). Regions of 1 kb and 300 bp were used to calculate the XP-CLR values for maize and rice,

respectively, and each point represents a value in a region. The red dashed lines indicate the positions of known selected genes detected in our study (**table S7**). (**D**) The distribution of selected regions (outer) and genes (inner) in maize (blue) and rice (red). The blue lines in the inner rings show the convergently selected genes that were syntenic in the maize and rice genomes. The red lines highlight the positions of genes that are known to have undergone convergent selection. (**E**) Convergent selection acts on the identified orthologs more often than that expected by chance between maize and different rice datasets. Pairwise comparison via permutation test; ***$P < 0.001$. (**F**) Enriched pathways in maize or rice identified using g:Profiler (adjusted $P < 0.05$, multiple-testing correction via the g:SCS algorithm) among the 490 orthologous gene pairs under convergent selection. Circle size indicates the number of genes from the common gene hit list included in each pathway; circle color and *x*-axis position indicate the $-\log_{10}$-transformed P value. The vertical dashed lines indicate the significant threshold $P < 0.05$. (**G**) Detailed molecular representation of genes implicated in the starch and sucrose metabolism pathway during selection. Detailed information for these genes is listed in **table S9**.

One-page Summary

INTRODUCTION: During the independent process of cereal evolution, many trait shifts appear to have been under convergent selection to meet the specific needs of humans. Identification of convergently selected genes across cereals could help understand the evolution of crop species as well as accelerate breeding programs. In the last more than two decades, researchers have debated whether convergent phenotypic selection in distinct lineages is driven by conserved molecular changes or by diverse molecular pathways. Two of the most economically important crops, maize and rice, display some conserved phenotypic shifts that include the loss of seed dispersal, decreased seed dormancy, and increased grain number during evolution, although they experienced independent selection. Hence, maize and rice can serve as excellent system for understanding the extent of convergent selection among cereals.

RATIONALE: Despite the identification of a few convergently selected genes, our understanding of the extent of molecular convergence on a genome-wide scale between maize and rice is very limited. To ask how often selection acts on orthologous genes, we investigated the functions and molecular evolution of the grain yield quantitative trait locus *KRN2* in maize and its rice ortholog *OsKRN2*. We also identified convergently selected genes on a genome-wide scale in maize and rice, using two large datasets.

RESULTS: We identified a selected gene, *KRN2* (*kernel row number2*), that differs between domesticated maize and its wild ancestor, teosinte. This gene underlies a major quantitative trait locus for kernel row number in maize. Selection in the non-coding

upstream regions resulted in a reduction of *KRN2* expression and an increased grain number via increasing kernel rows. The rice ortholog, *OsKRN2*, also underwent selection, and negatively regulates grain number via control of secondary panicle branches. These orthologs encode WD40 proteins, and function synergistically with a gene of unknown function, DUF1644, suggesting that a conserved protein interaction controls grain number in maize and rice. Field tests show that knockout of *KRN2* in maize or *OsKRN2* in rice increased grain yield by ~10% and ~8%, with no apparent trade-off in other agronomic traits, suggesting potential applications of *KRN2* and its orthologs for crop improvement.

On a genome-wide scale, we identified a set of 490 orthologous genes that underwent convergent selection during maize and rice evolution, including *KRN2/OsKRN2*. We found that the convergently selected orthologous genes appear to be significantly enriched in two specific pathways as starch and sucrose metabolism, and biosynthesis of cofactors in both maize and rice. A deep analysis of convergently selected genes in the starch metabolic pathway indicate that the degree of genetic convergence via convergent selection is related to the conservation and complexity of the gene network for a given selection.

CONCLUSION: Our findings demonstrate that common phenotypic shifts during maize and rice evolution acting on conserved genes are driven at least in part by convergent selection, which in maize and rice likely occurred both during and post domestication. We provide evolutionary and functional evidence on the convergent selection of *KRN2/OsKRN2* for grain number between maize and rice. We further found

that a complete loss-of-function allele of *KRN2*/*OsKRN2* increased grain yield without an apparent negative impact on other agronomic traits. Exploring the role of *KRN2/OsKRN2* and other convergently selected genes across the cereals could provide new opportunities to enhance production of other global crops.

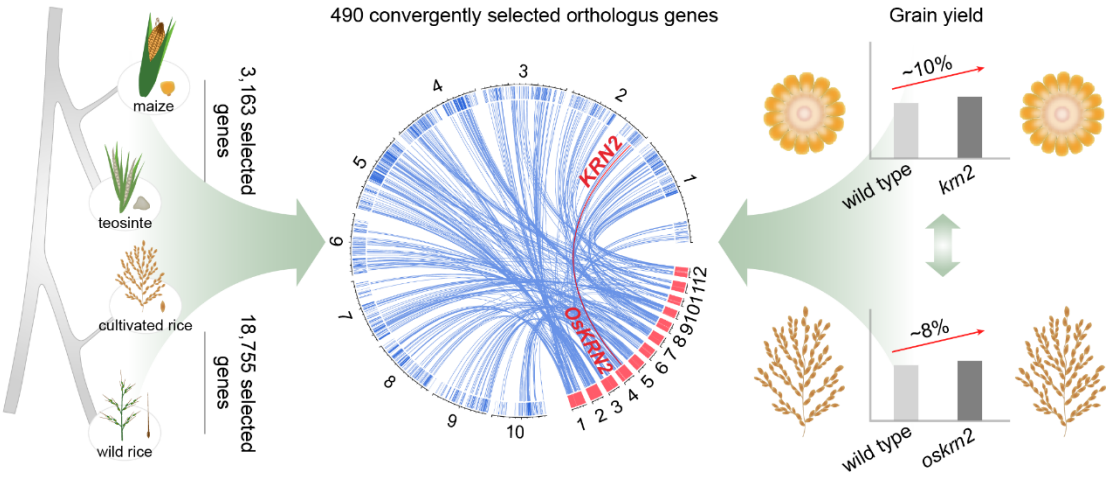

Fig. 0. Shared selected orthologous genes in maize and rice for convergent phenotypic shifts during domestication and improvement. By comparing 3,163 selected genes in maize and 18,755 selected genes in rice, 490 orthologous gene pairs, including *KRN2* and its rice ortholog, *OsKRN2*, are identified as having been convergently selected. Knockout of *KRN2* in maize or *OsKRN2* in rice increased grain yield by increasing kernel rows and secondary panicle branches, respectively.

Supplementary Materials for

Convergent selection of a WD40 protein that enhances grain yield in maize and rice

Wenkang Chen[1,3]*, Lu Chen[2]*‡, Xuan Zhang[1,3]*, Ning Yang[2,4]*, Jianghua Guo[1], Min Wang[1], Shenghui Ji[1], Xiangyu Zhao[1], Pengfei Yin[1], Lichun Cai[1], Jing Xu[1], Lili Zhang[1], Yingjia Han[1], Yingni Xiao[1], Gen Xu[1], Yuebin Wang[2], Shuhui Wang[1], Sheng Wu[1], Fang Yang[2], David Jackson[2,5], Jinkui Cheng[1,3], Saihua Chen[6], Chuanqing Sun[1], Feng Qin[1], Feng Tian[1,3], Alisdair R. Fernie[7], Jiansheng Li[1,3]†, Jianbing Yan[2,4]†, Xiaohong Yang[1,3]†

*These authors contributed equally to this work.

† Corresponding authors. Email: yxiaohong@cau.edu.cn (X.Y.); yjianbing@mail.hzau.edu.cn (J.Y.); lijiansheng@cau.edu.cn (J.L.)

This PDF file includes:

Materials and Methods
Figs. S1 to S19
Tables S1 to S3, S8, and S10
Captions and legends for tables S4 to S7, S9, S11, and S12

Other Supplementary Materials for this manuscript include the following:

Tables S4 to S7, S9, S11, and S12

Materials and Methods

Plant materials

A recombinant inbred line (RIL) population of 199 lines was developed from inbred lines MT-6 (6 kernel rows) and B73 (~16 kernel rows) to detect quantitative trait loci (QTLs) for kernel row number (KRN). MT-6 was derived from Mo17 and a teosinte accession, X26-4 (accession number: PI 566686; *Zea mays* ssp. *mexicana*) (*16*).

A total of 512 maize inbred lines; 39 maize landraces; and 75 *Zea mays* ssp. *parviglumis*, 570 *Oryza sativa*, and 257 *Oryza rufipogon* accessions (table S5) were used for selection and association analyses. Out of these plant materials, a set of 507 maize inbred lines and 70 *parviglumis*, 461 *sativa*, and 257 *rufipogon* accessions, which represent cultivated and wild relatives in maize and rice, was used for convergent selection on a genome-wide scale; a set of 379 maize inbred lines was used for *KRN2*-based association mapping; a set of 69 maize inbred lines, 39 maize landraces, and 34 *parviglumis* accessions was used for the molecular evolutionary analysis of *KRN2*; and a set of 109 *sativa* and 59 *rufipogon* accessions was used for the molecular evolutionary analysis of *OsKRN2*.

The *Mutator* mutant of *KRN2* (*Mu-krn2*; stock number: UFMu-09531) was ordered from the Maize Genetics Cooperation Stock Center and was backcrossed with maize inbred line W22 three times. The mutation site was genotyped by PCR with the primers TIR8-1 and *KRN2*-MU-R (table S10).

QTL mapping for KRN

Together with the two parental lines, the MT-6/B73 RIL population was planted in a randomized complete block design with one replicate in Beijing (39.9°N, 116.3°E) and Sanya (18.2°N, 109.1°E), China, in 2013. Each line was grown in a single-row plot (2.5-m rows, 0.5 m apart, with planting density of 63,000 plants/ha). KRN was counted in eight plants in each plot after maturity. To eliminate the influence of environmental effects, the best linear unbiased predictor (BLUP) value for each line was calculated using the linear mixed model considering both genotype and environment as random effects in the R function 'lme4'. The BLUP values for each line were used to perform QTL mapping.

All RILs, along with both parents, were genotyped by a genotyping-by-sequencing (GBS) strategy (*61*). The restriction enzyme *Ape*KI was used to construct GBS libraries, followed by single-end sequencing on the Illumina HiSeq 2000 platform at Huazhong Agricultural University in Wuhan, China. In total, 97,991 SNPs were identified using TASSEL version 5.0 (*62*). Next, the SNPs in a genomic region without recombination breakpoints were combined into a recombination bin (*63*), resulting in 3,081 bins that were defined as markers for the construction of a genetic linkage map (table S11). A genetic map of 1,138.8 cM with an average interval of 0.37 cM between adjacent markers was constructed using the R/qtl package function *est.map* with the Kosambi's mapping function (*64*).

QTL mapping was performed using composite interval mapping (*46*) implemented in Windows QTL Cartographer version 2.5 (https://brcwebportal.cos.ncsu.edu/qtlcart/WQTLCart.htm). Model six of the Zmapqtl

module was used to detect QTL throughout the genome by scanning with a 0.5-cM interval between markers and with a 10-cM window. Forward-backward stepwise regression with five controlling markers was used to control background from flanking markers. The LOD value for putative QTLs was determined after 1,000 permutations at a significance level of $P < 0.05$. The confidence interval for QTL position was estimated with the 1.5-LOD support interval method (*65*).

Fine mapping of *qKRN2*

A recombinant-derived progeny testing strategy (*47*) was used to fine map *qKRN2*. First, MT-6/B73 F_1 plants were backcrossed with B73 for five generations, and four molecular markers (IDP1, IDP2, IDP7, and IDP8 in table S10) were used to detect qKRN2 heterozygosity during each generation. Next, a BC_5F_2 population containing 1,114 individuals was used to screen recombinants with different breakpoints at the qKRN2 locus using six molecular markers (IDP1, IDP2, IDP5, IDP6, IDP7, and IDP8 in table S10). BC_5F_3 families derived from BC_5F_2 recombinants were planted in the field and genotyped with these six molecular markers to identify homozygous recombinants (HRs) and homozygous nonrecombinants (HNRs). Within each BC_5F_3 family, the significance of KRN differences between HR and HNR plants was determined using a Student's *t* test. If HR and HNR plants differed significantly in terms of KRN, the parental BC_5F_2 recombinant was assumed to be heterozygous for the target QTL; otherwise, the parental BC_5F_2 recombinant was assumed to be homozygous. After integrating the QTL location information from all recombinants, qKRN2 was narrowed down from an 18.63-Mb genomic region to a 0.43-Mb region (fig. S1). To further fine map qKRN2, a BC_6F_2 population containing 5,942 individuals was used to screen recombinants using five molecular markers (IDP2, IDP3, IDP4, SNP1, and IDP5 in table S10) within the 0.43-Mb genomic region. Using the same testing strategy, qKRN2 was further delimited to a 5,799-bp genomic region (fig. S1). The fine-mapping populations were grown in the experimental field of China Agricultural University in Sanya (18.2°N, 109.1°E) and Bayan Nur (40.7°N, 107.5°E), China.

RNA isolation and expression analysis

Total RNA was isolated from maize and rice tissues using the EASYspin Plant RNA kit and treated with RNase-free DNase I to remove contaminating DNA (Aidlab). First-strand cDNA was synthesized using the PrimeScript II 1st Strand cDNA Synthesis kit (TAKARA). qPCR was conducted using TB Green *Premix Ex Taq* II (TAKARA) on a 7500 Real Time PCR System (Applied Biosystems). Expression levels of *KRN2* and *OsKRN2* were normalized to that of maize or rice *ACTIN* (table S10), respectively. The comparative CT ($2^{-\Delta CT}$) method (*66*) was used to quantify relative expression levels. Each tissue contained three biological replicates, and each replicate was collected from at least five maize/rice plants. For shoot apical meristem and inflorescence meristem of maize, each biological replicate was collected from at least 30 plants.

Transient expression assays in maize protoplasts

The ~2.0-kb and ~1.2-kp promoter fragments of *KRN2* were amplified from NIL-

KRN2^{B73} and NIL-*KRN2*^{teosinte} DNA, respectively, using specific primers *KRN2*-LUC-1955 and *KRN2*-LUC-1200 (table S10) and then inserted upstream of the LUC gene in vector pGreenII 0800-LUC that had been cleaved with *Kpn*I and *Pst*I, generating constructs p*KRN2*^{B73}::*LUC* and p*KRN2*^{teosinte}::*LUC*, respectively. The *Renilla luciferase* (*REN*) gene driven by the *35S* promoter in these constructs was used as the internal control to evaluate protoplast transfection efficiency. The isolation of protoplasts from leaves of 14-day-old etiolated B73 seedlings, the transformation of constructs into the protoplasts using polyethylene glycol–mediated transformation, the culturing of protoplasts, and detection of the LUC signal were carried out as described (*50*). Relative LUC activity was calculated by normalizing LUC activity to REN activity. Five biological replicates were assayed for each construct.

Overexpression of *KRN2* in maize

The full-length coding sequence of *KRN2* was amplified from NIL-*KRN2*^{B73} and NIL-*KRN2*^{teosinte} cDNA and cloned into vector pBCXUN that had been cleaved with *Xcm*I under the constitutive *ubiquitin* promoter to produce constructs *Ubi*::*KRN2*^{B73} and *Ubi*::*KRN2*^{teosinte}. The constructs were introduced into *Agrobacterium* strain EHA105 and transformed into immature embryos of inbred line LH244 through an *Agrobacterium*-mediated transformation system. The transgenic lines were generated at Center for Crop Functional Genomic and Molecular Breeding of China Agricultural University. The genotypes were confirmed by PCR, and *KRN2* expression was quantified by qPCR. The primers used for vector construction (*KRN2*-B73-OE and *KRN2*-MT-6-OE), genotyping (*KRN2*-QRT) and qPCR (*KRN2*-QRT) are listed in table S10.

Nucleotide diversity and molecular evolution of *KRN2* and *OsKRN2*

To determine whether the *KRN2* or *OsKRN2* locus has undergone molecular evolution, the ~2.0-kb promoter and 5'UTR and full-length *KRN2* coding sequence were sequenced in a set of 34 *parviglumis* accessions, 39 maize landraces, and 69 maize inbred lines (table S5), while 59 *rufipogon*, 44 *japonica*, and 65 *indica* accessions (table S5) were used to resequence the ~1,100-bp region upstream of the *OsKRN2* start codon. PCR products from maize inbred lines and cultivated rice were directly sequenced, whereas those from *parviglumis* accessions, maize landraces, and *rufipogon* accessions were cloned into a vector using the pEASY-T5 Zero Cloning kit (TransGen), and one clone per PCR product was randomly chosen for sequencing. The primers used for genotyping *KRN2* (*KRN2*-SEQ-1 to *KRN2*-SEQ-5) and *OsKRN2* (*OsKRN2*-SEQ) are listed in table S10. Nucleotide diversity (π) and Tajima's D-statistic were calculated using DnaSP version 5.0 (*52*). To further test whether the observed loss of genetic diversity in maize relative to that in teosinte could be explained by a domestication bottleneck alone, coalescent simulations that incorporated the domestication bottleneck (*53*, *67*, *68*) were performed for the regions of *KRN2* that were sequenced.

Subcellular localization

The coding sequences of *KRN2* and *DUF1644* were amplified from B73 using

gene-specific primers (*KRN2*-EGFP and *DUF1644*-EGFP, table S10) and introduced between the *Hin*dIII and *Bam*HI enzyme sites of the pGreenII-GFP vector to produce constructs *Ubi*::*KRN2-GFP* and *Ubi*::*DUF1644-GFP*, respectively. The isolation of protoplasts and transformation of cells with constructs were performed as described (*50*). The protoplasts were cultured at 22°C in the dark for 12–18 h, and GFP fluorescence was quantified with confocal microscopy (Zeiss).

Yeast two-hybrid (Y2H) assay

For Y2H screening, the ULTImate Y2H was performed by Hybrigenics Services (http://www.hybrigenics-services.com) using the full-length KRN2 protein from B73 as bait against a cDNA library prepared from maize developing ear/tassel inflorescences. The full-length coding sequence of *KRN2* was cloned into pB66 as an N-terminal fusion to GAL4. A total of 95.9 million clones were screened, and a total of 153 positive colonies were selected on medium lacking leucine (Leu), tryptophan (Trp), and histidine (His) and supplemented with 20 mM 3-aminotriazole (3-AT) (Sigma). The prey fragments of the positive clones were amplified by PCR and sequenced at their 5' and 3' junctions. The resulting sequences were used to identify the corresponding interacting proteins in GenBank. A confidence score (predicted biological score) was attributed to each interaction as described (*69*). The six candidate interactors with high confidence scores are listed in table S2.

To validate the interaction between KRN2 and its candidate interactor DUF1644, we cloned the full-length *KRN2* and *DUF1644* coding sequences into vectors pGBKT7 and pGADT7 using primers *KRN2*-BD and *DUF1644*-AD (table S10), to generate constructs BD-KRN2 and AD-DUF1644, respectively. These two constructs were cotransformed into the yeast strain Y2H Gold. Y2H assays were performed using the Matchmaker Gold Yeast Two-Hybrid System (Clontech). The resulting transformants with appropriate positive and negative controls were spotted on SD (–Trp/–Leu) medium containing 20 mM 3-AT to check for growth in the absence of selection. The transformants were then spotted on SD (–Trp/–Leu/–Ade/–His) selection medium containing 20 mM 3-AT. Plates were incubated at 30°C for 3 days to observe yeast growth. Similar methods were performed for vector construction and transformation of BD-OsKRN2 and AD-OsDUF1644, except that 3-AT was not used in the SD medium. The primers used for constructing BD-OsKRN2 (*OsKRN2*-BD) and AD-OsDUF1644 (*OsDUF1644*-AD) vectors are listed in table S10.

Split firefly luciferase (LUC) complementation assay

The split firefly LUC complementation assays were performed to examine the interactions between KRN2 and DUF1644 using constructs JW771 (nLUC) and JW772 (cLUC) (*51*). The full-length coding sequences of *KRN2* and *DUF1644* were amplified using primers *KRN2*-nLUC and *DUF1644*-cLUC (table S10), and cloned into JW771 and JW772, respectively, to generate *35S*::*KRN2-nLUC* and *35S*::*cLUC-DUF1644*, respectively. The fused constructs were transformed into *Agrobacterium* strain GV3101 and co-transformed into tobacco (*Nicotiana benthamiana*) leaves. After 3 days of growth, luciferin (1 mM) was injected into tobacco to activate LUC, and the

fluorescence signals were observed by the Chemiluminescent Imaging System (Tanon-5200). Similar methods were used to construct *35S*::*OsDUF1644-nLUC* and *35S*::*cLUC-OsKRN2* and co-transform into the tobacco leaves. The primers used to amplify the full-length coding sequences of *OsKRN2* (*OsKRN2*-cLUC) and *OsDUF1644* (*OsDUF1644*-nLUC) are listed in table S10.

Inflorescence meristem (IM) imaging and measurements

The IM isolated from fresh tissue was imaged with a scanning electron microscope (S-3000N, Hitachi). Samples were dissected and mounted on a stub. Imaging was performed under vacuum using 4-kV accelerating voltage and a secondary electron detector. The IM diameter was measured with an EZ4 HD stereo microscope (Leica) and corresponding LAS EZ software. The diameter was measured in at least 20 plants for each genotype.

Phylogenetic analysis of KRN2, DUF1644, and their orthologs

Amino acid sequences of KRN2 orthologs were obtained for *Arabidopsis* (AT5G53500, AT5G24320, AT1G64610, AT5G42010), rice (Os04g0568400 in *japonica* and BGIOSGA016939 in *indica*), sorghum (SORBI_3006G182500), foxtail millet (SETIT_009524mg), and wheat (TraesCS2A02G402000) (Gramene, http://www.gramene.org/). Similarly, for DUF1644 orthologs, amino acid sequences were obtained for *Arabidopsis* (AT4G08460, AT1G77770, AT1G68140), rice (Os02g0566500 in *japonica* and BGIOSGA006228 in *indica*), sorghum (SORBI3004G185600), foxtail millet (SETIT017622mg), and wheat (TraesCS3A02G128000) (Gramene). These amino acid sequences were aligned by ClustalW, and a phylogenetic tree was constructed using the neighbor-joining method in MEGA version 6.0 (*70*) with 1,000 bootstraps.

Minimum spanning tree

A set of 59 *rufipogon*, 44 *japonica*, and 65 *indica* accessions (table S5) was used to construct a minimum spanning tree for *OsKRN2*. The polymorphic sites in the ~1,100-bp region upstream of the *OsKRN2* start codon were extracted from the aligned sequences for nucleotide diversity analysis using TASSEL version 5.0 (*62*). Next, Arlequin version 3.5 (*54*) was used to define the haplotypes and construct the minimum spanning tree among haplotypes. Arlequin's distance matrix output was used in HapStar version 0.6 (*71*) to draw the minimum spanning tree.

Transgenic functional validation of *OsKRN2*

To generate the overexpression construct, the full-length *OsKRN2* coding sequence was amplified from the *japonica* cultivar Nipponbare and cloned into vector pCUbi1390 that had been cleaved with *Kpn*I and *Bam*HI to produce *Ubi*::*OsKRN2*. The construct was introduced into the mature embryo-derived callus of Nipponbare via *Agrobacterium*-mediated transformation. The genotypes were confirmed by PCR, and the enhanced expression of *OsKRN2* was confirmed by qPCR. All plants were cultivated in the transgenic experimental field of China Agricultural University in

Beijing and Huazhong Agricultural University in Wuhan, China. The primers used for vector construction (*OsKRN2*-OE), genotyping (*OsKRN2*-CR) and qPCR (*OsKRN2*-QRT) are listed in table S10.

CRISPR-Cas9 gene editing and genotyping

The CRISPR-Cas9 knockout constructs for *KRN2*, *DUF1644*, and *OsKRN2* were designed to produce defined deletions in the first exon using two, one, and one guide RNAs (table S10), respectively, together with the *Cas9* endonuclease gene. *Agrobacterium*-mediated transformation was carried out with the aforementioned methods. The gene-specific primers (*KRN2*-CR, *DUF1644*-CR, and *OsKRN2*-CR for *KRN2*, *DUF1644*, and *OsKRN2*, respectively; table S10) were designed to amplify the DNA fragments of target genes encompassing the guide RNA–targeted sites in transgenic T_1 plants, and PCR products were sequenced to confirm their genotypes.

To test for off-target effects of gene-edited mutations, genomic DNA was extracted from the seedling leaves of two *KRN2*-edited plants, two *DUF1644*-edited plants, and one wild-type plant in maize, and three *OsKRN2*-edited plants and one wild-type plant in rice. All samples (accession number in NCBI: PRJNA771523) were genotyped by paired-end (150-bp) sequencing on the Illumina NovaSeq platform (Novogene, Tianjin, China). The average sequencing data for each plant was 16.2 Gb in maize and 3.0 Gb in rice, with the average depth being 7.7× in maize and 8.1× in rice (table S12). Fastp version 0.22 (https://github.com/OpenGene/fastp) was used to filter low-quality bases according to the following criteria: (i) low-quality bases (quality score < 20) were removed from both ends of the reads; (ii) then, the sliding window trimmer was used to remove low-quality sequences at the 3' end, using an average quality score of 20 over four bases; and (iii) reads with > 20% unqualified bases were further filtered. The clean reads in maize and rice were mapped to the B73 reference genome version 4.0 (*30*) and the Nipponbare reference genome IRGSP-1.0 (*33*) using Bowtie2 version 2.4.4 (*72*), respectively. The mean genome mapping ratio of the reads was ~98.0% in both maize and rice, and the average genome coverage was 90.3% and 97.7%, respectively. SAMtools version 1.9 (*73*) was used to sort the BAM files. The unique mapping reads were used for variant calling using Genome Analysis Toolkit (GATK version 4.2) (https://software.broadinstitute.org/gatk/). Low-quality variants were filtered using bcftools version 1.9 (http://github.com/samtools/bcftools). The following filter criteria was used for single-nucleotide variants (SNVs): "QUAL < 30.0 || QD < 2.0 || MQ < 40.0 || FS > 60.0 || SOR > 3.0 || MQRankSum < -12.5 || ReadPosRankSum < -8.0 || FORMAT/DP < 5". The filtering criteria for InDels was as follows: "QUAL < 30.0 || QD < 2.0 || FS > 200.0 || ReadPosRankSum < -20.0 || FORMAT/DP < 5". Subsequently, the SNVs and InDels identified by whole-genome sequencing in gene-edited plants were compared with the off-target mutations predicted by using the Cas-OFFinder tool (http://www.rgenome.net/cas-offinder/). None of the variants in the seven gene-edited plants concurred in the predicted off-target sites (table S12).

Field trials of the gene-edited plants

Gene-edited plants, together with their wild-type plants, were used for field trials

that were carried out in a randomized block design with three replicates. For maize, *CR-krn2-1*, *CR-krn2-2*, and wild-type plants were grown in three locations, Bayan Nur (40.7°N, 107.5°E), Tieling (41.5°N, 123.2°E), and Sanya (18.2°N, 109.1°E), China, in 2018 and 2019. Each genotype was planted in a four-row plot, and rows were 0.5 m apart, with a planting density of 63,000 plants/ha. All plants were open-pollinated, 12 important agronomic traits were investigated after pollination, and 14 grain yield–related traits were assessed after harvest (table S3). For the measurement of grain yield in a plot, 26–38 ears were quantified in each plot, and 25–58 plants were measured for the remaining agronomic traits. For rice, *CR-oskrn2-1*, *CR-oskrn2-2*, and wild-type plants were planted in Wuhan (30.5°N, 114.4°E), China, in 2020. Each genotype was planted with 20 × 30 cm spacing under standard paddy conditions. Agronomic traits were assessed at maturation, and yield-related data were collected after harvest. For the measurement of grain yield per plant, 19–21 plants were quantified in each plot, and 19–30 plants were measured for the remaining agronomic traits.

Candidate-gene association mapping

KRN2-based association mapping was performed using a subset of 379 maize inbred lines (table S4) (*49*). SNPs in the promoter region and full-length *KRN2* were extracted from the published resequencing data (table S4) (*74*). An ~1,200-bp fragment in the promoter and 5'UTR regions was sequenced in 379 inbred lines using primers *KRN2*-SEQ-2 (table S10), and the polymorphic sites including SNPs and InDels were extracted using TASSEL version 5.0 (*62*). The associations between all polymorphic sites with minor allele frequency (MAF) ≥ 0.05 and KRN were analyzed using a mixed linear model (*48*) in TASSEL version 5.0 (*62*) considering population structure and the kinship matrix, which was conducted with ADMIXTURE version 1.3.0 (*55*) and TASSEL version 5.0 (*62*), respectively. A Bonferroni adjusted significance threshold ($P < 0.01/40 = 2.5 \times 10^{-4}$) was used to identify significant associations.

Genotyping and SNP calling of plant materials used for genome-wide selection analysis

In maize and *parviglumis*, ~65 million SNPs were download from ZEAMAP database (http://www.zeamap.com/ftp/02_Variants/PAN_Zea_Variants/SNPs/). Whole-genome resequencing and SNP calling were carried out as previously described (*74*). In brief, 507 maize inbred lines and 70 *parviglumis* accessions were genotyped by paired-end (150-bp) sequencing on the Illumina HiSeq3000 platform (BGI, Shenzhen, China). Trimmomatic version 0.33 (*75*) was used to trim reads containing adaptor sequences and low-quality bases according to the following criteria: (i) low-quality bases (quality score < 3) were removed from both ends of the reads; (ii) then, the sliding window trimmer was used to remove low-quality sequences at the 3' end, using an average quality score of 15 over four bases; and (iii) reads < 36 bp were further filtered. Filtered reads were mapped to the B73 reference genome version 4.0 using Bowtie2 version 2.1.0 (*72*) (--very-fast), and variants were called with SAMtools version 1.3.1 (*73*) and GATK version 3.5 (https://software.broadinstitute.org/gatk/).

In the cultivated and wild rice, the high-depth sequencing dataset of 534 *sativa* and 228 *rufipogon* accessions are accessible from the published data: 400 *sativa*

accessions were from the public 3000 Rice Genomes Project (*76*); 186 *rufipogon* accessions (accession number in NCBI: PRJNA657701) (*77*), and 134 *sativa* and 42 *rufipogon* accessions (accession number in NCBI: PRJNA407820) (*8*) are from the published data. In addition, to enrich the genetic diversity of wild rice, 80 more *rufipogon* accessions (accession number in NCBI: PRJNA771230) (table S5) were genotyped by paired-end (150-bp) sequencing on the Illumina NovaSeq platform (Novogene, Tianjin, China). In all sequenced cultivated and wild rice accessions, the SNPs from 400 *sativa* accessions were accessed from the published 3000 Rice Genomes Project (https://aws.amazon.com/public-data-sets/3000-rice-genome/) (*76*), and SNPs of the remaining 134 *sativa* accessions and 308 wild relatives were recalled using the same method as that used for the 3000 Rice Genomes Project (*76*). In brief, filtered reads were mapped to the reference genome IRGSP-1.0 using BWA-MEM version 0.7.17 (r1188) (*78*). Duplicated reads were masked by using picard version 1.119 (http://broadinstitute.github.io/picard/), and variants were called using GATK version 3.5 (-glm BOTH -mbq 20 -genotyping_mode DISCOVERY -out_mode EMIT_ALL_SITES) (https://software.broadinstitute.org/gatk/). To correctly infer the genetic relationships among all rice accessions used in our study, the SNPs of a published low-depth sequencing dataset of 1,082 *sativa* and 446 *rufipogon* accessions (accession numbers in EBI: ERP001143, ERP000729, and ERP000106) (*3*) were recalled using the same pipeline. Taken together, ~111 million bi-allelic SNPs in all collected cultivated and wild rice accessions (https://ngdc.cncb.ac.cn/gvm/getProjectDetail?Project=GVM000285) were filtered via VCFtools version 0.1.13 (--min-alleles 2 --max-alleles 2 --remove-indels) (*79*) for subsequent analysis.

Genetic structure in the genus *Oryza*

Together with the recalled SNPs from the study of Huang *et al*. (*3*), the hierarchical population structure of all cultivated and wild rice accessions was estimated using ADMIXTURE version 1.3.0 (*55*), which implemented a structure-based model of the maximum likelihood clustering algorithm. The accessions or varieties with membership probabilities of ≥ 0.60 were assigned to corresponding groups, and accessions or varieties with probabilities of < 0.60 were assigned to a mixed group. The reanalyzed genetic structure assigned all cultivated and wild rice accessions to the groups defined in Huang *et al*.'s study (*3*). Using 292,444 SNPs filtered by PLINK version 1.9 (*80*) with "--geno 0.75 --maf 0.05 --biallelic-only --snps-only --indep-pairwise 50 10 0.1", we classified these cultivated and wild rice accessions into three main groups containing *rufipogon* (n = 257 accessions), *indica* (n = 208 accessions), and *japonica* (n = 253 accessions). The 257 *rufipogon* accessions were further classified into three main subgroups: Or-I (n = 26 accessions), Or-II (n = 107 accessions), and Or-III (n = 124 accessions) (table S5). The inferred genetic relationships were confirmed by PCA (fig. S17C) that were conducted with the same SNPs by using GCTA version 1.26 (*56*). Specifically, one *rufipogon* accession (21DX370) was corrected to an *indica* accession, and 74 *sativa* and 50 *rufipogon* accessions were re-classified into mixed groups and were not used for subsequent phylogenetic tree construction and genome-wide selection

analysis. As a consequence, the rice accessions used for subsequent analysis comprise 366 *sativa* accessions from the 3000 Rice Genomes Project (*76*), 153 *rufipogon* accessions from Zheng *et al*.'s study (*77*), 94 *sativa* and 42 *rufipogon* accessions from Wang *et al*.'s study (*8*), and 1 *sativa* and 62 *rufipogon* accessions resequenced in the current study (table S5).

Phylogenetic tree construction

Phylogenetic trees of maize and rice were constructed by using the SNPhylo version 20180901 pipeline, which indicates evolutionary relationships among populations (*58*). The resulting SNP alignment for phylogenetic tree construction was available on the Figshare repository (*57*). Before tree construction, we filtered the SNPs with MAF < 0.01 and missing rate > 0.5 from ~65 million SNPs in maize and ~111 million SNPs in rice. In total, 23,642,849 SNPs in maize and *parviglumis*, and 14,455,996 SNPs in *sativa* and *rufipogon* were ultimately selected for the SNPhylo pipeline. iTOL version 6 (*81*) was used to visualize the trees.

Identification of regions and genes that have undergone selection

Genomic regions under selection should have significantly lower diversity and altered allele frequencies in cultivated as compared with wild accessions. Thus, we identified the selected regions using ~65 million SNPs in maize (table S5) (*74*) and ~71 million SNPs (after removing all accessions from Huang *et al*.'s study) in rice (table S5) (*8*, *76*, *77*) via a cross-population composite likelihood ratio (XP-CLR) method, which is based on modeling the likelihood of multi-locus allele frequency differentiation between two populations (*29*), followed by cross-validation on the basis of permutation tests for the ratio of nucleotide diversity between wild and cultivated accessions in the corresponding regions = (*2*, *57*). The nucleotide diversity of cultivated and wild accessions was calculated using VCFtools version 0.1.13 (*79*). The regions with the top 10% XP-CLR scores were set as the candidate selection regions. Then a more stringent criterion was applied for identification of selected regions via filtering out the regions in which the ratio of nucleotide diversity between wild and cultivated accessions was lower than the median ratio observed from 1,000 randomly picked windows of the same size (*2*). In maize, the XP-CLR analysis was performed by comparing 110 randomly selected maize inbred lines (table S5) to *parviglumis* with a 0.5-cM sliding window and a 1-kb step size. Genetic distances between SNPs were interpolated according to their physical distances in an ultra-high-density genetic map from a maize-teosinte population (*82*), with physical distances being converted to B73 version 4.0 by CrossMap (*83*). The nucleotide diversity ratio between *parviglumis* and maize was calculated based on a 1-kb region. In rice, we carried out the XP-CLR analysis and nucleotide diversity ratio assessment with a 0.005-cM sliding window and a 300-bp step size by comparing *japonica*, *indica* (50 accessions randomly selected from 208 *indica* in table S5), and *sativa* with Or-III, Or-I, and *rufipogon*, respectively (*3*). For XP-CLR analysis, the genetic distance was converted by using the genetic map from a Zhengshan97 and Minhui63 RIL population (*84*). To identify genes that have undergone selection, we extracted the

physical regions of all annotated genes in maize and rice from the annotation files of B73 version 4.36 from the Gramene database and IRGSP-1.0_2019-06-26 from the rice annotation project database (RAP-DB; https://rapdb.dna.affrc.go.jp/index.html), respectively. The genes that are located within the selected regions were regarded as having undergone selection. For genes that were previously shown to have undergone selection (table S7), we also regarded them as selected genes if a selected region located in the up/downstream intergenic regions of these genes and did not overlap with adjacent genes.

Identification of orthologs under convergent selection

To identify the global orthologous genes in the maize and rice genome, we downloaded the protein sequence of maize (B73, version 4.36) from the Gramene database and that of rice (IRGSP-1.0_2019-06-26) from the RAP-DB. The maximum-length protein sequence for each gene was selected for sequence comparisons with a custom script (*57*). The maize and rice orthologs were identified utilizing reciprocal blastp (version 2.81), and the protein sequences with coverage ≥ 0.7 were deemed orthologous genes. We identified a total of 10,516 orthologous gene pairs between maize and rice, and then compared all identified selected genes in both maize and rice within these 10,516 orthologous gene pairs. We regarded that subset of selected gene pairs as genes that have undergone convergent selection. Collinearity analysis was conducted by MCScanX (*59*) with blastp (version 2.8.1; -evalue 1e-10; -num_alignments 5 -outfmt 6) using the maximum-length transcripts in maize and rice as input. Our null hypothesis is that each gene in maize and rice has the same possibility of undergoing selection without any constraints. Using a permutation test repeated 1,000 times, we randomly picked 3,163 genes from 39,398 maize genes (B73 version 4.0) (*30*) and 18,755 genes from 45,969 rice genes (IRGSP-1.0) (*33*) and recoded the number of randomly chosen gene pairs that belong to the 10,516 ortholog pairs. Then we sorted the resulting number of gene pairs in each of the 1,000 permutations from largest to smallest, and we found that the number of observed gene pairs under convergent selection (n = 490) was greater than the largest number (n = 393) from the permutation tests, which means that the gene pairs that were candidates for having undergone convergent selection between maize and rice were statistically unlikely to be a random occurrence ($P < 0.001$). Consequently, we rejected the null hypothesis that each gene in maize and rice has the same probability of having undergone selection without any constraints.

KEGG enrichment analysis of selected genes

An enrichment analysis of KEGG pathways (KEGG FTP Release 2021-05-03) (*85*) was carried out for the 490 pairs of orthologous genes under convergent selection using g:Profiler version e104_eg51_p15_3922dba (*60*) following a published protocol (*86*). Statistical significance for pathway enrichment was auto-calculated via the g: Profiler g:SCS algorithm for multiple-testing correction. The g:SCS threshold ($P < 0.05$) suggested by g:Profiler was used for the multiple-testing correction. For the maize genome, we used version Zm-B73-REFERENCE-NAM-5.0, and the gene

IDs from version 4.0 were converted to version 5.0 on MaizeGDB (https://www.maizegdb.org/). For the rice genome, we used IRGSP-1.0. Only the genes with at least one annotation were considered in the reference background.

Statistical analysis

An unpaired two-tailed Student's *t* test was used to compare the differences in gene expression levels (Fig. 1F and fig. S4), LUC activity (Fig. 1H), and tested traits (Figs. 1E, 2, C and E, 4, B and D, and figs. S1, S2D and S10B) between two samples. A one-way analysis of variance (ANOVA) followed by Tukey's multiple comparison test was used to compare the differences in gene expression levels (Fig. 3H and fig. S5C) and tested traits (Fig. 3, F and I, and figs. S5D, S9, C and D, S10C, S13, S15 and S16, B to M) among three or more samples. Both the two-tailed Student's *t* test and ANOVA were carried out in Microsoft Excel.

Tajima's D test presented in DnaSP version 5.0 (*52*) was used to test whether *KRN2* experienced direct selection during maize domestication (fig. S6). In addition, a coalescent simulation (1,000 random permutations) was used to determine whether the observed loss of *KRN2* genetic diversity in maize relative to that in teosinte could be explained by a domestication bottleneck alone (fig. S6). Coalescent simulations were performed for each region using the MS program (*53*). All parameters in the model were assigned to previously established values (*67*, *68*).

A permutation test after XP-CLR, as described above, was carried out to identify the selected regions on a genome-wide scale. The regions that had the top 10% of XP-CLRs and for which the nucleotide diversity ratio between wild and cultivated accessions was higher than the median observed from 1,000 randomly picked windows of the same size were regarded as selected regions. We also used a permutation test to determine whether the convergent selection was enriched on a genome-wide scale (Fig. 5E). To assess the significance of the convergent selection, we compared the real data to randomly selected data, as described above. The custom scripts for these permutation tests can be accessed from the Figshare repository (*57*).

The g: Profiler g:SCS algorithm, as described above, was performed for multiple-testing correction of the enrichment test of KEGG pathways for the 490 pairs of orthologous genes under convergent selection (Fig. 5F).

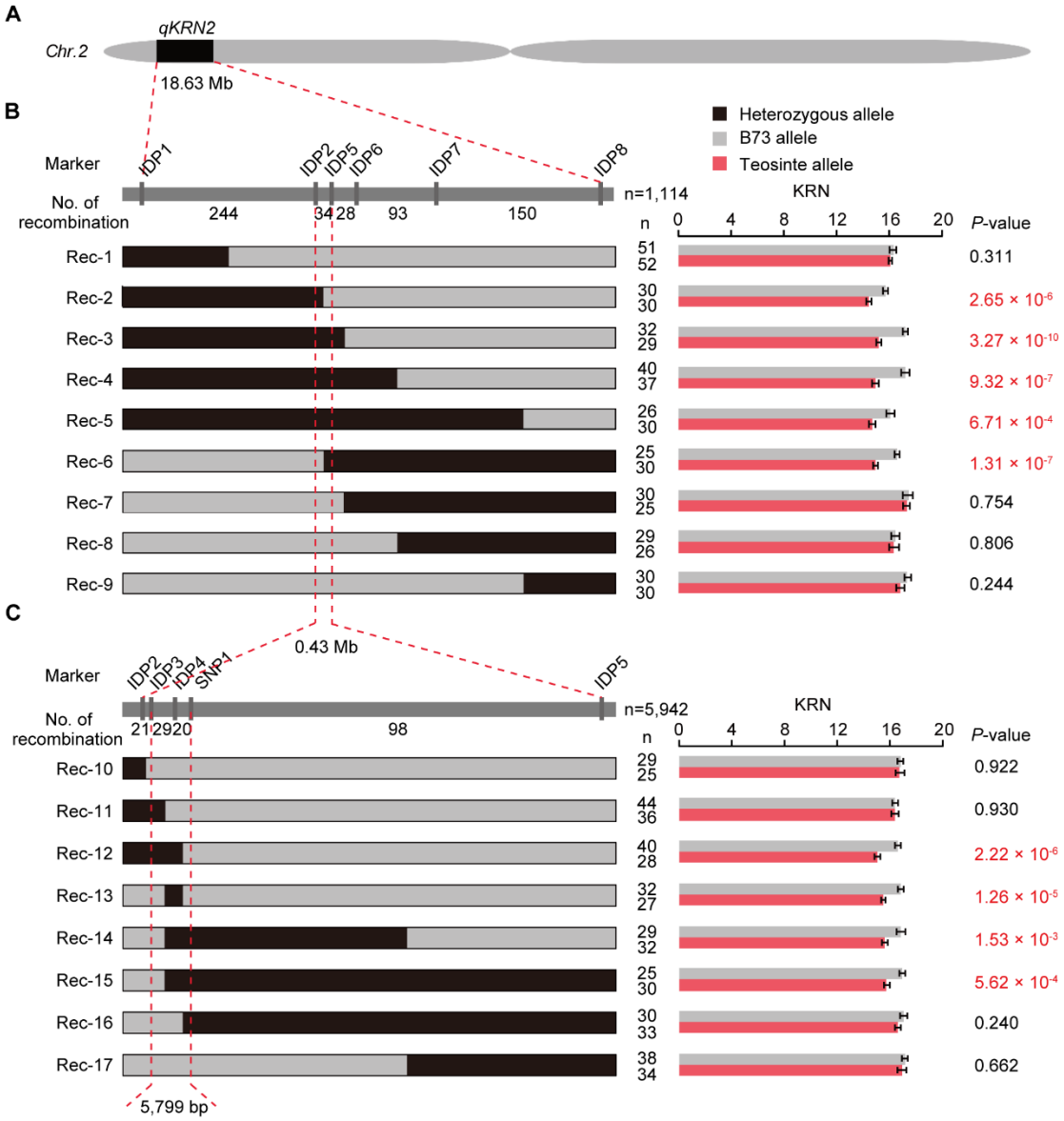

Fig. S1 Fine mapping of *qKRN2*. (**A**) qKRN2 *was coarsely mapped between IDP1 and IDP8 on chromosome 2.* (***B***) qKRN2 was *fine mapped to a 0.43-Mb genomic region flanked by markers IDP2 and IDP5 using 1,114 individuals of* a BC_5F_2 population *and* (***C***) *very fine mapped to a 5,799-bp genomic region flanked by markers IDP3 and SNP1 using 5,942 individuals of* a BC_6F_2 population. Graphical genotypes of different heterozygous recombinant types are shown on the left, and the phenotypes of their self-pollinated homozygous progenies are shown on the right. The vertical gray lines represent the positions of molecular markers *in the* qKRN2 *region. The number of recombinants between two markers is shown below the graphical* qKRN2 *region. In each bar, the gray-filled space represents alleles homozygous for B73, whereas the black-filled space represents heterozygous alleles.* The red vertical dashed lines show the boundary of the fine-mapped interval of *qKRN2*. *One representative family per recombinant type is shown for comparison of KRN between the* self-pollinated homozygous recombinant and nonrecombinant progenies. *The data for KRN represent the mean ± s.e.m.;* P *values were determined by the two-tailed Student's* t *test.*

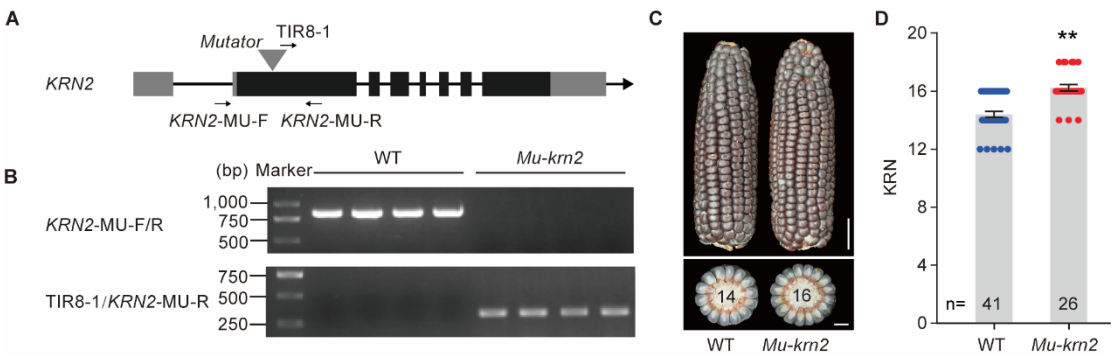

Fig. S2 Knockout of *KRN2* increases KRN. (*A*) Position of *Mutator* transposon insertion in *KRN2* of *Mu-krn2*. Black shading, exons; gray shading, UTRs. The triangle indicates the site of *Mutator* insertion. *KRN2*-MU-F and *KRN2*-MU-R were the primers flanking the *Mutator* insertion, and TIR8-1 was used as a forward primer located at the end of *Mutator*. (*B*) PCR assays of the *Mutator* insertion in wild type (WT) and *Mu-krn2*. (*C*) Ear performance of WT and *Mu-krn2*. Scale bars: 2 cm for the ears, and 1 cm for the ear transverse sections. (*D*) Quantification of KRN between WT and *Mu-krn2*. *The data for KRN represent the mean ± s.e.m.; the* P *value was determined by the two-tailed Student's* t *test.* $^{**}P < 0.01$.

```
B73 GAGAATTAAAATATCTGGCGGACAAAACTAGATGCTTGCCGCCCCATCTTTTAGAAGGAAAAAAAG 66
Teo GAGAATTAAAATATCTGGCGGACAAAACTAGATGCTTGCCGCCCCATCTTTTAGAAGGAAAAAAA- 65

B73 AAAGAAAAGAAAGCAGTGGACACCTGATCAACTACCGAGCCTGCTTCGGTGCCGTGACCGGGAAAT 132
Teo AAAGAAAAGAAAGCAGTGGACACCTGATCAACTACCGAGCCTGCTTCGGTGCCGTGACCGGGAAAT 131

B73 CTTTCGGAGCAGGAGGAGGCTCTCCGTGTCCGTACGTCCCAACGGAGGTGGTAGACCGA------G 192
Teo CTTTCGGAGCAGGAGGAGGCTCTCCGTGTCCGTACGTCCCAACGGAGGTGGTAGACCGAGACCGGG 197

B73 ACGCCGGATAAGTCTAAGGACGAAATTTAGTGACCAGAGATTACGAGAGGATCGAGGGATTAAAAA 258
Teo ACGCCGGATAAGTCTAAGGACGAAATTTAGTGACCAGAGATTACGGGAGGATCGAGGGATTAAAGA 263

B73 GAAATAAACTACCCTTTAATCCTCTAATCCTCTTGTAATCTCGTTGTCACCAAATCAACCAGCTGG 324
Teo GAAATAAACTACCCTTTAATCCTCTAATCCTCTCGTAATCTCGTTGTTACCAAATCAACCAGCTGG 329

B73 TAAACCTCCCTTCCCTCCCAGGCTCCCAGCAGAGAGCAGCAGCTTTCGTGCAAAGATGGGCACGTG 390
Teo TAAACCTCCCTCCCCTCCCAGGCTCCCAGCAGAGAGCAGCAGCTTTCGTGCAAAGATGGGCACGTG 395

B73 GATAAAATAGATATAAACAAAACACAAAGGCTTGGACG-------------------CATGGGGTT 437
Teo GATAAAATAGATATAAACAAAACACAAAGGCTTGGACGCAGGAGAGTCGCGTACATCCATGGGGTT 461

B73 GCTGCCGTGCCGCC------CTCGCGCTCGCGTTGCCATCTTCGCCCAACCACGAATCAACTCTGG 497
Teo GTTGCCGTGCCGCCCTCGCGCTCGCGCTCGCGTTGCCATCTTCGCCCAACCACGAATCAACTCTGG 527

B73 AGCTGCAGGGTTGTTGGGGTTAGCTAGAGATGGATACGTCGTCCATGC----ATCTGCTCATGCAT 559
Teo AGCTGCAGGGTTGTTGGGGTTAGCTAGAGATGGATACG-CGTCCATGCATCTATCTGCTCATGCAT 592

B73 ATCCAGCTGGGTTCTTTAAACTAGCGG------ACGTACAGCTCGAATCTACGTACTTAGCCCATT 619
Teo ATCCAGCTGGGTTCTGTAAACTATTGGACGTACACGTACAGCTCGAATCAACGTAC--------TT 650

B73 ATCAGCACCTATCTTTGTGTTTTTTTCCCCAGTCTGCTCACTCATGTATCAAAAGCCACCACACAT 685
Teo ATCAGCACCTATCTTTGTG-TTTTTTCCCCAGTCTGCTCACTCATGTAGCAAAAGCCACCACACAA 715

B73 GCAGAGCAGGTGGCTGCGTTCCATGCATGCAGAGTTTTTTTTAACGTCACTGCTGACCGATGCGTC 751
Teo GCAGAGCAGGTGGCTACGTTCCACGCATGCAGAG--TTTTTTAACGTCACTGCTGACCGAT----- 774

B73 TTTAGGGCCCGTATGTAATCCAGCTTATTTTATATAAATTATATAATCTGGATTGTGTAATCTAGT 817
Teo -----------------------GCTTATTTTATATAAATTATATAATCTGGATTTTACAATCTAGT 818

B73 TTATATAATCCTATTACAGATGTTTGTTTACATAAATTATTAGTAGATAAAAAGCTAAACAATAAT 883
Teo TTATATAATCCTATTAGAGATGTTTGTTTACATAAATTATTAGTGGGCAAAAAGCTAAACAATAAT 884

B73 CTAAAAT-AAGCATCTACTAATTTATTTATGAATTATCATAACCTAGACATCTAGATTATATAATT 948
Teo CTAGAATAAAGTATCTAAGTACTTGTTTATGGATTATCATAATCTAG-CACCTATATTATGTAATT 949

B73 CACTCCAATACCTAGAGCCGGCTAGCCGCTGCAACGACTGTT----AATAAATAAATAAATTCCCT 1010
Teo CACTCCAATACCTAGAGCCGGCTAGCCGCTGCGACGACTGTTCATAAATAAATAAATAAATTCCCG 1015

B73 CGTCCAAAAAGGGCTGGAATTGATGCAGGCTAAAATCAAAATGCTCGGCACTACTGACCGTCTGAC 1076
Teo CGTCCTAATAGGGCTGGAATTGATGCAGGCTAAAATCAAAATGCTCGGCACTA--------CTGAC 1073

B73 CCGAA----CACAGACAGAGCAGCAGCCCCAGCTGACGGGTTGACCCAGACCGAGTCGCCACTCGC 1138
Teo CCGAAAAAGCACAGACAGAGCAGCAGCCCCAGCTGACGGGTTGACCTAGACCGAG-------TCGC 1132

B73 CAACAAGAGATCGAGCTCTGTGAAATAGTTTTGACGTGTTCCCGTTTTTTTTTTCTTTTTCTTGCG 1204
Teo CAACAAGGGATCGATCTCTGCGAAATAGTTTTGA-----------------------------CG 1168

B73 TGAATAGGTAAAAGAAGAAATCGCACCGCGCGCCTGCATCCTGCACCTGTACGCGCAAGGGG--GG 1268
Teo TGAATAGGTAAAAGAAAAATCGCAC--CGCGCCTGCATCCTGCACCTGTACGCGCAAGGGGGAGG 1232

B73 ACCAAGCAGCGGACGGCAGTAGCATGTTAGGTGCATCAAACTGTTCCCCTCCCCCGCTTTGATGAG 1334
Teo ACCAGGCAGCGGACGGCAGTAGCATGTTAGGTGCATCAAACTGTTCCCCTCCCCCGCTTTGATGAG 1298

B73 CGCCTTTGTTTGGCGCAACGCGAGCGCCCAGCCCAGCTAGTAATTTGCCGTTTCCAAGCAACACTT 1400
Teo CGCCTTTGTTTGGCGCAACGCGAGCGCCCAGCCCAGCTAGTAA-TTGCCGTTTCCAAGCAACGCTT 1363

B73 TGCAGCTGCAGAGCACACAACACAAGCTAGCTAGAGTCAGATTTGTGCCAAC-------------- 1452
Teo TGCAGCTGCAGAGCACACAACACAAGCTAGCTAGAGTCAGATTTGTGCCAACATATACATACATAC 1429

B73 ----ATACATATACATGTGTTCCCCCTTCGTCGCTGCTCAGAA-CCAACGGCAGGGATCGATCGTA 1513
Teo ATATATACATATACATGTGTT-CCCCTTCGTCGCTGCTCAGAATCCAACGGCAGAGATTGATCGTA 1494

B73 GTAGTAATCCTCCTACTCTCGTTCGTTCTGCCCAATGCAGAGCCGAGCAGTACTGTACTGTGCTGT 1579
Teo GTAGTAATCCT--GACTCTCGTTCGTTCTGCCCAATGCAGAGCCGAGTAGTACTGTGCTGTGCTGT 1558

B73 TTCTGTTACAATTCACTGCC---ACGACGAATGGCTCGTGTCGTGGCATGCAGGCCATGCGCCTGC 1642
Teo TTCTGTTACAATTTACTGCCACGACGACGAATGGCTCGT-------------GGCCATGTACCTGC 1611

B73 TGTTGCTAATGCTAACCTCAGCACATCGGTTTTCCACAGCAGAAAAAAAGATCTCTTTCTCTCTGC 1708
Teo TGTTGCTAATGCTAACCTCAGCACATCGATTTCCCACAGCAGAAAAAAAGATCTCTTTCTCTCTGC 1677

B73 GGAC-GGTCCTATCAGGCAAGGGTTACACGAGCAGATCGGTGTGCTGCAGCGCCGATGCACCCGGT 1773
Teo GGACGGGTCCTATCAGGCAAGGGTTACACGAGCAGATCGGTGTGCTGCAGCGCCGATGCACCCGGT 1743
```

```
B73 TGCAGTACGCATAGACCCAGGCCTAGACCTGCACGATTTATTGCCGCTGCTACTACAGCAGCTCAC 1839
Teo TGCAGTACGCATAGACCCAGGCCTAGACCTGCACGATTTATTGCCGCTGCTACTACAGCAGCTCAC 1809

B73 CACCTATTACTGCTACAAAACGACGACCGGAAGTGAGACGAAAAGGAGAGAAAAA--ACATACATA 1903
Teo CACCTATTACTGCTACAAAACGACGACCGAGAGTGAGACGAAAAGGAAAGAAAACATACATACATA 1875

B73 CCGAAGAACAGAAGAACAAAGGAAAGATAAAAAGAAAGGAAAGTGTGAGAGGCGTCATCAGAGGGT 1969
Teo CCGAAGAAAAGAAGAAC----------AAAGGAAAGTGTGAGAGGCGTCATCAGAGG-- 1922

B73 GTGAGATGAACCAACCCAGCAGCAAGAAATGAT---------------------------------- 2002
Teo GTGAGATGAACCAACCCAGCAGCAAGAAATGATTAAGGAGGTGTTTGGTTGCTCCTGCTAAAGTTT 1988

B73 ------------------------------------------------------------------
Teo AGTCCGAGTCACATCAAGCGTTTGATTTTTAAATAGGAGTATGAAATATAGACCCAACCAACTGGA 2054

B73 ------------------------------------------------------------------
Teo CTAGATTCGTCTCGTCTTTTAATATTCGGCTGACAAATTAGTTTTATAATCCGACTACATTTAATA 2120

B73 ------------------------------------------------------------------
Teo CTCGGAACGGAGGTTCAAACATTCGATGGGACAGGGGCTAAATTTTAGTTTGGGGTAACCAAACAC 2186

B73 ----TAAGAGGCAAGAGGCAAATCTGCGACAGTGCATTGTTTTAGCGGGAACTGTGCAGTATTTTC 2064
Teo CCCCTAAGAGGCAAGAGGCAAATCTGCGACAGTGCATTGTTTTAGCGGGAACTGTGCAGTATTTTC 2252

B73 CTCGTTTTTTTC---CCTCTGAGCAGCACAGTGCATCTTCAGAAATTTATTTTTGCGTCCGTCCTC 2127
Teo CTCGTTTTTTTCTTGCCTCTGAGCAGCACAGTGCATCTTCAGAAATTTATTTTTGCGTCCGTCCTC 2318
                                B73_TSS
B73 CAAATCTGGCGATGGTGATGGGGGACTCGGACGGGACTGGGACCCCCACACACCCAGCACGGCTGG 2193
Teo CAAATCTGGCGATGGTGATGGGGGACTCGGACGGGACTGGGACCCCCACTCACCCAGCACGGCTGG 2384
                                                    Teo_TSS
B73 CCAGCTCCTCTCCTCCTCCTCCT----CCGCCTCCCACGTCCGTCGTAAT-AAATCGCCCCGTCGT 2254
Teo CCAGCTCCTCTCCTCCTCCTCCTCCGCCCGCCTCCCACGTCCGTCGTAATAAAATCGCCCCGTCGT 2450

B73 CTCCAATTCCCCCCCTCCTCTCCTTTCTCCCCGCCCGCGTGAGATCGGCTCGAATCCAATCCTCTC 2320
Teo CTCCAATTCCCCCCCTCCTCTCCTTTCTCCCCGCCCGCGTGAGATCGGCTCGAATCCAATCCTCTC 2516

B73 CAATAATACGCACCGGCACCCATTTGCGCCATGCTGCCGCGGCCGGCCACCACGACGAGCCAAGAA 2386
Teo CAATAATACGCACCGCCACCCATTTGCGCCATGCTGCCGCGGCCGGCGACCACGACGAGCCAAGAA 2582

B73 CACGCGCGGCATCCCTGAGCCACCCACCCAGGCT--TACCAAAACGGATTCCTTTTCCCTCTTGGA 2450
Teo CACGCGCGGCATCCCTGAGCCACCCACCCAGGCTGCTACCAAAACGGATTCCTTTTCCCTCTTGGA 2648

B73 TCCCAGCCGCTCCCAAGCGTGCGCGCGAATTCTCTGCTTGCCTCGCCCAGGTGAGCTTCTCCCCCC 2516
Teo TCCCAGCCGCTCCCAAGCGTGCGCGCGAATTCTCTGCTTGCCTCGCCCAGGTGAGCTTCTCCCCCC 2714

B73 ACCCCCCACCCCTGCCATCAGTTTCTTCCTTTTCTAATCCCTCATTATTCCCCCTCTACCATCATC 2582
Teo ACCCCCCACCCCTGCCATCAGTTTCTTCCTTTTCTAATCCCTCATTATTCCCCCTCTACCATCATC 2780

B73 AATCAATCTATTGGTTTCGACGAGATATGTGGTGGTGAATTCGGCGGGTCTTGAGAGGGGGAAGGG 2648
Teo AATCAATCTATTGGTTTCGACGAGATATGTGGTGGTGAATTCGGCGGGTCTTGAGAGGGGGAAGGG 2846

B73 ATTTTTAAAAAAAAAACCCTGAAATTTTGTCAGCGGTTCCTTGGCCTGGCTGCCCGCTTTAATAAT 2714
Teo ATTTTTTAAAAAAAAACCCTGAAATTTTGTCAGCGGTTCCTTGGCCTGGCTGCCCGCTTTAATAAT 2912

B73 GGCCGCGCGGCTGGTTGGCTTGCCAGGCCAGATGCATTGCTCAGGAGGCAGGAGCGCTTGGGCCGT 2780
Teo GGCCGCGCGGCTGGTTGGCTTGCCAGGCCAGATGCATTGCTCAGGAGGCAGGAGCGCTTGGGCCGT 2978

B73 GCGAGCTGCGGGATTTGGGAGATGCGTGCAGTTGAATGCGTGGGATTCGCCGTGATTTGTTTATGC 2846
Teo GCGAGCTGCGGGATTTGGGAGATGCGTGCAGTTGAATGCGTGGGATTCGCCGTGATTTGTTTATGC 3044

B73 TGATCGCCCTCTCCTCCCGACCCGTGCTCCCTCCGCGTCCGCTCTCTCCCTTTTTCTCGTCCCCAG 2912
Teo TGATCGCCCTCTCCTCCCGACCCGTGCTCCCTCCGCGTCCGCTCTCTCCC-TTTTCTCGTCCCCAG 3109

B73 TTGCCGCCGAGCCAATTCAGCGCCGCTTTACTGTTATATAAGCCGCGCCTCCGCACCGGACCAGGG 2978
Teo TTGCCGCCGAGCCAATTCAGCGCCGCTTTACTGTTATATAAGCCGCGCCTCCGCACCGGACCAGGG 3175

B73 CTCTGAGATGTGTTTATCTTTCTCTCCTCGCAGCGCCGTGTGCTCTTGTGCTGAAGATCCATCCCA 3044
Teo CTCTGAGATGTGTTTATCTTTCTCTCCTCGCAGCGCCGTGTGCTCTTGTGCTGAAGATCCATCCCA 3241
      Exon1
B73 TCCATGGAAGGGTGCCAACTGCTAGTAGGCTGTAGGATGGAGATGGAGGAGGAAGCGTTCTTTGAC 3110
Teo TCCATGGAGGGGTGCCAACTGCTAGTAGGCTGTAGGATCGAGATGGAGGAGGAAGCGTTCTTTGAC 3307

B73 TCGCGAGAGGAGCTCACGGCGTCGCCGGCGCCCAGCCCGGGCCCTGCATTGCCGTGGTCGGGAAGC 3176
Teo TCGCGAGAGGAGCTCACGGCGTCGCCGGCGCCCAGCCCGGGCCCTGCATTGCCGTGGTCGGGAAGC 3373

B73 CTCGACAGTGTGTGTCAGAGGAGGGAGCGGTTCATGAGAAGCATGGGCCTAGAGTGCTGCCCGGCT 3242
Teo CTCGACAGTGTGTGTCAGAGGAGGGAGCGGTTCATGAGAAGCATGGGCCTAGAGTGCTGCCCGGCT 3439

B73 CCCCTGCAGGCCGATGCCGTGGCCACCGTGGGCGATGTCGACAAGGAGGAAGAGGCTGTGCCGGAA 3308
Teo CCCCTGCAGGCCGATGCCGTGGCCACCGTGGGCGATGTCGACAAGGAGGAAGAGGCTGTGCCGGAA 3505

B73 TTTGGGAGATCGTGGTCGCAGTCGGATGAGAACGACTGCTCCATGTCGAGTTGGTCCACGGAGGAG 3374
Teo TTTGGGAGATCGTGGTCGCAGTCGGATGAGAACGACTGCTCCATGTCGAGTTGGTCCACGGAGGAG 3571
```

```
B73 ACGAAGAGCTTAGAGGATGGTGTCTCGGATGACAATTCTGTCAGTGGATCCAGCCGGGATGATGCT 3440
Teo ACGAAGAGCTTAGAGGATGGTGTCTCGGATGACAATTCTGTCAGTGGATCCAGCCGGGATGATGCT 3637

B73 AGCAGCAAGGTGAGCAGGAGTTTCAGTTCGTTGTCCTTCATCCAGAGGCTCATGAGCCGCAGTGGT 3506
Teo AGCAGCAAGGTGAGCAGGAGTTTCAGTTCGTTGTCCTTCATCCAGAGGCTCATGAGCCGCAGTGGT 3703

B73 AAGCTCTCTGGTGTTCCCAAGGCGGTCGAGAGGAGGAGAAACGGATGGCTTCGGAGGCTGGGCTTG 3572
Teo AAGCTCTCTGGTGTTCCCAAGGCGGTCGAGAGGAGGAGAAACGGATGGCTTCGGAGGCTGGGCTTG 3769

B73 AGGTCTGGTATCCTCGATCATGGAGGCGATGAGGCTAGCACCAGCTCCTCAGAGAGTGAGCAAAAC 3638
Teo AGGTCTGGTATCCTCGATCATGGAGGCGATGAGGCTAGCACCAGCTCCTCAGAGAGTGAGCAAAAC 3835

B73 AGGGGTGGAAGGTATGAAAGGGTCAAGGTCCGCAGCTACAGGAAGCGGTCGAAAGAACTGTCAGCA 3704
Teo AGGGGTGGAAGGTATGAAAGGGTCAAGGTCCGCAGCTACAGGAAGCGGTCGAAAGAACTGTCAGCA 3901

B73 GTTTATCAAGGCCAAGTGATTAAGGGCCATGATGGTGCCATCCTGGCTATGAAGTTTAGTCCGGAT 3770
Teo GTTTATCAAGGCCAAGTGATTAAGGGCCATGATGGTGCCATCCTGGCTATGAAGTTTAGTCCGGAT 3967

B73 GGGCAGTTTCTTGCTACTGGAGGGGAAGATGGAGTTGTCAGGGTCTGGGGCGTCGCGCAGTCTGAG 3836
Teo GGGCAGTTTCTTGCTACTGGAGGGGAAGATGGAGTTGTCAGGGTCTGGGGCGTCGCGCAGTCTGAG 4033

B73 GACTGCAAAATCCCAATGGATGATCCTTCTTGTGTTTACCTCAAAGCTCATCGCCAGAGTGGCTTG 3902
Teo GACTGCAAAATCCCAATGGATGATCCTTCTTGTGTTTACCTCAAAGCTCATCGCCAGAGTGGCTTG 4099

B73 GGTCCTGTTGATGCTGACAATGAGAAGAAATGCAAAGTTAAGGGCGTGAAGCAATCTGCAGATTCT 3968
Teo GGTCCTGTTGATGCTGACAATGAGAAGAAATGCAAAGTTAAGGGCGTGAAGCAATCTGCAGATTCT 4165

B73 GCCTGTGTTGTGATTCCAACAGTGGTGTTCCAGATCTCAAAGCAACCACTGCATGAGTTCCGTGGT 4034
Teo GCCTGTGTTGTGATTCCAACAGTGGTGTTCCAGATCTCAAAGCAACCACTGCATGAGTTCCGTGGT 4231

B73 CACTCTGGTGACGTACTGAGTCTGTCATGGTCTAACAACAAGGTCAGTACAATTATTGAATGAATT 4100
Teo CACTCTGGTGATGTACTGAATCTGTCATGGTCTAACAACAAGGTCAGTACAATTATTGAATGAATT 4297

B73 GCCCCCCTCTGTAAGGTTTGATTGCATTTTTTTATTTATTTTGTCCTTTCCTTTCTGATGATTGAA 4166
Teo GCCCCCCTCTGTAAGGTTTGATTGCATTTTTTTATTTATTTTGTCCTTTCCTTTCTGATGATTGAA 4363
                        Exon2
B73 ATTTTCTACCTTGCAGCATCTACTGTCAGCATCAACAGACAAATCTGTTCGCTTGTGGGAAATTGG 4232
Teo ATTTTCTACCTTGCAGCATCTACTGTCAGCATCAACAGACAAAACTGTTCGCTTGTGGGAAATTGG 4429

B73 ATCTGCAAACTGCATCACTGTTTTTCCGCACAGCAACTTTGGTAGGTCTATAGTCTC-TTACTTGC 4297
Teo ATCTGCAAACTGCATCACTGTTTTTCCGCACAGCAACTTTGGTAGGTCTATAGTCTCTTTACTTGC 4495

B73 TGCTCCAAAACTTTTCAACTATGCTTCTGAATTTGACCTCACCATTTCGCTATGAAAATTTACTTT 4363
Teo TGCTCCAAAACTTTTCAACTATGCTTCTGAATTTGACCTCACCATTTCGCTATGAAAATTTACTTT 4561
          Exon3
B73 TGCAGTGACTTGTGTCCAGTTGAATCCAACCAATGAGAATCAATTCATCAGTGGATCCATAGATGG 4429
Teo TGCAGTGACTTGTGTCCAGTTCAATCCAACCAATGAGAATCAATTCATCAGTGGATCCATAGATGG 4627

B73 CAAAATCCGTGTGTGGGATATTCCCAGATGCAGTGTCATTGATTGGGTGGATATTAGAGACATAAT 4495
Teo CAAAATCCGTGTGTGGGATATTCCCAGATGCAGTGTCATTGATTGGGTGGATATTAGAGACATAAT 4693

B73 AACAGCGGTTTGCTATCGACCTGACGGAAAGGTATCAGCATGCATTCTGAAGTGGGGTTTTTATGG 4561
Teo AACAGCGGTTTGCTATCGACCTGATGGAAAGGTATCAGCATGCATTCTGAAGTGGGGTTTTTATGG 4759
                                                                Exon4
B73 CTAACTTGTTATTTCAGTGGTTTGTGAGATTGATTTTCTCTGTCTTTTATATCTTGCAGGGAGCAG 4627
Teo CTAACTTGTTATTTCAGTAGTTTGTGAGATTGATTTTCTCTGTCTTTTATATCTTGCAGGGAGCAG 4825

B73 TGGTCGGAACCATTACTGGAAATTGTCGATTTTATGATGCATCAGGTACAAAAAAAAAAGTGAAAT 4693
Teo TGGTTGGAACCATTACTGGAAATTGTCGATTTTATGATGCATCAGGTAC--AAAAAGAAGTGAAAC 4889

B73 CTCTACTAGCTTTTCGTTACCATTTCAGTACCTCTCTGCTTTTACTTGAATGATACTCCATAAATA 4759
Teo CTCTACTAGCTTTTCAATACCATTTGGGTACTTCTGTGCTTTTACTTGAATGATACTCCATAAATA 4955
                                      Exon5
B73 CTGACTATAACTACATCTTGATGGATCAGATAATCTCCTGAGGTTTGAAACACAAGTTGCACTCAG 4825
Teo CTGACTATAACTACATCTTGATGGATCAGATAATCTCCTGAGGTTTGAAACACAAGTTGCAGTCAG 5021

B73 TGGCAAGAAAAAGTCTTCTCTTAAAAGAATCACTGCTTTCGAGGTAAATATCTTGACGAGAAGGAA 4891
Teo TGGCAAGAAAAAGTCTTCTCTTAAAAGAATCACTGCTTTCGAGGTAAATATCTTGACGAGAAGGAA 5087

B73 GGCTTTTATTGCACAGTTCACTTCATCAGTCATTTTTTTCGCTCGTATGTTCTGACTGTTTATTTT 4957
Teo GGCTTTTATTGCACAGTTCACTTCATCAGTCA--TTTTTCGCTCCTATGTTCTGACTATTTATTTT 5151
                        Exon6
B73 ATTTTTCATGTCAGTTCTCACCAAGCAACCCAAGTAAATTAATGGTTACCTCTGCTGACTCGAAGG 5023
Teo ATTTTTCATGTCAGTTCTCACCAAGCAACCCAAGTAAATTAATGGTTACCTCTGCTGACTCGAAGA 5217

B73 TTAAAATTCTTGAAGGAACCACTGTGACTCAGAATTATAGTGGTACTTTCCACATGCTTAGCTTTC 5089
Teo TCAAAATTCTTGAAGGAACCACTGTGACTCAGAATTATAGCGGTACAGTCCACATGCTTAGCTTTC 5283

B73 ATTCTTATTGATCTAAGCAATCGATACATTTTATGTATTATGAGCTCATCATTTTATTCATTCAAT 5155
Teo ATTCTTATTGATCTAAGCAATCGATGCA-TTTATGTATTATGAGCTCATCATTTTATTCATTCAAT 5348
        Exon7
B73 CAGGACTCCGTACTGGGTCTTGCCAGTCCTTGGCAACATTCACTCCTGATGGGCAGCATATAGTTT 5221
Teo CAGGACTCCGTACTGGGTCTTGCCAGTCCTTGGCAACATTCACTCCTGATGGGCAGCATATAGTTT 5414
```

```
B73 GTGCAAGCGAAGACTCCAATATTTATGTATGGAACCATGAAAACCAAGACGAGGCTTCACTGAAAC 5287
Teo GTGCAAGCGAAGACTCCAATATTTATGTATGGAACCATGAAAACCAAGACGAGGCTTCACTGAAAC 5480

B73 ATGCGAAAACCATATGGTCCTCAGAGCGCTTCTACTCCAACAATGCAGCCATCGCAATACCATGGA 5353
Teo ATGCGAAAACCATATGGTCCTCAGAGCGCTTCTACTCCAACAATGCAGCCATCGCAATACCATGGA 5546

B73 ATGGCCCGAAACCCAGAAACCCGGTCTCTCTGGCCTCCCAAATCTTGTCACCACAAGGAGATAACT 5419
Teo ATGGCCCGAAACCCAGAAACCCGGTCTCTCTGGCCTCCCAAATCTTGTCACCACAAGGAGATAACT 5612

B73 TGTGGTGCATGAGTAAGGCTGTCAAGTGCAGTTCGAGTCAGAGCGAAGATTCTGCTATCAACAGTT 5485
Teo TGTGGTGCATGAGTAAGGCTGTGAAGTGCAGTTCGAGTCAGAGCGAAGATTCTGCTATCAACAGTT 5678

B73 TTGTGTCAAGGTTTGCTCCTGGTATTTTCAATTTGAATCAGGAGTTCTCCTCTGAGTCCACTTGCA 5551
Teo TTGTGTCAAGGTTTGCTCCTGGTATTTTCAATTTGAATCAGGAGTTCTCCTCTGAGTCCACTTGCA 5744

B73 GAAGTTCAGCGACCTGGCCAGAGGAAATCCTGCCGTCTCGCTCGATTCGTGCAATTCTGGACGAGT 5617
Teo GAAGTTCAGCGACCTGGCCAGAGGAAATCCTGCCGTCTCGCTCGATTCGTGCAATTCTGGACGAGT 5810

B73 CGCAGTACAAGTTCCTAAGGAACTGTTTCCAGAGCACACCAAACTCGTGGGGTCAAGTGATAGTCA 5683
Teo CGCAGTACAAGTTCCTAAGGAACTGTTTCCAGAGCACACCAAACTCCTGGGGTCAAGTGATAGTCA 5876
                                                                 3'UTR
B73 CTGCAGGATGGGATGGCAAGATCAGGTCGTTCCAGAACTATGGCTTACCGGCGCACCAGTGAACAA 5749
Teo CTGCAGGATGGGATGGCAAGATCAGGTCGTTCCAGAACTATGGCTTACCGGCGCACCAGTGATCAA 5942

B73 CAGCTGGAGCATCTGCTGAAACTACACCGGCAGTTTTGGC-ACCTCACATG               5799
Teo CAGCTGGAGCATCTGCTGAAACTACACCGGCAGTTTTGGCAACCTCACATG               5993
```

Fig. S3 Sequence comparisons of the 5,799-bp genomic region at the *KRN2* locus between B73 and teosinte (Teo) alleles. The numbers on the right indicate the nucleotide positions in the full-length sequences. Polymorphic sites between B73 and teosinte alleles are shaded in light blue. The seven exons and UTRs are shaded in dark blue. The ATG start codon and TGA stop codon are shown in red type.

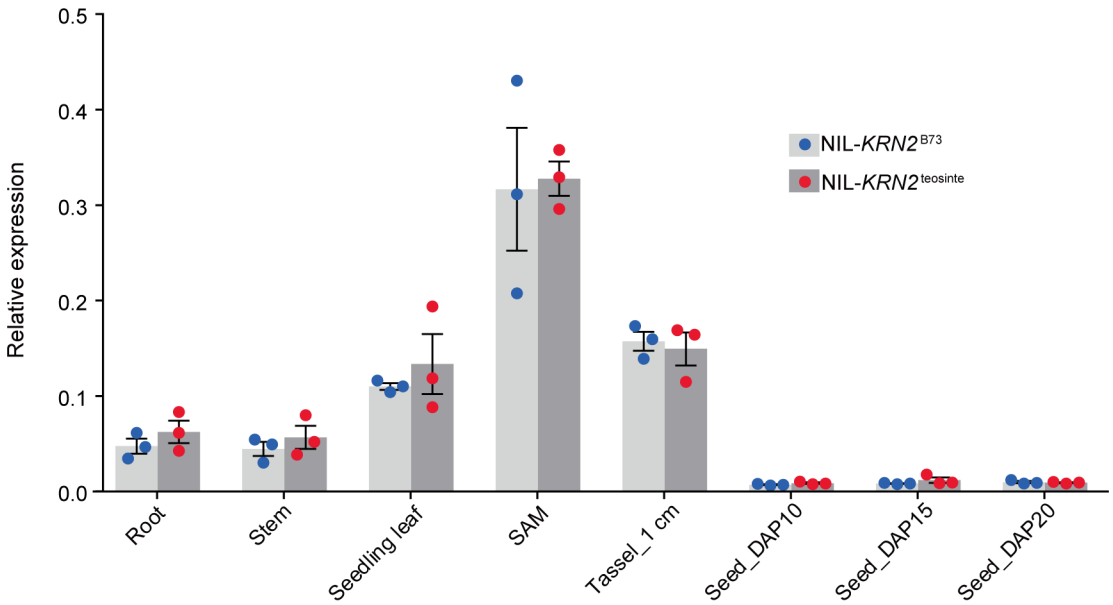

Fig. S4 *KRN2* expression in various tissues from NIL-*KRN2*^{B73} and NIL-*KRN2*^{teosinte}. The expression levels of *KRN2* were quantified using qPCR, and normalized to that of maize *ACTIN*. The statistical significance of differences between NILs was evaluated *using the two-tailed Student's* t *test*, and no significant differences were observed for the tested tissues. *The data for relative expression represent the mean ± s.e.m. (n = 3).* SAM, shoot apical meristem; DAP, days after pollination.

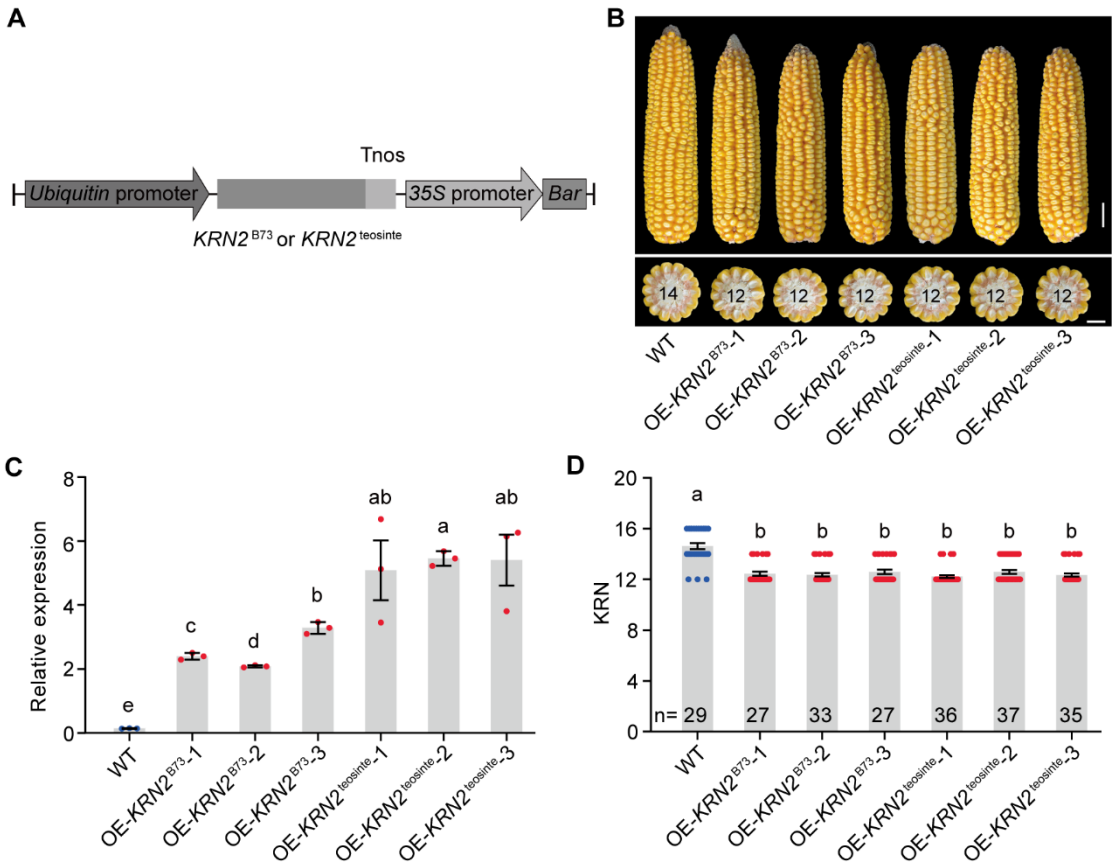

Fig. S5 *KRN2* overexpression decreases KRN. (**A**) Constructs overexpressing the *KRN2* alleles of B73 and teosinte driven by the *ubiquitin* promoter. (**B**) Ear performance of wild type (WT), three independent *Ubi*::*KRN2*^{B73} transgenic lines (OE-*KRN2*^{B73}-1, OE-*KRN2*^{B73}-2, OE-*KRN2*^{B73}-3), and three independent *Ubi*::*KRN2*^{teosinte} transgenic lines (OE-*KRN2*^{teosinte}-1, OE-*KRN2*^{teosinte}-2, OE-*KRN2*^{teosinte}-3). Scale bars: 2 cm for ears, and 1 cm for ear transverse sections. (**C**) *KRN2* expression in WT and transgenic overexpressing lines. The expression levels of *KRN2* were quantified using qPCR, and normalized to that of maize *ACTIN*. (**D**) Quantification of KRN in WT and transgenic overexpressing lines. In (C) and (D), the data represent the mean ± s.e.m., n = 3 in (C); different letters indicate significant differences among groups at $P < 0.05$ (one-way ANOVA followed by Tukey's multiple comparison test).

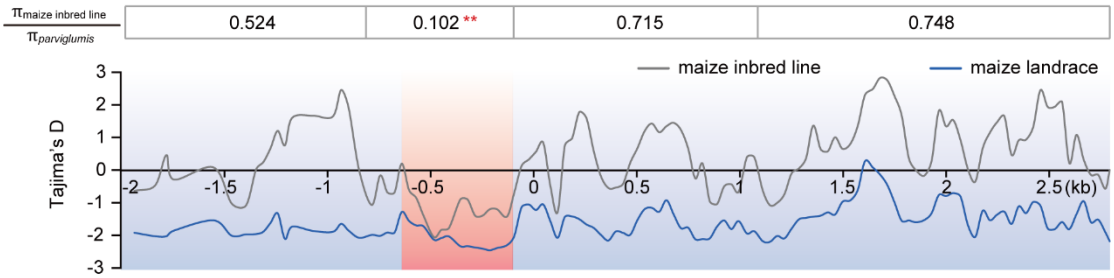

Fig. S6 Molecular evolution of *KRN2*. The nucleotide diversity ratio ($\pi_{\text{maize inbred line}}/\pi_{parviglumis}$) was calculated for four fragments, and coalescent simulations were performed to determine the significance. $^{**}P < 0.01$. Tajima's D tests were performed with 39 maize landraces (blue line) and 69 maize inbred lines (gray line). Regions with statistically significant differences (negative values) estimated with Tajima's D test (red shading, $P < 0.05$), indicate those genomic regions exhibiting evidence of selection.

```
Zm00001d002641     MEGCQLLVG-------CRMEMEEEAFFDSREELTASPAPSPGPALPWSG----SLDSVCQR  50
SORBI_3006G182500  MEGCQLLVG-------CRIEMEEEAFFDSREELTASPAPSPGPALPWSG----SLDSVCQR  50
SETIT_009524mg     MEGCQLLVG-------CRMEMEEETFFDSREELTASPAHSPGQALPWSG----SLDSVWQR  50
Os04g0568400       MEGCQLVARCSSSSSSSRMEVEEEAFFDTREELLP---PSPAAALPWSG----GLDSVRQR  54
BGIOSGA016939      --------------------MEVEEEAFFDTREELLP---PSPAAALPWSG----GLDSVRQR  36
TraesCS2A02G402000 MESCQLARE---SSSSGRVEAEEEAFFDTRQDLLPSPAPSPAPALPWSSGGLDGLDSVRDR  58
AT5G53500          MD---------------YLSQEEDLQFFDANEEMMALN-PSGFGFDVWND----SPGSVVER  42

Consensus          MEGCQLLVG                CRMEMEEEAFFDSREELLASPAPSPALPWSG    SLDSVCQR

Zm00001d002641     RERFMRSMGLE--CCPAPLQ-ADAVATVGDVD-KEEEAVPEF-----GRSWSQSDENDCSM 102
SORBI_3006G182500  RERFMRSMGLE--CCPAPPQ-ADAVATVGDVE-KEE-VVPEF-----GRLWSQSDENDCSM 101
SETIT_009524mg     RERFMRSMGLE--CSPSPRK-ADAAATVGDVE-KEE-VVPEF-----GRLWSQSDENDCSM 101
Os04g0568400       RERFMRSMGLE--RSPSLRQ-ADFADVVGDVE-EEGEVAAEA---EIGRWSSQSDENECSM 108
BGIOSGA016939      RERFMRSMGLE--RSPSLRQ-ADFADVVGDVE-EEGEVAAEAAAAEIGRWSSQSDENECSM  93
TraesCS2A02G402000 KERFFRSMGLE--CGPSPRQAVDPACAAGEVEKQQEEAVPET-----GRLSSHSEDNDCSM 112
AT5G53500          RRKFLEWMGVEEEGRVETKDSVSGSSVESCFDGGEENSVEAE--ERSGECSSSSSEVSLSG 101

Consensus          RERFMRSMGLE                PSPRQ ADAAATVGDVE    EEEVVPEF    GRLSSQSDENDCSM

Zm00001d002641     SSWSTEETKSLEDG-VSDDNSVSGSSRDDASSKVSRSFSSLSFIQRLMSRSGKLSGVPKAV 162
SORBI_3006G182500  SSWSTEETGSSVDG-VSDDNSVSGSSRDDASSKVSRSFSSLSFIQRLMSRSGKLSGVPKAI 161
SETIT_009524mg     SSWSTEDTGSYEDG-ASDDNSMSGSSRDDASSKVGRSFSSLSFIQRLVSRSGKLSGVPKAV 161
Os04g0568400       SSWSTEETTSYDDG-ASDDNSVSGSG------KASRSFSSLSFIQRLMSRNGKPSGAPKTI 162
BGIOSGA016939      SSWSTEETTSYDDG-ASDDNSVSGSG------KASRSFSSLSFIQRLMSRNGKPSGAPKTI 147
TraesCS2A02G402000 SSWSTEETTSYDEGGASDDNSVGGSSKDDGSSKVSRSSSSFSFIRRLMSRNGKPSGAPRTV 173
AT5G53500          SSVEVSEELSLR-----VDRNVGGCDVTRRQSSSMASCSSSRYCQ--VKETEKQRNIAGLV

Consensus          SSWSTEETSYDG ASDDNSVSGSSRDDASSKVSRSFSSLSFIQRLMSRNGKLSGVPKAV

Zm00001d002641     ERRRNGWLRRLGLRSGILDHGG-DEASTSSSESEQNRGGRYERVKVRSYRKRSKELSAVYQ 222
SORBI_3006G182500  ERRRNGWLRRLGLRAGILDHGA-DEASTSSSESEQNRGGRYERVKVRCYRKWSKELSAVYQ 221
SETIT_009524mg     ERRRNGWLRRLGLRASVLDHGG-DEASTSSSESEQNRGGRYERVKVRCYRKRSKELSAVYQ 221
Os04g0568400       DRRRNGWLRRLGVSACVVDSGAADEASTSSSDSEQIGAGRYERIKVHSYRKRSKELSAVYQ 223
BGIOSGA016939      DRRRNGWLRRLGVSACVVDSGAADEASTSSSDSEQIEAGRYERIKVHSYRKRSKELSAVYQ 208
TraesCS2A02G402000 ERRRSGWLERLGVAVCAVDNAA-DEPSTSSSDSEQIHGGRYERVKVRSYRKRSKELSALYQ 233
AT5G53500          TSFKKGWLSRLRSMGCTADTNIESGGRMRASSG---YGDVISRVKVKHCKKQAKELSALYQ 213

Consensus          ERRRNGWLRRLGLRACVLDHGA DEASTSSSDSEQIRGGRYERVKVRSYRKRSKELSAVYQ

R1

Zm00001d002641     GQVIKGHDGAILAMKFSPDGQFLATGGEDGVVRVWGVAQSEDCKIPMD-----DPSCVYLK 278
SORBI_3006G182500  GQVIKGHDGAILTMKFSPDGQFLASGGEDGVVRVWAVTQSEDCKIPVD-----DPSCVYLK 277
SETIT_009524mg     GQVIKAHDGAILTMKFSPDGQFLASGGEDGVVRIWGVTQSEDCKIPMD-----DPSCVYLK 277
Os04g0568400       GQVIKAHDGAILTMKFSPDGQLLATGGEDGVVRVWAVMQSEDCKIPLD-----DPSCVYLK 279
BGIOSGA016939      GQVIKAHDGAILTMKFSPDGQLLATGGEDGVVRVWAVMQSEDCKIPLD-----DPSCVYLK 264
TraesCS2A02G402000 GQVIKGHDGAILTMKFSPDGQFLASGGEDGVVRVWGVLQSDDCKIPLD-----DPSCVYLK 289
AT5G53500          SQDIKAHDGAILAMKFSNDGKFLASSGEDGIVRVWKVVEDKKSRLRRDCLNEIDPSCMYFE 274

Consensus          GQVIKAHDGAILTMKFSPDGQFLASGGEDGVVRVWAVMQSEDCKIPLD     DPSCVYLK

R2

Zm00001d002641     AHRQSGLGPVDADNE--KKCKVKGVKQSADSACVVIPTVVFQISKQPLHEFRGHSGDVLSL 337
SORBI_3006G182500  AHRQSGLAPVVADNE--KKCKVKGVKQSADSACVVIPTMVFQISEEPLHEFCGHSGDVLCL 336
SETIT_009524mg     AHRKSGLAPADAENG--KKCKVKGVKQSADSACVVIPAMVFQISEEPLHEFRGHSGDVLDL 336
Os04g0568400       ARRKYGLAPVNAESE--KKSKINGLKK-SDSACIVVPTMVFQISEEPVHEFRGHSGDVLDL 337
BGIOSGA016939      ARRKYGLAPVNAESE--KKSKINGLKK-SDSACIVVPTMVFQISEEPVHEFRGHSGDVLDL 322
TraesCS2A02G402000 ARRKNGLAPVSVDSEKLRKSKSMGMKKTGDSACIVIPTMVFQISEEPLHEFYGHSADVLDL 350
AT5G53500          VNDLSQLKPVLVNEEK-PKKTTESFRKTSDSACVVFPPKVFRIMEKPLYEFRGHTGEVLDI 334

Consensus          ARRKSGLAPVVADNE KKCKVKGVKQSADSACVVIPTMVFQISEEPLHEFRGHSGDVLDL
```

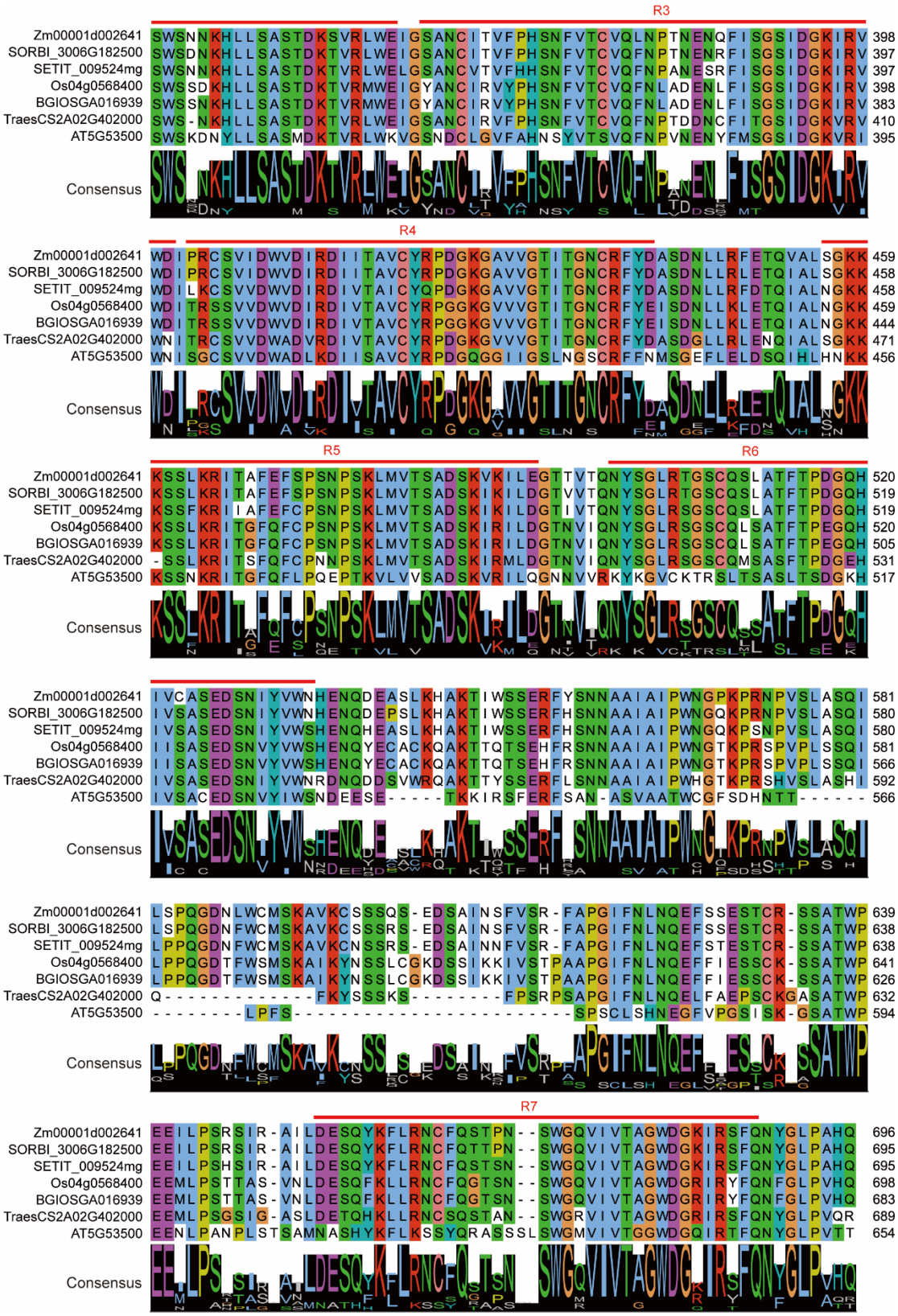

Fig. S7 Amino acid sequence alignment of KRN2 and its orthologs in various species. Zm00001d002641 (KRN2), SORBI_3006G182500, SETIT_009524mg, Os04g0568400 (OsKRN2), BGIOSGA016939, TraesCS2A02G402000, and AT5G53500 were from *Zea mays*, *Sorghum bicolor*, *Setaria italica*, *O. japonica*, *O.*

indica, *Triticum aestivum*, and *Arabidopsis thaliana*, respectively. The numbers to the right indicate the amino acid sequence positions. R1 to R7 indicate the seven WD40 repeats, which are marked by red lines. In the consensus plot, the size of each letter reflects its relative conservation among the various sequences.

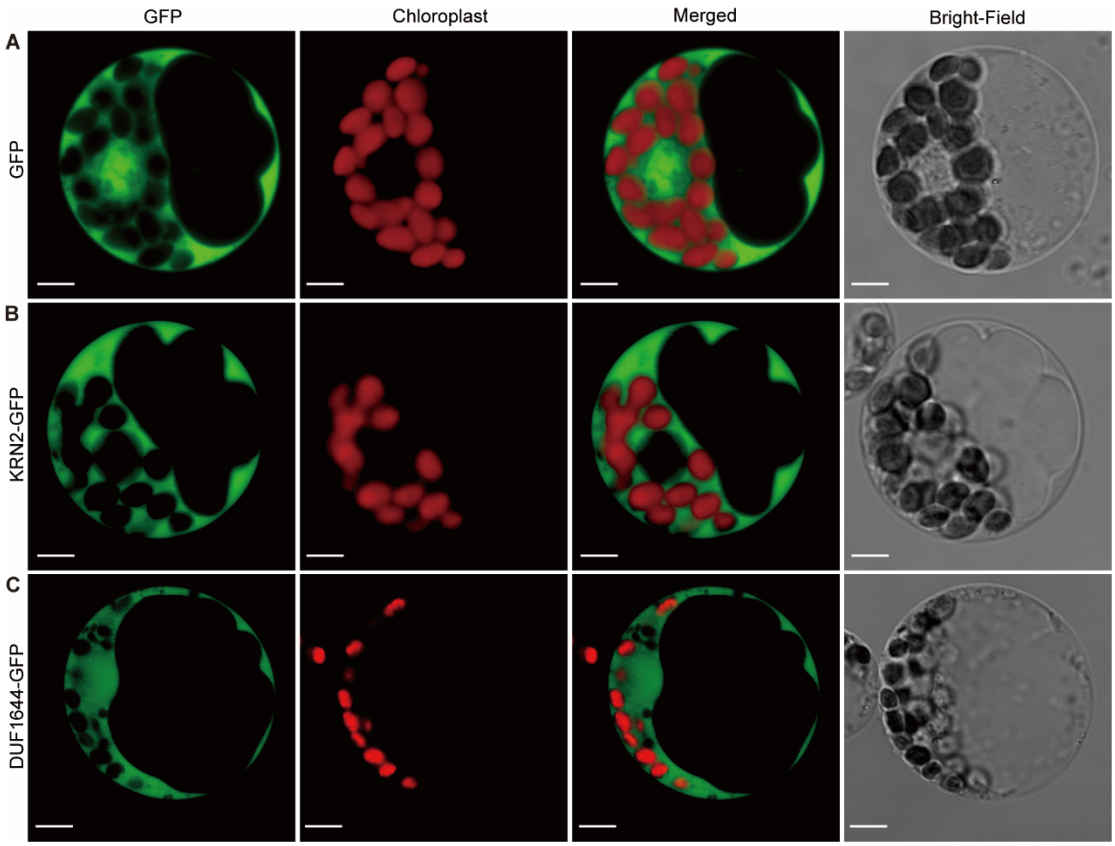

Fig. S8 The subcellular localization patterns of KRN2-GFP and DUF1644-GFP in the cells of maize protoplast. Under the control of GFP expression driven by the Ubi promotor (A), KRN2 is only localized in the cytoplasm (B), whereas DUF1644 is localized in the nucleus and the cytoplasm (C). Images of chlorophyll autofluorescence (red) and GFP fluorescence (green) in maize protoplast cells were separately collected and merged using a laser-scanning microscope (Zeiss LSM 710). Bright-field images are shown in the far-right panel. Scale bars: 5 μm.

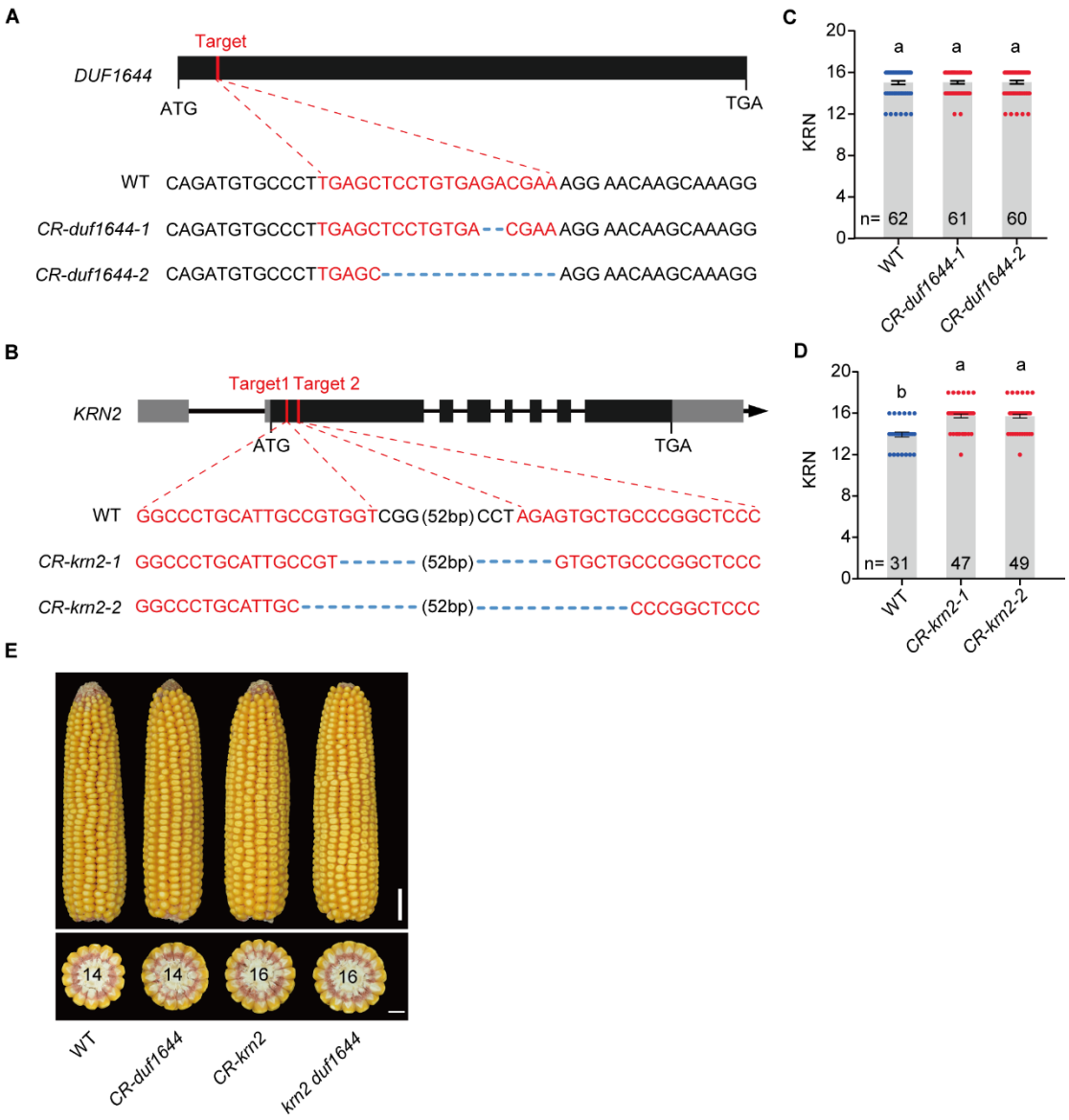

Fig. S9 CRISPR/Cas9-induced knockout of *DUF1644* and *KRN2* and the generation of double-knockout mutants. (**A, B**) Null coding sequences of *krn2* and *duf1644* mutants generated by CRISPR-Cas9 technology. Gene diagrams are shown. Black shading, exons; gray shading, UTRs. Red lines indicate the gRNA sites. (**C, D**) Loss of *DUF1644* function does not change the KRN (C), and *KRN2* loss-of-function increases KRN (D). The data *represent the mean ± s.e.m.;* different letters indicate significant differences among groups at $P < 0.05$ (one-way ANOVA followed by Tukey's multiple comparison test). (**E**) Ear performance of WT, single, and double knockout mutants of *DUF1644* and *KRN2*. The *krn2 duf1644* double mutant was generated using *CR-krn2-1* carrying a 64-bp deletion allele and *CR-duf1644-2* carrying a 14-bp deletion allele. Scale bars: 2 cm for ears, and 1 cm for ear transverse sections. The number within each ear transverse section indicates the representative KRN value for that plant.

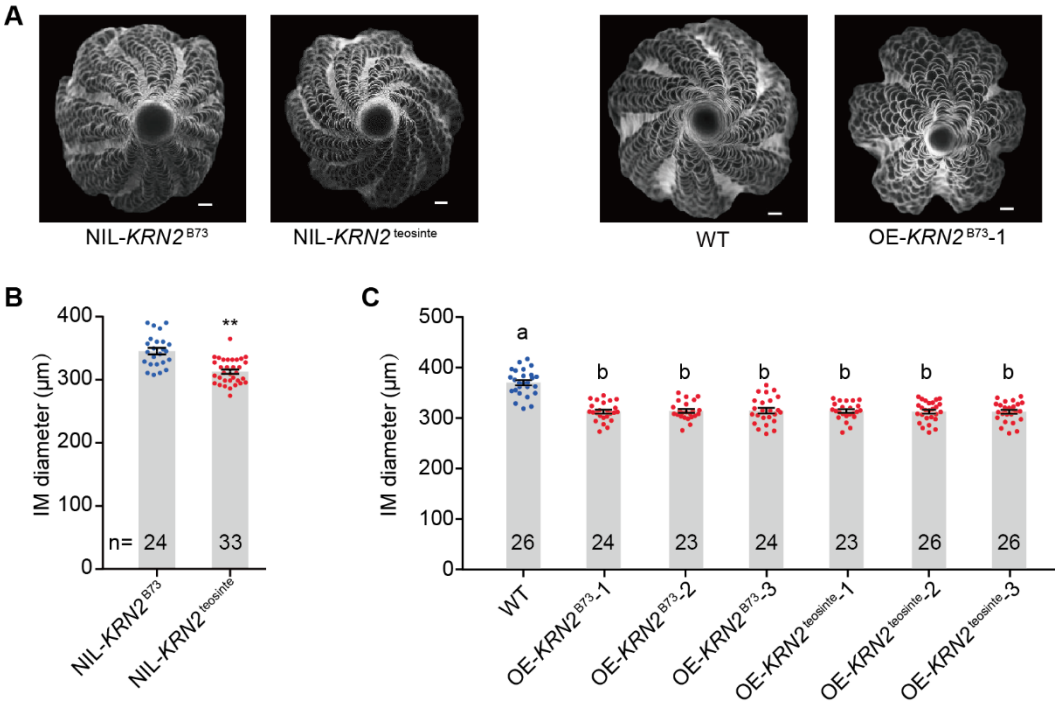

Fig. S10 *KRN2* regulates KRN by altering inflorescence meristem size. (**A**) *Top-down scanning electron microscopy views of* NIL-*KRN2*^{B73}, NIL-*KRN2*^{teosinte}, wild-type *(WT),* and OE-*KRN2*^{B73}-1 *ear primordia.* Scale bars: 100 μm. (**B**) Quantification of inflorescence meristem width from NIL-*KRN2*^{B73} and NIL-*KRN2*^{teosinte}. The data represent the mean ± s.e.m.; the *P* value was determined by the two-tailed Student's *t* test. $^{**}P < 0.01$. (**C**) Quantification of inflorescence meristem width from WT and transgenic plants. The data *represent the mean ± s.e.m.;* different letters indicate significant differences among groups at $P < 0.05$ (one-way ANOVA followed by Tukey's multiple comparison test).

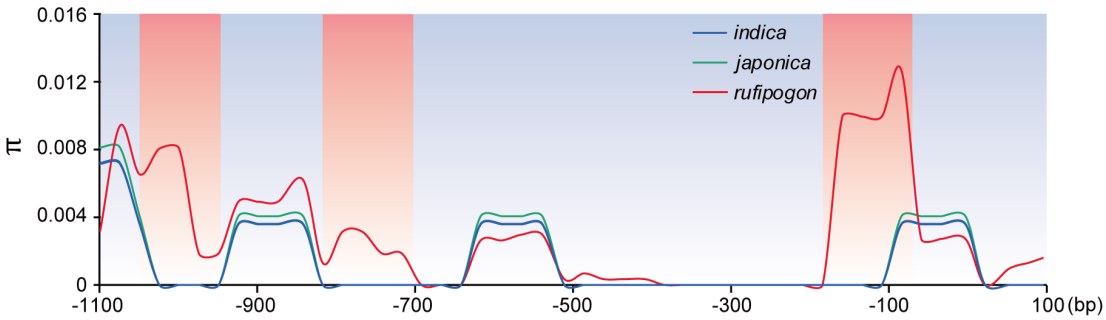

Fig. S11 Nucleotide diversity of the *OsKRN2* locus. A total of 65 *indica* (blue), 44 *japonica* (green), and 59 *rufipogon* (red) accessions were resequenced to estimate the nucleotide diversity (π) of ~1,100-bp regions upstream of the start codon of *OsKRN2*. A 100-bp sliding window with a 25-bp step size was used to calculate the nucleotide diversity (π). Regions with reduced nucleotide diversity in cultivated rice are shaded in red.

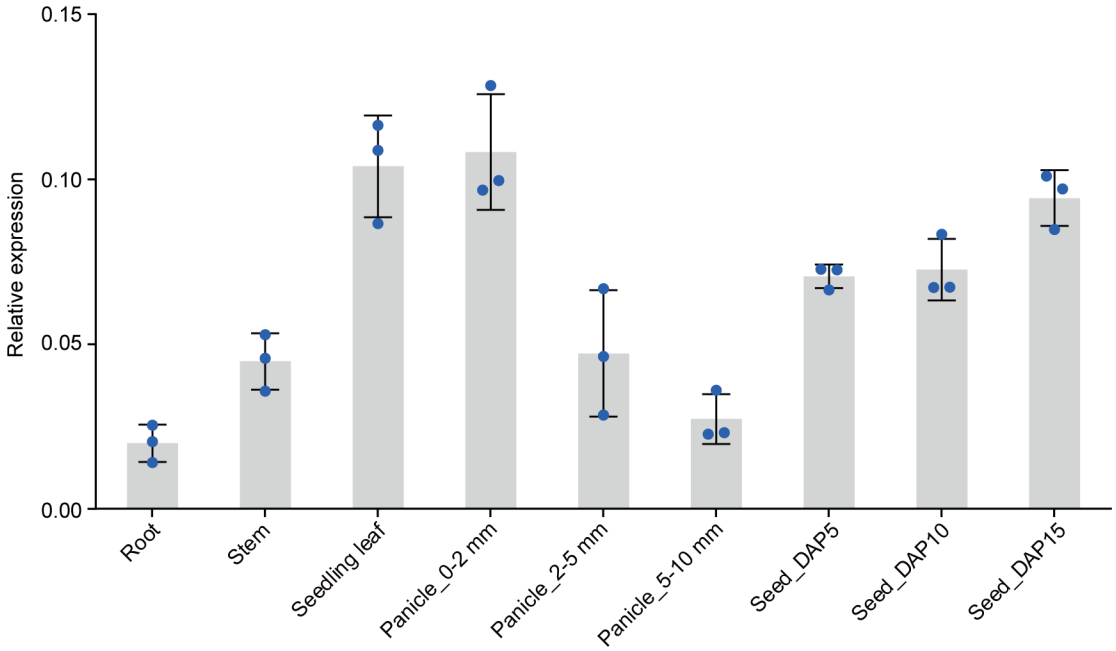

Fig. S12 *OsKRN2* expression patterns in various tissues from the *japonica* cultivar Nipponbare. The expression levels of *OsKRN2* were quantified using qPCR, and normalized to that of rice *ACTIN*. *The data for relative expression represent the mean ± s.e.m. (n = 3).* DAP, days after pollination.

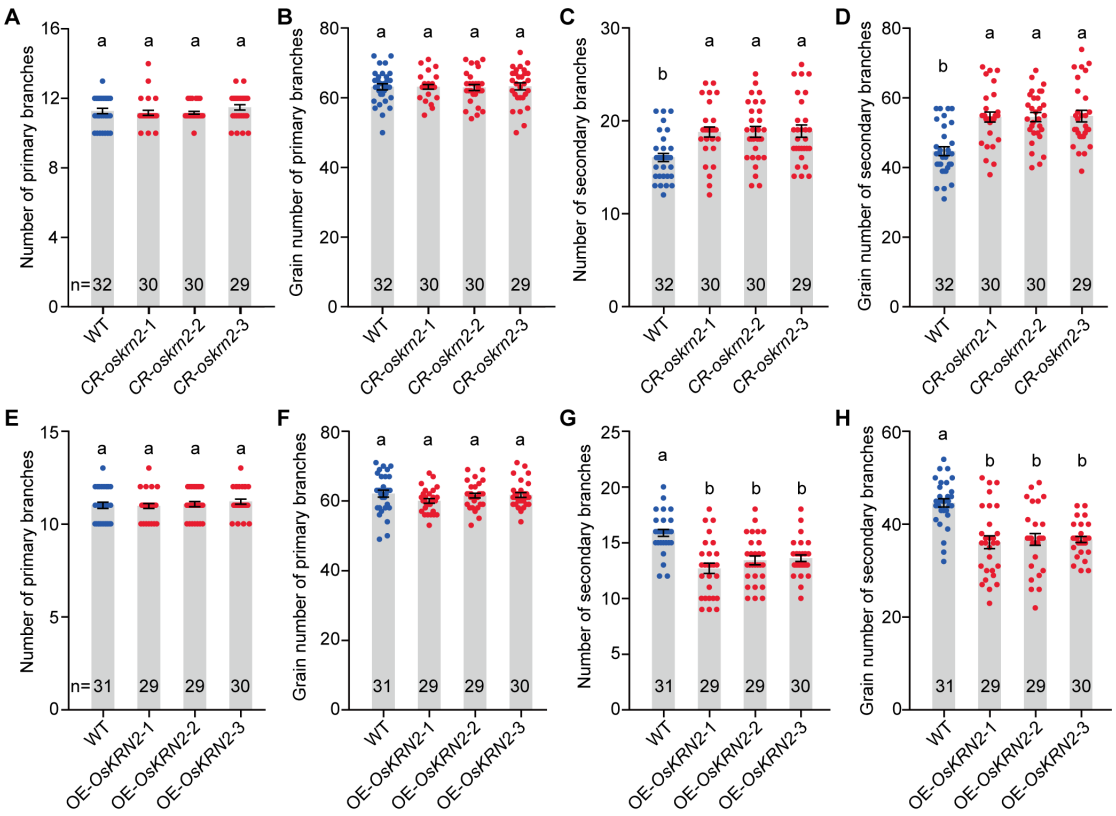

Fig. S13 Knockout of *OsKRN2* increases the number of secondary branches and grain number of secondary branches, and *OsKRN2*-overexpressing lines reduce these traits. (**A** to **D**) Quantification of primary branches (A), grain number of primary branches (B), secondary branches (C), and grain number of secondary branches (D) between wild-type (WT) plants and three *CR-oskrn2* mutants (*CR-oskrn2*-1, *CR-oskrn2*-2, *CR-oskrn2*-3). (**E** to **H**) Quantification of primary branches (E), grain number of primary branches (F), number of secondary branches (G), and grain number of secondary branches (H) between WT and *OsKRN2*-overexpressing transgenic lines (OE-*OsKRN2*-1, OE-*OsKRN2*-2, OE-*OsKRN2*-3). In (A) to (H), values *represent the mean ± s.e.m.;* different letters indicate significant differences among groups at $P < 0.05$ (one-way ANOVA followed by Tukey's multiple comparison test).

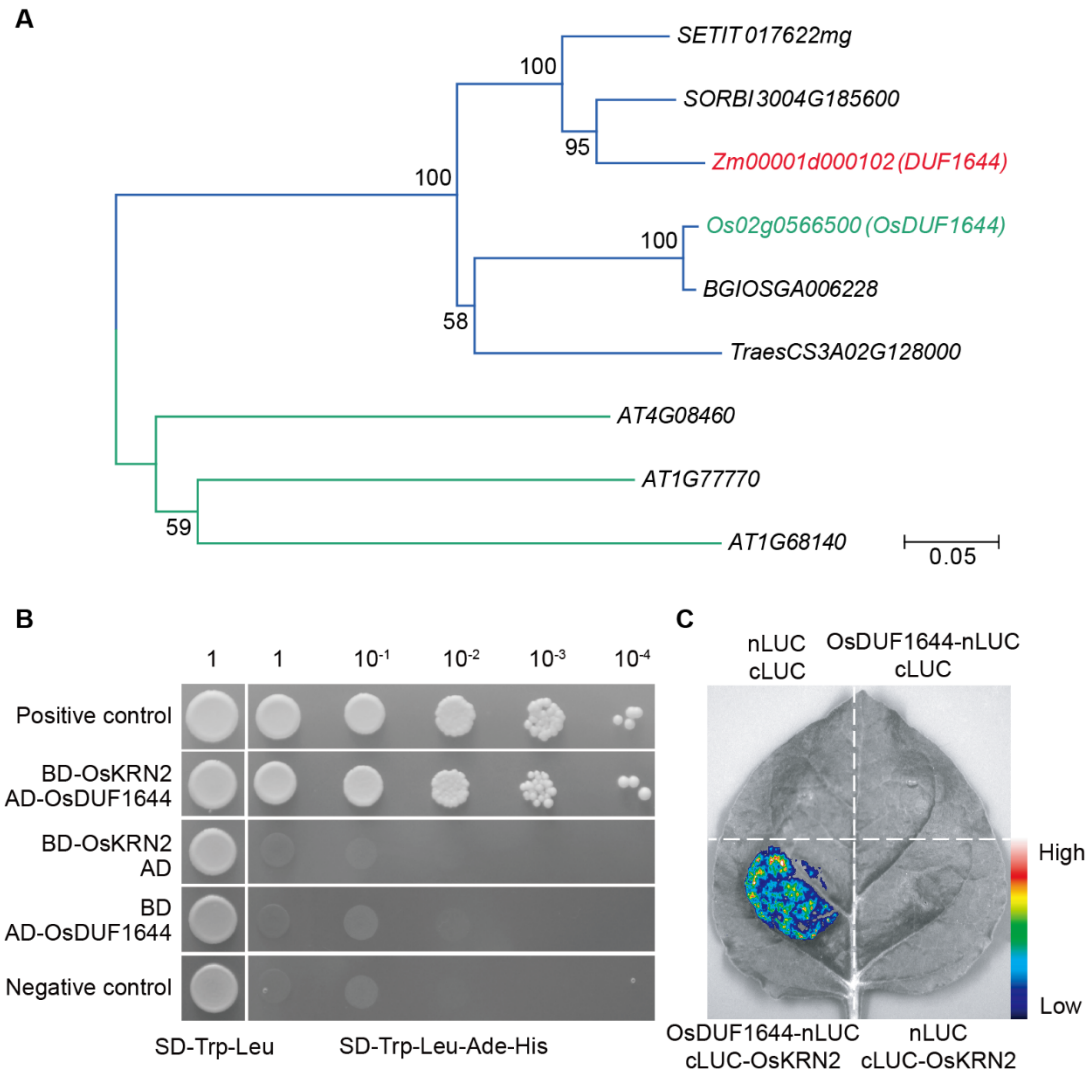

Fig. S14 OsKRN2 interacts with OsDUF1644. (**A**) The neighbor-joining phylogenetic tree of *DUF1644* and its orthologs from major cereals and *Arabidopsis*. Bootstrap values from 1,000 replicates are indicated at each node, and the scale represents branch length. (**B** and **C**) Interaction between OsKRN2 and OsDUF1644 confirmed by Y2H assays (B) and the split firefly LUC complementation assay in tobacco (C). BD, binding domain; AD, activation domain; Trp, tryptophan; Leu, leucine; Ade, adenine; His, histidine. The fluorescence signal intensity represents the strength of the interaction.

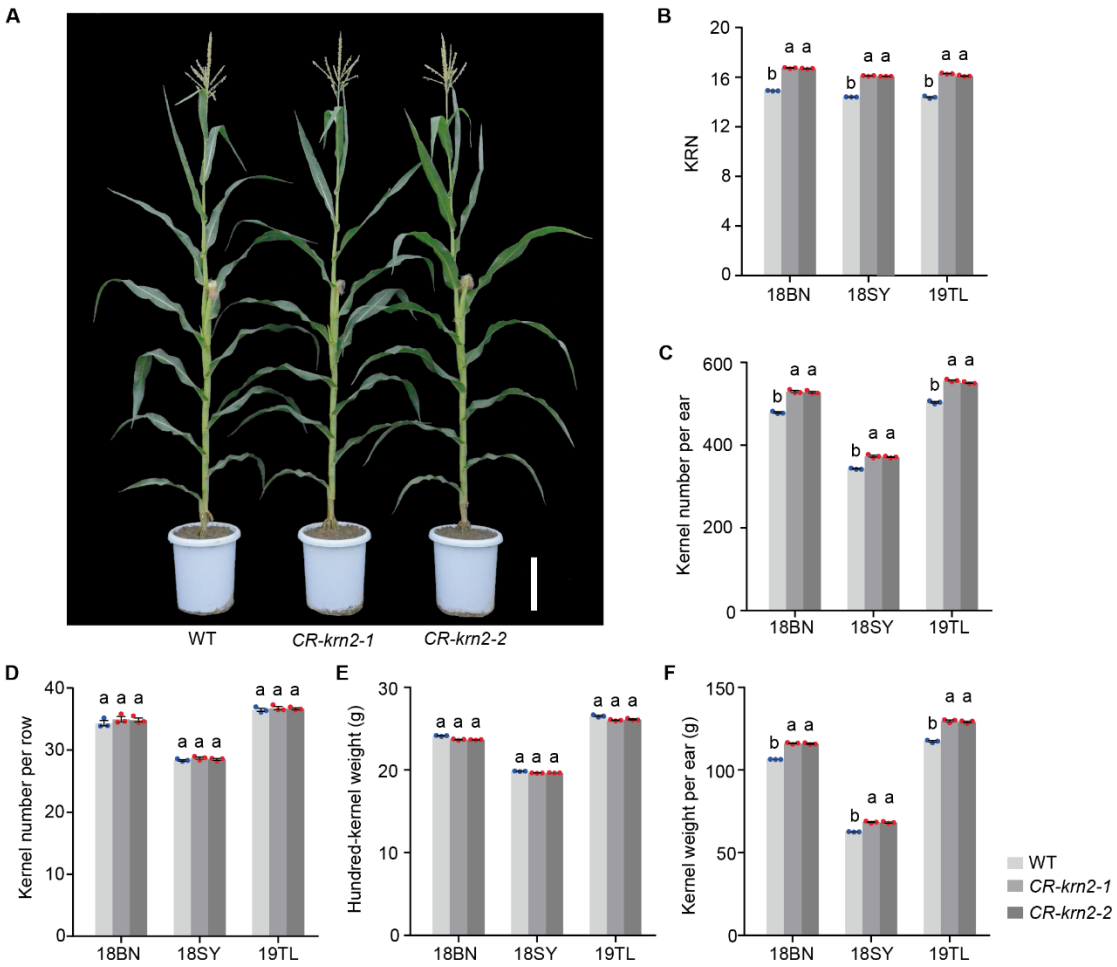

Fig. S15 Plant morphologies and performance of grain-yield component traits of *KRN2*-edited lines in three environments. (**A**) Morphologies of wild-type (WT), *CR-krn2-1*, and *CR-krn2-1* plants. Scale bars: 20 cm. (**B** to **F**) Quantification of KRN (B), kernel number per ear (C), kernel number per row (D), hundred-kernel weight (E), and kernel weight per ear (F) from wild-type (WT), *CR-krn2-1*, and *CR-krn2-2* plants in three environments. 18BN, 18SY, and 19TL indicate the field trials performed in Bayan Nur in 2018, Sanya in 2018, and Tieling in 2019, respectively. In each environment, the tested traits for each genotype were measured in three replicates, with each replicate containing 25–58 plants. Values *represent the mean ± s.e.m. of three replicates;* different letters indicate significant differences among groups at $P < 0.05$ (one-way ANOVA followed by Tukey's multiple comparison test).

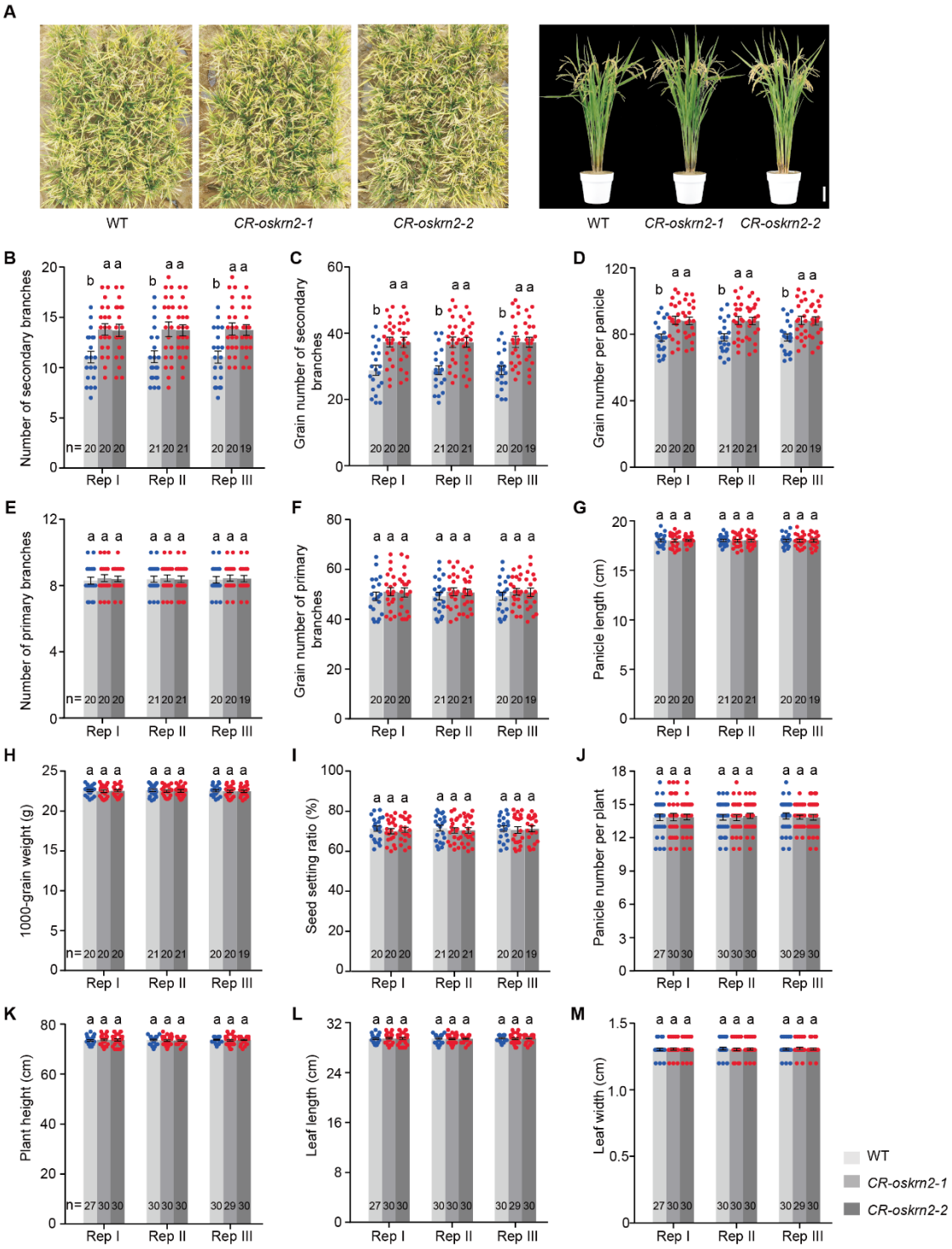

Fig. S16 Agronomic and yield-related traits of *OsKRN2*-edited lines in Wuhan, China, 2020. (**A**) Gross morphology of wild-type (WT) plants and two *CR-oskrn2* mutants (*CR-oskrn2-1* and *CR-oskrn2-2*) under field trials. The plants shown to the right are typical of the corresponding genotype. Scale bars: 10 cm. (**B** to **M**) Quantification of secondary branches (B), grain number of secondary branches (C), grain number per panicle (D), primary branches (E), grain number of primary branches (F), panicle length (G), 1,000-grain weight (H), seed setting ratio (I), panicle number per plant (J), plant height (K), leaf length (L), and leaf width (M) from WT, *CR-oskrn2-*

1, and *CR-oskrn2-2*. Each genotype was tested in three replicates (Rep I to Rep III) with each replicate containing 19–30 plants. Values *represent the mean ± s.e.m. of the measured plants;* different letters indicate significant differences among groups at $P < 0.05$ (one-way ANOVA followed by Tukey's multiple comparison test).

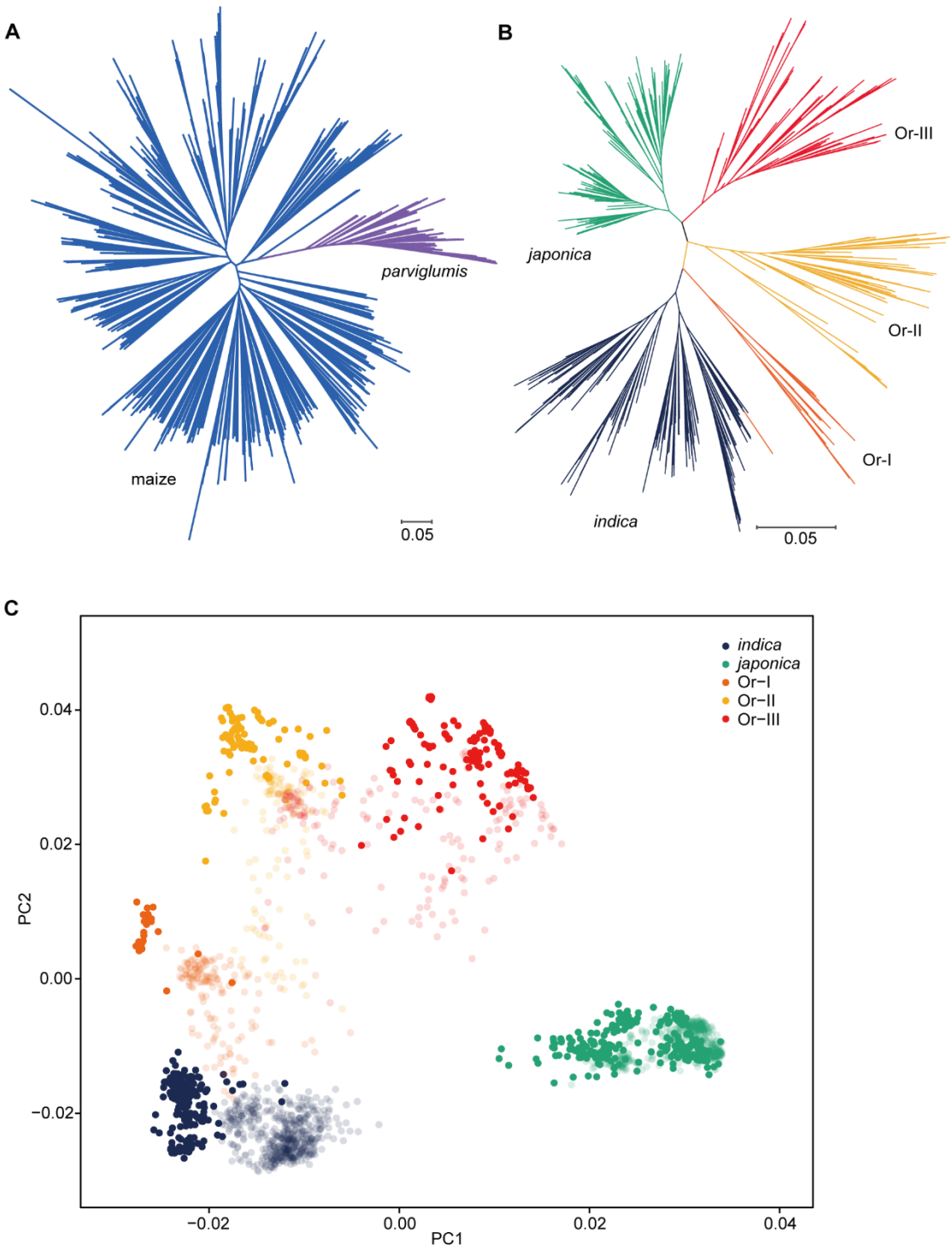

Fig. S17. The genetic relationships of cultivated maize and rice and their wild relatives used for the genome-wide scan for convergent selection. (A and **B)** Maximum likelihood trees of maize and *parviglumis* (A) as well as cultivated and wild rice (B). These phylogenetic trees were generated by using the SNPhylo pipeline. In rice, each colored cluster represents a subpopulation inferred using the program ADMIXTURE (table S5). (**C**) Genetic relationships of cultivated and wild rice assessed by PCA. All accessions are marked according to the inferred clusters from the ADMIXTURE analysis using 292,444 SNPs in 461 cultivated rice and 257 wild rice

accessions in our study (dark color) and 1,082 cultivated rice and 446 wild rice accessions in Huang *et al*.'s study (*3*) (light color). The SNPs of the published low-depth sequencing dataset from Huang *et al*.'s study were recalled using the same pipeline as that used for the 461 cultivated rice and 257 wild rice accessions in our study.

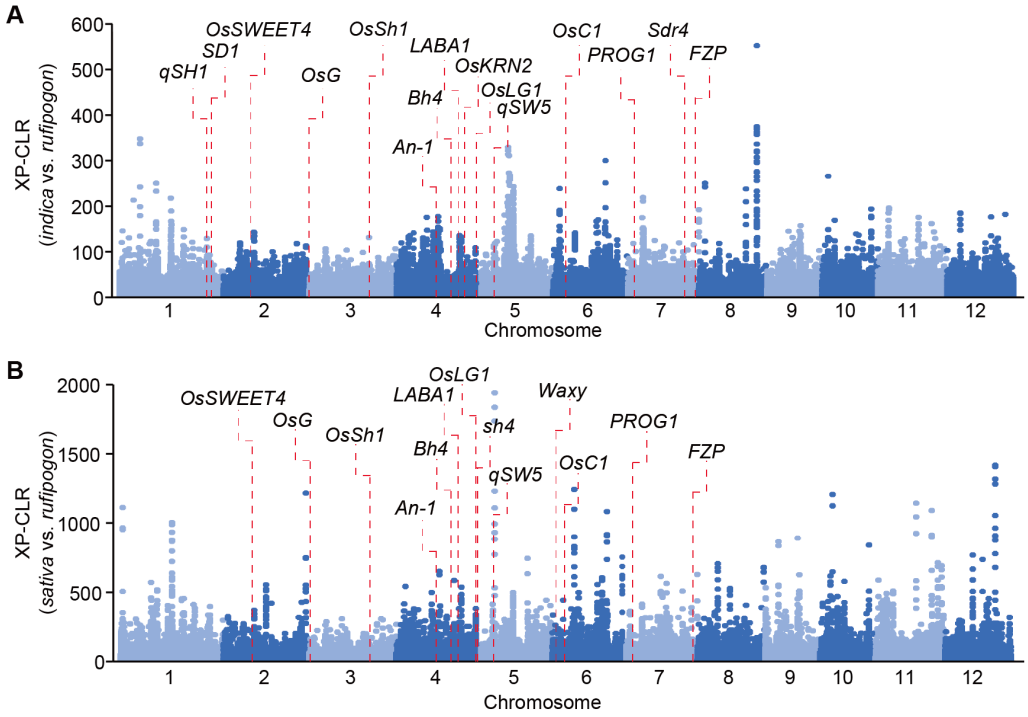

Fig. S18 Genome-wide XP-CLR values between two cultivated rice groups and wild rice. (A) The XP-CLR values estimated by comparing *indica* and *rufipogon*. **(B)** The XP-CLR values estimated by comparing *sativa* and *rufipogon*. The 300-bp regions were used to calculate the XP-CLR values, and each point represents a value in a region. The red dashed lines indicate the positions of the genes known to have undergone selection (table S7) and falling within or near the selected regions.

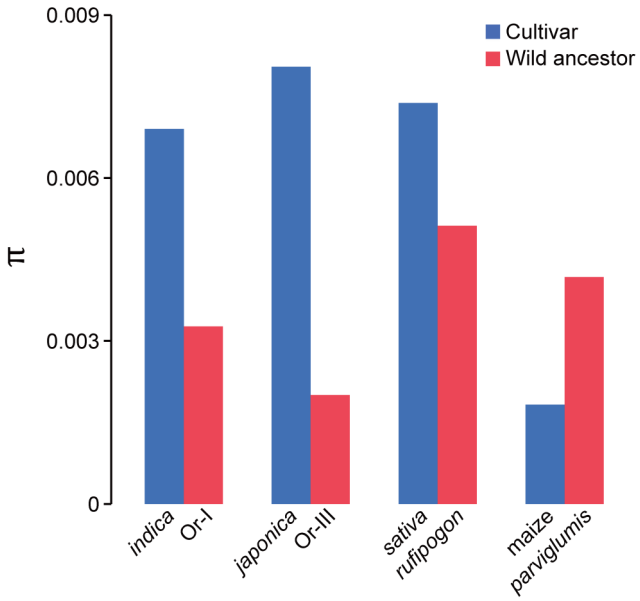

Fig. S19 Nucleotide diversity of the *TPS4* locus in wild ancestors and cultivars. A 300-bp sliding window was used to calculate the nucleotide diversity (π) across the *TPS4* locus in *indica*, Or-I, *japonica*, Or-III, *sativa*, *rufipogon*, maize inbred lines, and *parviglumis*.

Table S1. QTLs for KRN identified in the MT-6/B73 RIL population

QTL	Chr	Peak position (cM)	Left marker[a]	Right marker[a]	Additive effect[b]	LOD	PVE (%)[c]
qKRN1	1	163.97	chr1_295585779	chr1_303283055	0.41	5.28	5.15
qKRN2	2	32.56	chr2_10614197	chr2_28746618	0.79	16.89	19.10
qKRN4-1	4	56.75	chr4_154759197	chr4_160041575	0.59	10.24	10.78
qKRN4-2	4	95.83	chr4_199309320	chr4_205048956	0.34	3.91	3.45
qKRN5-1	5	22.41	chr5_7949729	chr5_11811621	0.41	4.75	4.60
qKRN5-2	5	55.18	chr5_82115827	chr5_146955915	0.59	9.18	9.31
qKRN6	6	55.60	chr6_155081087	chr6_157478216	0.38	4.79	4.24
qKRN7	7	51.06	chr7_138263125	chr7_145650361	0.34	4.07	3.57

[a]The marker name is defined by the chromosome and its physical position in B73 reference genome sequence version 4.0.
[b]Positive values indicate that the increasing alleles come from B73.
[c]Percentage of phenotypic variation explained by the additive effect of the identified QTL.

Table S2. List of candidate interactors screened with the yeast two-hybrid assay

Gene ID	Description
Zm00001d052941	Zinc knuckle (CCHC-type) family protein
Zm00001d032555	Expressed protein
Zm00001d028669	Kinesin-like protein KIN-5B
Zm00001d041489	Homeobox-leucine zipper protein ATHB-14
Zm00001d000102	Protein of unknown function DUF1644
Zm00001d010842	Pentatricopeptide repeat-containing protein

Table S3. Field tests of all agronomic and yield-related traits for *CR-krn2-1* and *CR-krn2-2* in three environments

Trait	Environment[a]	Replicate	WT		*CR-krn2-1*		*CR-krn2-2*		Difference[b]	
			Mean ± SD	N	Mean ± SD	N	Mean ± SD	N	*CR-krn2-1*	*CR-krn2-2*
Days to heading	18BN	1	67.16 ± 1.76	43	67.20 ± 1.90	44	67.18 ± 1.49	38	0.04	0.02
Days to heading	18BN	2	67.33 ± 1.75	49	67.26 ± 1.87	47	67.26 ± 2.03	47	-0.07	-0.07
Days to heading	18BN	3	67.33 ± 1.65	42	67.28 ± 1.67	39	67.33 ± 1.75	40	-0.05	-0.01
Days to anthesis	18BN	1	72.30 ± 2.04	43	72.36 ± 1.98	44	72.34 ± 1.77	38	0.06	0.04
Days to anthesis	18BN	2	72.43 ± 1.70	49	72.39 ± 1.98	46	72.40 ± 1.90	47	-0.04	-0.02
Days to anthesis	18BN	3	72.40 ± 1.98	42	72.41 ± 1.83	39	72.38 ± 1.80	39	0.01	-0.02
Days to silking	18BN	1	74.60 ± 2.14	43	74.68 ± 2.12	44	74.66 ± 1.88	38	0.08	0.05
Days to silking	18BN	2	74.61 ± 1.72	49	74.61 ± 1.97	46	74.61 ± 1.99	46	0.00	0.00
Days to silking	18BN	3	74.62 ± 1.67	42	74.62 ± 1.82	37	74.64 ± 1.83	39	0.00	0.02
Plant height (cm)	18BN	1	211.00 ± 6.59	43	211.09 ± 6.19	44	211.05 ± 7.34	38	0.09	0.05
Plant height (cm)	18BN	2	210.81 ± 7.88	48	211.38 ± 6.57	45	211.34 ± 7.81	44	0.57	0.53
Plant height (cm)	18BN	3	210.95 ± 7.19	41	211.42 ± 6.37	38	211.59 ± 7.34	39	0.47	0.64
Ear height (cm)	18BN	1	68.72 ± 7.14	43	69.00 ± 5.66	43	68.97 ± 5.70	38	0.28	0.25
Ear height (cm)	18BN	2	68.21 ± 6.56	47	68.36 ± 6.17	45	68.66 ± 6.00	44	0.14	0.45
Ear height (cm)	18BN	3	68.50 ± 6.95	40	68.57 ± 6.51	37	68.62 ± 6.93	39	0.07	0.12
Leaf number	18BN	1	20.16 ± 0.48	43	20.23 ± 0.48	43	20.29 ± 0.52	38	0.07	0.13
Leaf number	18BN	2	20.19 ± 0.54	47	20.27 ± 0.50	45	20.20 ± 0.51	44	0.08	0.01
Leaf number	18BN	3	20.20 ± 0.56	41	20.21 ± 0.52	39	20.18 ± 0.60	39	0.01	-0.02
Leaf number above ear	18BN	1	6.44 ± 0.50	43	6.47 ± 0.50	43	6.46 ± 0.51	37	0.02	0.02
Leaf number above ear	18BN	2	6.40 ± 0.50	47	6.43 ± 0.50	44	6.43 ± 0.50	44	0.03	0.03
Leaf number above ear	18BN	3	6.44 ± 0.50	41	6.46 ± 0.51	37	6.43 ± 0.50	37	0.02	-0.01
Leaf length (cm)	18BN	1	62.34 ± 2.79	43	62.33 ± 3.60	43	62.45 ± 3.51	36	-0.02	0.10
Leaf length (cm)	18BN	2	62.35 ± 2.67	45	62.52 ± 3.85	43	62.37 ± 3.48	43	0.18	0.02
Leaf length (cm)	18BN	3	62.21 ± 2.88	40	62.32 ± 3.50	37	62.11 ± 2.99	37	0.11	-0.10
Leaf width (cm)	18BN	1	7.40 ± 0.52	43	7.37 ± 0.55	43	7.36 ± 0.54	36	-0.02	-0.04

Trait	Environment[a]	Replicate	WT		*CR-krn2-1*		*CR-krn2-2*		Difference[b]	
			Mean ± SD	N	Mean ± SD	N	Mean ± SD	N	*CR-krn2-1*	*CR-krn2-2*
Leaf width (cm)	18BN	2	7.43 ± 0.56	45	7.55 ± 0.54	43	7.55 ± 0.53	43	0.12	0.12
Leaf width (cm)	18BN	3	7.42 ± 0.54	40	7.49 ± 0.55	37	7.48 ± 0.56	37	0.07	0.06
Leaf angle (°)	18BN	1	24.18 ± 3.05	43	23.95 ± 3.43	43	23.83 ± 3.62	36	-0.23	-0.35
Leaf angle (°)	18BN	2	24.39 ± 3.64	45	24.37 ± 3.68	43	24.20 ± 4.31	43	-0.02	-0.19
Leaf angle (°)	18BN	3	24.01 ± 3.75	40	24.02 ± 3.82	37	24.15 ± 3.46	37	0.01	0.14
Branch number	18BN	1	7.38 ± 1.35	40	7.35 ± 1.37	40	7.30 ± 1.42	33	-0.03	-0.07
Branch number	18BN	2	7.29 ± 1.17	49	7.33 ± 1.23	46	7.42 ± 1.08	45	0.04	0.14
Branch number	18BN	3	7.32 ± 1.19	41	7.32 ± 1.19	38	7.42 ± 1.11	38	0.00	0.10
Tassel length (cm)	18BN	1	34.02 ± 1.98	40	34.11 ± 1.93	40	34.15 ± 2.19	33	0.09	0.13
Tassel length (cm)	18BN	2	34.05 ± 2.20	49	34.43 ± 1.98	46	34.35 ± 1.99	45	0.38	0.30
Tassel length (cm)	18BN	3	34.06 ± 2.10	41	34.35 ± 2.18	38	34.03 ± 2.23	38	0.29	-0.04
Ear length (cm)	18BN	1	16.94 ± 0.82	32	17.05 ± 0.78	30	17.05 ± 0.81	28	0.11	0.10
Ear length (cm)	18BN	2	17.45 ± 0.83	35	17.59 ± 0.89	34	17.55 ± 0.91	33	0.13	0.10
Ear length (cm)	18BN	3	16.91 ± 0.79	31	17.03 ± 0.82	30	17.05 ± 0.74	30	0.12	0.14
Kernel number per row	18BN	1	33.88 ± 2.51	32	34.47 ± 2.46	30	34.43 ± 2.41	28	0.59	0.55
Kernel number per row	18BN	2	35.20 ± 2.59	35	35.82 ± 2.43	34	35.52 ± 2.44	33	0.62	0.32
Kernel number per row	18BN	3	33.94 ± 2.25	31	34.63 ± 2.44	30	34.60 ± 2.36	30	0.70	0.66
Kernel row number	18BN	1	14.92 ± 1.01	37	16.78 ± 1.20	36	16.71 ± 1.32	31	1.86**	1.79**
Kernel row number	18BN	2	14.88 ± 1.35	41	16.75 ± 0.98	40	16.70 ± 0.97	40	1.87**	1.82**
Kernel row number	18BN	3	14.89 ± 1.39	36	16.69 ± 1.08	35	16.63 ± 1.06	35	1.80**	1.74**
Ear diameter (cm)	18BN	1	4.21 ± 0.10	37	4.35 ± 0.15	36	4.35 ± 0.15	31	0.14**	0.14**
Ear diameter (cm)	18BN	2	4.19 ± 0.13	41	4.33 ± 0.12	40	4.33 ± 0.12	40	0.14**	0.14**
Ear diameter (cm)	18BN	3	4.19 ± 0.14	36	4.32 ± 0.12	35	4.32 ± 0.12	35	0.13**	0.13**
Ear weight (g)	18BN	1	130.62 ± 12.03	32	144.19 ± 13.99	30	144.04 ± 13.59	28	13.57**	13.42**
Ear weight (g)	18BN	2	131.40 ± 13.05	35	146.02 ± 15.78	34	145.84 ± 14.65	33	14.62**	14.44**
Ear weight (g)	18BN	3	130.46 ± 12.94	31	144.06 ± 14.25	30	144.08 ± 14.60	30	13.60**	13.62**
Cob diameter (cm)	18BN	1	2.51 ± 0.11	32	2.57 ± 0.12	30	2.57 ± 0.13	28	0.05	0.05

Trait	Environment[a]	Replicate	WT		*CR-krn2-1*		*CR-krn2-2*		Difference[b]	
			Mean ± SD	N	Mean ± SD	N	Mean ± SD	N	*CR-krn2-1*	*CR-krn2-2*
Cob diameter (cm)	18BN	2	2.53 ± 0.10	34	2.57 ± 0.11	34	2.57 ± 0.10	33	0.05	0.05
Cob diameter (cm)	18BN	3	2.51 ± 0.10	30	2.54 ± 0.10	30	2.55 ± 0.10	30	0.03	0.04
Cob weight (g)	18BN	1	18.90 ± 2.27	32	19.39 ± 2.72	29	19.33 ± 2.85	28	0.49	0.43
Cob weight (g)	18BN	2	19.12 ± 2.52	34	19.89 ± 2.73	32	19.79 ± 2.53	32	0.77	0.66
Cob weight (g)	18BN	3	18.86 ± 2.71	30	19.52 ± 2.78	30	19.50 ± 2.74	30	0.67	0.64
Hundred-kernel weight (g)	18BN	1	24.19 ± 1.07	32	23.75 ± 1.41	30	23.69 ± 1.39	28	-0.44	-0.49
Hundred-kernel weight (g)	18BN	2	24.06 ± 1.20	34	23.59 ± 1.34	32	23.60 ± 1.24	32	-0.48	-0.47
Hundred-kernel weight (g)	18BN	3	24.16 ± 1.26	30	23.70 ± 1.26	29	23.69 ± 1.20	29	-0.46	-0.48
Kernel length (mm)	18BN	1	10.62 ± 0.25	32	10.87 ± 0.25	30	10.86 ± 0.21	28	0.24**	0.24**
Kernel length (mm)	18BN	2	10.65 ± 0.24	34	10.85 ± 0.25	32	10.85 ± 0.23	32	0.20**	0.21**
Kernel length (mm)	18BN	3	10.65 ± 0.25	30	10.85 ± 0.25	29	10.85 ± 0.27	29	0.20**	0.21**
Kernel width (mm)	18BN	1	7.41 ± 0.23	32	7.14 ± 0.31	30	7.15 ± 0.32	28	-0.27**	-0.25**
Kernel width (mm)	18BN	2	7.45 ± 0.27	34	7.18 ± 0.25	32	7.20 ± 0.24	32	-0.27**	-0.25**
Kernel width (mm)	18BN	3	7.40 ± 0.26	30	7.16 ± 0.26	29	7.16 ± 0.23	29	-0.24**	-0.24**
Kernel thickness (mm)	18BN	1	4.11 ± 0.12	32	4.11 ± 0.13	30	4.11 ± 0.14	28	0.00	0.00
Kernel thickness (mm)	18BN	2	4.11 ± 0.12	34	4.11 ± 0.13	32	4.10 ± 0.13	32	0.00	-0.01
Kernel thickness (mm)	18BN	3	4.10 ± 0.13	30	4.11 ± 0.13	29	4.11 ± 0.13	29	0.00	0.00
Kernel volume (mm^3)	18BN	1	200.47 ± 8.74	32	199.33 ± 8.98	30	198.93 ± 10.22	28	-1.14	-1.54
Kernel volume (mm^3)	18BN	2	199.56 ± 9.64	34	197.97 ± 9.91	32	198.44 ± 8.65	32	-1.59	-1.12
Kernel volume (mm^3)	18BN	3	200.00 ± 9.38	30	199.14 ± 10.53	29	199.48 ± 9.48	29	-0.86	-0.52
Kernel number per ear	18BN	1	477.55 ± 50.75	31	527.57 ± 61.13	30	525.93 ± 59.45	28	50.02**	48.38**
Kernel number per ear	18BN	2	482.35 ± 56.98	34	534.58 ± 68.83	33	532.69 ± 62.56	32	52.22**	50.33**
Kernel number per ear	18BN	3	476.57 ± 50.79	30	526.90 ± 66.86	30	525.53 ± 61.55	30	50.33**	48.97**
Kernel weight per ear (g)	18BN	1	106.42 ± 9.79	31	116.22 ± 12.03	30	116.01 ± 9.44	28	9.80**	9.39**
Kernel weight per ear (g)	18BN	2	106.53 ± 8.78	34	116.55 ± 10.42	33	116.46 ± 9.15	32	10.02**	9.93**
Kernel weight per ear (g)	18BN	3	106.42 ± 9.80	30	115.58 ± 8.72	30	115.75 ± 9.11	30	9.16**	9.03**
Grain yield (kg/ha)	18BN		6706.79 ± 3.90	3	7315.40 ± 31.01	3	7312.74 ± 22.50	3	608.61 (9.07%)**	605.95 (9.03%)**

Trait	Environment[a]	Replicate	WT		*CR-krn2-1*		*CR-krn2-2*		Difference[b]	
			Mean ± SD	N	Mean ± SD	N	Mean ± SD	N	*CR-krn2-1*	*CR-krn2-2*
Days to heading	18SY	1	52.55 ± 1.97	38	52.57 ± 1.84	35	52.56 ± 2.26	43	0.02	0.01
Days to heading	18SY	2	52.23 ± 1.83	35	52.39 ± 1.98	33	52.31 ± 1.91	35	0.17	0.09
Days to heading	18SY	3	52.00 ± 2.03	39	52.06 ± 2.13	31	52.00 ± 1.83	38	0.06	0.00
Days to anthesis	18SY	1	56.55 ± 1.70	38	56.86 ± 1.87	35	56.65 ± 1.88	43	0.30	0.10
Days to anthesis	18SY	2	56.54 ± 1.74	35	56.64 ± 1.76	33	56.63 ± 1.78	35	0.09	0.09
Days to anthesis	18SY	3	56.23 ± 2.12	39	56.52 ± 2.10	31	56.34 ± 1.63	38	0.29	0.11
Days to silking	18SY	1	56.61 ± 2.76	38	56.77 ± 2.43	35	56.67 ± 2.72	43	0.17	0.07
Days to silking	18SY	2	56.40 ± 2.68	35	56.44 ± 2.21	33	56.40 ± 2.44	35	0.04	0.00
Days to silking	18SY	3	56.38 ± 3.15	39	56.48 ± 2.55	31	56.53 ± 2.15	38	0.10	0.14
Plant height (cm)	18SY	1	235.83 ± 5.79	36	235.38 ± 6.45	32	235.28 ± 6.04	40	-0.46	-0.56
Plant height (cm)	18SY	2	235.11 ± 7.56	35	235.39 ± 6.69	33	234.66 ± 6.74	35	0.28	-0.46
Plant height (cm)	18SY	3	235.56 ± 6.81	39	235.42 ± 6.88	31	235.40 ± 7.69	35	-0.14	-0.16
Ear height (cm)	18SY	1	76.24 ± 8.02	38	76.18 ± 6.34	34	76.05 ± 7.56	39	-0.06	-0.19
Ear height (cm)	18SY	2	76.23 ± 7.19	35	76.36 ± 7.54	33	76.20 ± 7.68	35	0.14	-0.03
Ear height (cm)	18SY	3	76.18 ± 5.65	39	76.13 ± 8.02	31	76.09 ± 7.04	35	-0.05	-0.09
Leaf number	18SY	1	17.58 ± 0.72	38	17.53 ± 0.75	34	17.44 ± 0.55	39	-0.05	-0.14
Leaf number	18SY	2	17.51 ± 0.70	35	17.67 ± 0.74	33	17.49 ± 0.74	35	0.15	-0.03
Leaf number	18SY	3	17.51 ± 0.76	39	17.48 ± 0.63	31	17.50 ± 0.73	38	-0.03	-0.01
Leaf number above ear	18SY	1	6.29 ± 0.52	38	6.26 ± 0.45	34	6.28 ± 0.51	39	-0.02	-0.01
Leaf number above ear	18SY	2	6.29 ± 0.52	35	6.30 ± 0.47	33	6.26 ± 0.44	35	0.02	-0.03
Leaf number above ear	18SY	3	6.28 ± 0.56	39	6.29 ± 0.53	31	6.29 ± 0.61	38	0.01	0.01
Leaf length (cm)	18SY	1	75.09 ± 3.08	37	75.25 ± 2.27	34	75.30 ± 2.56	38	0.16	0.21
Leaf length (cm)	18SY	2	75.20 ± 3.22	35	75.56 ± 2.50	33	75.22 ± 2.87	35	0.36	0.02
Leaf length (cm)	18SY	3	75.67 ± 3.30	39	75.32 ± 2.93	31	75.21 ± 2.49	38	-0.34	-0.46
Leaf width (cm)	18SY	1	7.55 ± 0.30	37	7.56 ± 0.34	34	7.56 ± 0.37	38	0.01	0.00
Leaf width (cm)	18SY	2	7.44 ± 0.50	35	7.42 ± 0.42	33	7.41 ± 0.44	35	-0.02	-0.03
Leaf width (cm)	18SY	3	7.38 ± 0.50	38	7.39 ± 0.46	31	7.39 ± 0.50	36	0.01	0.00

Trait	Environment[a]	Replicate	WT		*CR-krn2-1*		*CR-krn2-2*		Difference[b]	
			Mean ± SD	N	Mean ± SD	N	Mean ± SD	N	*CR-krn2-1*	*CR-krn2-2*
Leaf angle (°)	18SY	1	20.91 ± 3.24	37	21.24 ± 3.32	34	20.85 ± 2.82	38	0.33	-0.06
Leaf angle (°)	18SY	2	21.54 ± 3.24	35	21.35 ± 2.95	33	21.29 ± 3.10	35	-0.19	-0.25
Leaf angle (°)	18SY	3	21.64 ± 3.06	38	21.64 ± 3.04	31	21.66 ± 3.07	36	0.00	0.02
Branch number	18SY	1	6.78 ± 0.87	36	6.79 ± 0.84	34	6.76 ± 0.91	38	0.02	-0.01
Branch number	18SY	2	6.77 ± 0.73	35	6.79 ± 0.86	33	6.80 ± 0.99	35	0.02	0.03
Branch number	18SY	3	6.67 ± 0.81	39	6.74 ± 0.82	31	6.68 ± 1.02	37	0.08	0.02
Tassel length (cm)	18SY	1	29.25 ± 1.56	36	29.21 ± 1.63	34	29.24 ± 2.25	38	-0.04	-0.01
Tassel length (cm)	18SY	2	29.00 ± 1.68	35	29.18 ± 1.72	33	29.23 ± 1.70	35	0.18	0.23
Tassel length (cm)	18SY	3	29.46 ± 1.94	39	29.58 ± 1.84	31	29.51 ± 2.08	38	0.12	0.05
Ear length (cm)	18SY	1	13.62 ± 0.77	32	13.74 ± 0.80	30	13.63 ± 0.90	32	0.12	0.01
Ear length (cm)	18SY	2	13.43 ± 0.92	33	13.63 ± 0.92	30	13.60 ± 0.93	31	0.20	0.16
Ear length (cm)	18SY	3	13.55 ± 0.89	31	13.59 ± 1.07	30	13.52 ± 0.75	29	0.04	-0.03
Kernel number per row	18SY	1	28.59 ± 3.01	32	29.00 ± 2.24	30	28.59 ± 2.41	32	0.41	0.00
Kernel number per row	18SY	2	28.33 ± 2.47	33	28.77 ± 2.40	30	28.68 ± 2.48	31	0.43	0.34
Kernel number per row	18SY	3	28.19 ± 2.44	31	28.37 ± 2.09	30	28.21 ± 2.02	29	0.17	0.01
Kernel row number	18SY	1	14.41 ± 1.28	34	16.13 ± 1.02	31	16.06 ± 1.31	36	1.72**	1.64**
Kernel row number	18SY	2	14.40 ± 1.26	35	16.06 ± 1.08	32	16.06 ± 1.48	32	1.66**	1.66**
Kernel row number	18SY	3	14.40 ± 1.06	35	16.13 ± 1.15	31	16.06 ± 1.25	34	1.73**	1.66**
Ear diameter (cm)	18SY	1	3.71 ± 0.11	33	3.80 ± 0.14	31	3.80 ± 0.13	33	0.09**	0.09**
Ear diameter (cm)	18SY	2	3.68 ± 0.12	33	3.78 ± 0.14	31	3.78 ± 0.12	31	0.10**	0.09**
Ear diameter (cm)	18SY	3	3.67 ± 0.13	32	3.77 ± 0.13	30	3.76 ± 0.11	31	0.10**	0.09**
Ear weight (g)	18SY	1	67.66 ± 5.44	32	74.90 ± 6.33	30	74.07 ± 6.34	31	7.24**	6.41**
Ear weight (g)	18SY	2	67.02 ± 5.54	33	74.11 ± 7.68	30	74.06 ± 6.33	31	7.09**	7.04**
Ear weight (g)	18SY	3	67.25 ± 5.52	31	74.09 ± 6.61	30	74.02 ± 6.72	29	6.84**	6.77**
Cob diameter (cm)	18SY	1	2.09 ± 0.09	33	2.13 ± 0.08	31	2.12 ± 0.10	33	0.04	0.03
Cob diameter (cm)	18SY	2	2.07 ± 0.08	33	2.11 ± 0.09	31	2.11 ± 0.08	31	0.04	0.04
Cob diameter (cm)	18SY	3	2.08 ± 0.10	32	2.11 ± 0.09	30	2.11 ± 0.11	31	0.03	0.03

Trait	Environment[a]	Replicate	WT		*CR-krn2-1*		*CR-krn2-2*		Difference[b]	
			Mean ± SD	N	Mean ± SD	N	Mean ± SD	N	*CR-krn2-1*	*CR-krn2-2*
Cob weight (g)	18SY	1	8.40 ± 0.96	33	8.81 ± 0.95	31	8.71 ± 1.03	33	0.42	0.31
Cob weight (g)	18SY	2	7.97 ± 0.74	33	8.31 ± 0.83	31	8.30 ± 0.98	31	0.35	0.33
Cob weight (g)	18SY	3	7.94 ± 0.85	32	8.28 ± 0.80	30	8.26 ± 0.83	30	0.34	0.32
Hundred-kernel weight (g)	18SY	1	19.83 ± 1.02	31	19.61 ± 1.15	30	19.65 ± 1.44	31	-0.23	-0.18
Hundred-kernel weight (g)	18SY	2	19.87 ± 1.51	32	19.63 ± 1.39	30	19.63 ± 1.37	30	-0.24	-0.24
Hundred-kernel weight (g)	18SY	3	19.90 ± 1.53	31	19.65 ± 1.37	30	19.67 ± 1.30	29	-0.25	-0.23
Kernel length (mm)	18SY	1	10.05 ± 0.24	31	10.24 ± 0.26	30	10.22 ± 0.24	31	0.19**	0.17**
Kernel length (mm)	18SY	2	10.04 ± 0.24	32	10.23 ± 0.25	30	10.22 ± 0.25	30	0.18**	0.17**
Kernel length (mm)	18SY	3	10.04 ± 0.23	31	10.21 ± 0.24	30	10.22 ± 0.25	29	0.17**	0.18**
Kernel width (mm)	18SY	1	7.02 ± 0.27	31	6.83 ± 0.26	30	6.83 ± 0.27	31	-0.19**	-0.18**
Kernel width (mm)	18SY	2	7.04 ± 0.24	32	6.84 ± 0.25	30	6.83 ± 0.28	30	-0.20**	-0.20**
Kernel width (mm)	18SY	3	7.04 ± 0.22	31	6.83 ± 0.25	30	6.84 ± 0.27	29	-0.21**	-0.20**
Kernel thickness (mm)	18SY	1	4.01 ± 0.11	31	4.01 ± 0.10	30	4.01 ± 0.11	31	0.00	0.00
Kernel thickness (mm)	18SY	2	4.01 ± 0.10	32	4.01 ± 0.11	30	4.01 ± 0.10	30	0.00	0.00
Kernel thickness (mm)	18SY	3	4.01 ± 0.11	31	4.01 ± 0.09	30	4.01 ± 0.12	29	0.00	0.00
Kernel volume (mm^3)	18SY	1	148.71 ± 9.31	31	148.5 ± 10.43	30	148.55 ± 10.18	31	-0.21	-0.16
Kernel volume (mm^3)	18SY	2	149.84 ± 9.71	32	148.5 ± 10.18	30	148.50 ± 10.76	30	-1.34	-1.34
Kernel volume (mm^3)	18SY	3	149.84 ± 9.96	31	148.83 ± 9.89	30	149.14 ± 10.09	29	-1.01	-0.70
Kernel number per ear	18SY	1	344.42 ± 35.01	31	377.60 ± 34.95	30	373.16 ± 34.96	31	33.18**	28.74**
Kernel number per ear	18SY	2	341.94 ± 35.86	32	372.90 ± 32.00	30	371.37 ± 33.35	30	30.96**	29.43**
Kernel number per ear	18SY	3	341.94 ± 42.92	31	369.43 ± 30.20	30	368.86 ± 28.66	29	27.50**	26.93**
Kernel weight per ear (g)	18SY	1	62.82 ± 6.51	31	69.11 ± 6.79	30	68.93 ± 5.75	31	6.29**	6.11**
Kernel weight per ear (g)	18SY	2	62.53 ± 5.51	32	68.54 ± 6.92	30	68.24 ± 7.71	30	6.01**	5.71**
Kernel weight per ear (g)	18SY	3	62.63 ± 7.52	31	67.86 ± 6.38	30	67.78 ± 6.41	29	5.23**	5.15**
Grain yield (kg/ha)	18SY		3947.64 ± 9.21	3	4315.71 ± 39.31	3	4304.05 ± 36.55	3	368.07 (9.32%)**	356.41 (9.03%)**
Days to heading	19TL	1	74.49 ± 1.90	53	74.44 ± 1.71	55	74.11 ± 2.00	53	-0.05	-0.38
Days to heading	19TL	2	75.48 ± 1.83	58	75.61 ± 2.23	46	75.64 ± 2.28	56	0.13	0.16

Trait	Environment[a]	Replicate	WT		*CR-krn2-1*		*CR-krn2-2*		Difference[b]	
			Mean ± SD	N	Mean ± SD	N	Mean ± SD	N	*CR-krn2-1*	*CR-krn2-2*
Days to heading	19TL	3	76.91 ± 2.03	54	76.61 ± 1.98	57	76.84 ± 2.22	50	-0.29	-0.07
Days to anthesis	19TL	1	76.38 ± 1.67	53	76.31 ± 1.68	55	76.23 ± 1.66	53	-0.07	-0.15
Days to anthesis	19TL	2	77.00 ± 1.63	58	77.24 ± 1.95	46	77.27 ± 2.02	56	0.24	0.27
Days to anthesis	19TL	3	79.10 ± 2.11	52	78.89 ± 1.83	57	78.94 ± 2.17	47	-0.20	-0.16
Days to silking	19TL	1	76.60 ± 1.72	53	76.69 ± 1.57	55	76.68 ± 1.37	53	0.09	0.08
Days to silking	19TL	2	77.47 ± 1.58	58	77.95 ± 1.83	44	78.00 ± 1.94	55	0.49	0.53
Days to silking	19TL	3	80.14 ± 1.94	50	79.89 ± 1.70	56	80.02 ± 2.07	47	-0.25	-0.12
Plant height (cm)	19TL	1	262.52 ± 9.52	50	260.96 ± 6.29	54	260.57 ± 7.95	51	-1.56	-1.95
Plant height (cm)	19TL	2	255.46 ± 8.71	54	256.09 ± 7.01	45	256.93 ± 8.36	55	0.63	1.46
Plant height (cm)	19TL	3	250.29 ± 6.40	51	250.72 ± 6.97	57	249.90 ± 9.61	48	0.43	-0.40
Ear height (cm)	19TL	1	102.06 ± 9.02	50	100.59 ± 7.52	54	100.41 ± 7.05	51	-1.47	-1.65
Ear height (cm)	19TL	2	96.69 ± 10.00	54	97.02 ± 9.02	45	97.38 ± 9.52	55	0.34	0.70
Ear height (cm)	19TL	3	96.22 ± 10.34	51	96.32 ± 9.49	57	95.81 ± 8.46	48	0.10	-0.40
Leaf number	19TL	1	20.31 ± 0.62	49	20.30 ± 0.79	50	20.31 ± 0.80	49	-0.01	0.00
Leaf number	19TL	2	20.57 ± 0.77	54	20.67 ± 0.77	45	20.80 ± 0.83	55	0.09	0.23
Leaf number	19TL	3	21.86 ± 0.58	49	21.82 ± 0.75	50	21.64 ± 0.72	36	-0.04	-0.22
Leaf number above ear	19TL	1	6.13 ± 0.48	53	6.07 ± 0.47	55	6.17 ± 0.47	53	-0.06	0.04
Leaf number above ear	19TL	2	6.29 ± 0.46	58	6.20 ± 0.46	45	6.21 ± 0.41	56	-0.09	-0.08
Leaf number above ear	19TL	3	6.18 ± 0.43	51	6.23 ± 0.46	57	6.20 ± 0.54	46	0.05	0.02
Leaf length (cm)	19TL	1	75.21 ± 2.35	50	75.33 ± 2.36	54	75.82 ± 2.63	51	0.12	0.61
Leaf length (cm)	19TL	2	76.57 ± 2.41	54	76.22 ± 2.38	45	76.73 ± 2.72	55	-0.36	0.15
Leaf length (cm)	19TL	3	77.41 ± 3.83	51	77.31 ± 2.64	57	77.55 ± 3.62	48	-0.10	0.14
Leaf width (cm)	19TL	1	8.75 ± 0.49	50	8.85 ± 0.43	54	8.90 ± 0.45	51	0.10	0.15
Leaf width (cm)	19TL	2	8.88 ± 0.44	54	8.75 ± 0.55	45	8.90 ± 0.55	55	-0.14	0.01
Leaf width (cm)	19TL	3	9.05 ± 0.68	51	9.12 ± 0.44	57	9.04 ± 0.60	48	0.07	-0.01
Leaf angle (°)	19TL	1	24.68 ± 2.66	50	24.85 ± 3.46	54	24.82 ± 2.75	51	0.17	0.14
Leaf angle (°)	19TL	2	25.39 ± 2.89	54	25.27 ± 3.02	45	25.53 ± 3.60	55	-0.12	0.14

Trait	Environment[a]	Replicate	WT		*CR-krn2-1*		*CR-krn2-2*		Difference[b]	
			Mean ± SD	N	Mean ± SD	N	Mean ± SD	N	*CR-krn2-1*	*CR-krn2-2*
Leaf angle (°)	19TL	3	25.52 ± 3.22	51	25.88 ± 3.30	57	25.55 ± 3.40	48	0.36	0.02
Branch number	19TL	1	9.70 ± 1.64	50	9.46 ± 1.50	54	9.41 ± 1.42	51	-0.24	-0.29
Branch number	19TL	2	9.19 ± 1.47	54	9.00 ± 1.73	45	9.09 ± 1.64	53	-0.19	-0.09
Branch number	19TL	3	9.22 ± 1.81	51	9.42 ± 1.46	57	9.13 ± 1.63	48	0.21	-0.09
Tassel length (cm)	19TL	1	38.23 ± 2.42	50	38.25 ± 2.48	54	38.11 ± 2.09	51	0.02	-0.12
Tassel length (cm)	19TL	2	37.36 ± 2.57	54	37.37 ± 2.34	45	37.59 ± 2.72	53	0.01	0.23
Tassel length (cm)	19TL	3	37.10 ± 3.19	51	37.68 ± 2.47	57	37.30 ± 2.89	48	0.59	0.20
Ear length (cm)	19TL	1	18.70 ± 1.13	32	18.91 ± 1.01	41	18.91 ± 0.90	44	0.21	0.21
Ear length (cm)	19TL	2	18.83 ± 1.01	43	19.03 ± 1.03	30	19.01 ± 1.06	39	0.21	0.19
Ear length (cm)	19TL	3	18.66 ± 1.04	28	18.86 ± 0.90	39	18.88 ± 0.88	29	0.20	0.22
Kernel number per row	19TL	1	36.38 ± 2.72	32	36.49 ± 2.93	41	36.48 ± 2.84	44	0.11	0.10
Kernel number per row	19TL	2	36.98 ± 2.82	43	37.30 ± 2.55	30	36.95 ± 3.19	39	0.32	-0.03
Kernel number per row	19TL	3	36.11 ± 2.99	28	36.49 ± 2.54	39	36.59 ± 2.68	29	0.38	0.48
Kernel row number	19TL	1	14.38 ± 0.94	32	16.24 ± 1.20	41	16.05 ± 1.01	44	1.87**	1.67**
Kernel row number	19TL	2	14.47 ± 1.22	43	16.33 ± 1.30	30	16.15 ± 1.25	39	1.87**	1.69**
Kernel row number	19TL	3	14.29 ± 1.30	28	16.26 ± 1.04	39	16.07 ± 1.13	29	1.97**	1.78**
Ear diameter (cm)	19TL	1	4.18 ± 0.12	32	4.31 ± 0.13	41	4.30 ± 0.11	44	0.13**	0.12**
Ear diameter (cm)	19TL	2	4.22 ± 0.11	43	4.37 ± 0.12	30	4.36 ± 0.12	39	0.15**	0.13**
Ear diameter (cm)	19TL	3	4.16 ± 0.14	28	4.34 ± 0.13	39	4.34 ± 0.14	29	0.18**	0.18**
Ear weight (g)	19TL	1	155.52 ± 11.99	30	170.46 ± 14.35	37	169.89 ± 13.35	37	14.95**	14.37**
Ear weight (g)	19TL	2	156.59 ± 12.55	35	169.72 ± 16.18	29	169.22 ± 16.22	31	13.13**	12.63**
Ear weight (g)	19TL	3	155.67 ± 15.57	26	169.00 ± 15.99	38	169.16 ± 15.74	29	13.34**	13.49**
Cob diameter (cm)	19TL	1	2.58 ± 0.09	31	2.61 ± 0.09	40	2.60 ± 0.07	44	0.03	0.02
Cob diameter (cm)	19TL	2	2.57 ± 0.09	43	2.61 ± 0.08	30	2.61 ± 0.08	39	0.04	0.03
Cob diameter (cm)	19TL	3	2.57 ± 0.09	25	2.61 ± 0.07	39	2.60 ± 0.08	28	0.04	0.03
Cob weight (g)	19TL	1	19.94 ± 1.88	31	20.23 ± 1.97	40	20.21 ± 1.63	44	0.29	0.26
Cob weight (g)	19TL	2	20.00 ± 1.78	43	20.35 ± 1.78	30	20.30 ± 1.84	39	0.36	0.30

Trait	Environment[a]	Replicate	WT		*CR-krn2-1*		*CR-krn2-2*		Difference[b]	
			Mean ± SD	N	Mean ± SD	N	Mean ± SD	N	*CR-krn2-1*	*CR-krn2-2*
Cob weight (g)	19TL	3	20.06 ± 1.94	25	20.35 ± 1.83	39	20.37 ± 2.20	28	0.28	0.30
Hundred-kernel weight (g)	19TL	1	26.52 ± 2.54	31	26.00 ± 1.59	41	26.03 ± 1.72	44	-0.52	-0.48
Hundred-kernel weight (g)	19TL	2	26.40 ± 2.16	42	25.94 ± 2.00	30	26.06 ± 2.50	39	-0.47	-0.34
Hundred-kernel weight (g)	19TL	3	26.69 ± 2.47	25	26.10 ± 2.10	38	26.24 ± 2.16	28	-0.59	-0.45
Kernel length (mm)	19TL	1	10.94 ± 0.37	31	11.18 ± 0.29	41	11.18 ± 0.34	44	0.24**	0.24**
Kernel length (mm)	19TL	2	10.94 ± 0.23	42	11.20 ± 0.37	30	11.19 ± 0.35	39	0.26**	0.25**
Kernel length (mm)	19TL	3	10.93 ± 0.27	25	11.19 ± 0.28	38	11.19 ± 0.31	28	0.26**	0.26**
Kernel width (mm)	19TL	1	7.66 ± 0.25	31	7.42 ± 0.28	41	7.42 ± 0.28	44	-0.25**	-0.24**
Kernel width (mm)	19TL	2	7.68 ± 0.26	42	7.39 ± 0.31	30	7.40 ± 0.28	39	-0.29**	-0.28**
Kernel width (mm)	19TL	3	7.68 ± 0.28	25	7.40 ± 0.21	38	7.40 ± 0.24	28	-0.27**	-0.27**
Kernel thickness (mm)	19TL	1	4.14 ± 0.08	31	4.14 ± 0.09	41	4.15 ± 0.09	44	0.00	0.00
Kernel thickness (mm)	19TL	2	4.14 ± 0.08	42	4.14 ± 0.08	30	4.14 ± 0.10	39	0.00	0.00
Kernel thickness (mm)	19TL	3	4.14 ± 0.11	25	4.14 ± 0.08	38	4.14 ± 0.09	28	0.00	0.00
Kernel volume (mm^3)	19TL	1	186.45 ± 11.70	31	184.51 ± 10.11	41	184.20 ± 11.71	44	-1.94	-2.25
Kernel volume (mm^3)	19TL	2	186.19 ± 12.34	42	186.17 ± 12.15	30	186.15 ± 12.64	39	-0.02	-0.04
Kernel volume (mm^3)	19TL	3	186.20 ± 10.73	25	186.18 ± 11.82	38	186.07 ± 12.12	28	-0.02	-0.13
Kernel number per ear	19TL	1	504.03 ± 37.36	30	556.24 ± 34.00	37	549.39 ± 35.81	38	52.21**	45.36**
Kernel number per ear	19TL	2	507.26 ± 40.80	35	559.45 ± 39.51	29	553.71 ± 46.52	31	52.19**	46.45**
Kernel number per ear	19TL	3	500.15 ± 40.93	26	553.34 ± 47.18	38	548.50 ± 51.69	28	53.19**	48.35**
Kernel weight per ear (g)	19TL	1	117.49 ± 10.35	30	130.37 ± 12.27	37	129.65 ± 11.93	37	12.88**	12.16**
Kernel weight per ear (g)	19TL	2	118.00 ± 11.08	35	130.14 ± 13.09	29	129.52 ± 10.29	31	12.14**	11.52**
Kernel weight per ear (g)	19TL	3	116.54 ± 13.17	26	128.45 ± 13.60	38	128.13 ± 13.25	29	11.90**	11.51**
Grain yield (kg/ha)	19TL		7392.67 ± 46.45	3	8168.02 ± 66.01	3	8133.14 ± 53.12	3	775.36 (10.49%)**	740.47 (10.02%)**

[a] 18BN, 18SY, and 19TL indicate the field trials performed in Bayan Nur (40.7°N, 107.5°E) in 2018, Sanya (18.2°N, 109.1°E) in 2018, and Tieling (41.5°N, 123.2°E) in 2019, respectively.

[b] P values were determined by two-tailed Student's t test. ** $P < 0.01$

Table S4 (Separate file). Polymorphic sites of *KRN2* in a natural population consisting of 379 inbred lines and their association with KRN. The origin and pedigree of the public maize inbred lines were previously described (*49*), and the SNPs in the promoter region and full-length *KRN2* were extracted from the public data (*74*).

Table S5 (Separate file). List of plant materials used in this study. The excel file contains two sheets. The first lists the used maize inbred lines, maize landraces and teosinte. The second lists the used cultivated and wild rice. The origin, pedigree, and genotype for genome-wide selection of the public materials were previously described (*8*, *49*, *74*, *76*, *77*).

Table S6 (Separate file). List of selected regions identified in maize and rice. The excel file contains four sheets. The first lists the selected regions identified in maize by comparing maize and *parviglumis*. The second lists the selected regions identified in rice by comparing *japonica* and *rufipogon* Or-III. The third lists the selected regions identified in rice by comparing *indica* and *rufipogon* Or-I. The fourth lists the selected regions identified in rice by comparing *sativa* and *rufipogon*.

Table S7 (Separate file). Detailed information for identified selected genes including convergently selected genes in maize and rice. The excel file contains three sheets. The first lists the selected genes identified in maize. The second lists the selected genes identified in rice. The third lists the orthologous gene pairs that have undergone convergent selection between maize and rice.

Table S8. Summary of regions and genes identified as having undergone selection in maize and rice

Species	Comparison	Regions that have undergone selection				Gene number
		Number	Average length (bp)	Range (bp)	Total (Mb)	
Maize	Maize/*parviglumis*	38,495	1,807	1,000–45,000	69.6	3,163
Rice	*O. sativa*/*O. rufipogon*	47,017	559	300–16,200	26.3	7,864
	O. indica/Or-I	47,525	543	300–12,300	25.8	10,196
	O. japonica/Or-III	40,892	676	91–18,000	27.6	7,709
	Total	97,324	658	91–24,600	64.0	18,755

Table S9 (Separate file). List of convergently selected genes in the starch and sucrose metabolism pathways identified in maize and rice. The excel file contains two sheets. The first lists the convergently selected genes in the starch and sucrose metabolism pathways identified in maize. The second lists the convergently selected genes in the starch and sucrose metabolism pathways identified in rice.

Table S10. List of primers used in this study

Experiment	Primer name[a]	Forward sequence (5' to 3')	Reverse sequence (5' to 3')
Fine mapping of *qKRN2*	IDP1	AAGAACGAGTGGAAGAACGC	CCTGTCGTGGGAGTTGTAGG
	IDP2	ATGTCTCCCACTGCTGCTAC	CCTCCGTGACCTCATCGTC
	IDP3	CGTGGGGTCAAGTGATAGTC	GATCTCAAAGGACCACCAGG
	IDP4	GTTCCCCTCCCCCGCTTT	TCCGAGTCCCCCATCACC
	SNP1	TGAACGGCAGAACACCAG	GGAGGGAAGGGAGGTTTACC
	IDP5	ACGGGCGACGAGAAGAAC	CAGCATCAGACCCTCACTACC
	IDP6	AATTGCACATAACAGAGGCG	CTCTTCCAATCGGGTTTGC
	IDP7	GTCCTTACAGGCTTTGCAGC	GTGAACCGATCAACGAATCC
	IDP8	CGAGACAGAAAGTGAAGCCC	CCTCTGCTGATCCTTTGACC
qPCR	*KRN2*-QRT	GACGGAAAGGGAGCAGTGGT	GCTTGGTGAGAACTCGAAAGCAG
	ACTIN-maize	CCAAGGCCAACAGAGAGAAA	CCAAACGGAGAATAGCATGAG
	OsKRN2-QRT	GGTGGAAAGGGAGTGGTGGT	GCTTGGGCAAAACTGAAAGCCTG
	ACTIN-rice	TGCTATGTACGTCGCCATCCAG	AATGAGTAACCACGCTCCGTCA
Vector construction for generating overexpression transgenic plants	*KRN2*-B73-OE	CATGGAAGGGTGCCAACTGC	GTGAGGTGCCAAAACTGCC
	KRN2-MT-6-OE	CATGGAGGGGTGCCAACTGC	AAGGACCACCAGGTTTGATT
	OsKRN2-OE	ATGGAGGGGTGCCAATTGGT	TCACTGATGCACTGGTAAACC

Experiment	Primer name[a]	Forward sequence (5' to 3')	Reverse sequence (5' to 3')
Genotyping of the uniform *Mutator* mutant	*KRN2*-MU-F	CGCCGTGATTTGTTTATGC	
	KRN2-MU-R	GACCTTGACCCTTTCATACC	
	TIR8-1	CGCCTCCATTTCGTCGAATCCCCTG	
Nucleotide diversity analysis	*KRN2*-SEQ-1	GTTCCCCTCCCCCGCTTT	TCCGAGTCCCCCATCACC
	KRN2-SEQ-2	ACTGCTACAAAACGACGACC	GAAGGACAACGAACTGAAACTC
	KRN2-SEQ-3	CATGTCGAGTTGGTCCACG	CAATAAAAGCCTTCCTTCTCG
	KRN2-SEQ-4	GCAGTGTCATTGATTGGGTG	GGGTTTCTGGGTTTCGGG
	KRN2-SEQ-5	CAGTCCTTGGCAACATTC	CCCGACGAATGAAATGACG
	OsKRN2-SEQ	GCAGCACTGGACCAGTGGCAG	TGAACCGCTCCCTCCGCT
Vector construction for protoplast transient expression assay	*KRN2*-LUC-1955	ACTCACTATAGGGCGAATTGGGTACCCAGCAGCCCCAGCTGACG	GAACTAGTGGATCCCCCGGGCTGCAGGGATGGGATGGATCTTCAGCAC
	KRN2-LUC-1200	ACTCACTATAGGGCGAATTGGGTACCACTGCTACAAAACGACGACC	GAACTAGTGGATCCCCCGGGCTGCAGGGATGGGATGGATCTTCAGCAC
Vector construction for subcellular localization	*KRN2*-EGFP	GTTGTTTGGTGTTACTTAAGCTTATGGAAGGGTGCCAACTGC	GCCCTTGCTCACCATGGATCCCTGGTGCGCCGGTAAG
	DUF1644-EGFP	GTTGTTTGGTGTTACTTAAGCTTATGGCAAGATCACCAAAAG	GCCCTTGCTCACCATGGATCCTCTCTCAGCTGCCTCGC
Vector construction for Y2H assay	*KRN2*-BD	CCTGCATATGTCGGCCATTACGGCCATGGAAGGGTGCCAACTGC	CTGCAGGTCGAGGGCCGAGGCGGCCTCACTGGTGCGCCGGTAAG
	DUF1644-AD	GGAGGCCAGTGAATTCCACCCGGGCATGGCAAGATCACCAAAAGGT	CTGCAGCTCGAGCTCGATGGATCCTCATCTCTCAGCTGCCTCGC
	OsKRN2-BD	CCTGCATATGTCGGCCATTACGGCCATGGAGGGGTGCCAATTGG	CTGCAGGTCGAGGGCCGAGGCGGCCTCACTGATGCACTGGTAAAC
	OsDUF1644-AD	GGAGGCCAGTGAATTCCACCCGGGGATGGGTAGATCTCCAAGGGGC	CTGCAGCTCGAGCTCGATGGATCCTTAGATGCCATGTGTTGACC

Experiment	Primer name[a]	Forward sequence (5' to 3')	Reverse sequence (5' to 3')
Vector construction for split firefly LUC complementation assay	*KRN2*-nLUC	CACGGGGGACGAGCTCGGTACCATGGAAGGGTGCCAACTGC	GACGCGTACGAGATCTGGTCGACCTGGTGCGCCGGTAAG
	DUF1644-cLUC	CGTACGCGTCCCGGGGCGGTACCATGGCAAGATCACCAAAAGGT	GAACGAAAGCTCTGCAGGTCGACTCATCTCTCAGCTGCCTCGC
	OsDUF1644-nLUC	CACGGGGGACGAGCTCGGTACCATGGGTAGATCTCCAAGGGGC	GACGCGTACGAGATCTGGTCGACGATGCCATGTGTTGACC
	OsKRN2-cLUC	CGTACGCGTCCCGGGGCGGTACCATGGAGGGGTGCCAATTGG	GAACGAAAGCTCTGCAGGTCGACTCACTGATGCACTGGTAAAC
Vector construction for generating *KRN2*, *DUFF1644*, and *OsKRN2* null mutants via CRISPR-Cas9 technology	*KRN2*-Target1	GGCCCTGCATTGCCGTGGT	
	KRN2-Target2	GGGAGCCGGGCAGCACTCT	
	DUF1644-Target	TGAGCTCCTGTGAGACGAA	
	OsKRN2-Target	AGGTTCACTCGTACCGGAAG	
Genotyping of gene-editing plants	*KRN2*-CR	CGCCGTGATTTGTTTATGC	GAAGGACAACGAACTGAAACTC
	DUF1644-CR	TAAGTTTGGCTTTGCGTGTT	TTGCTGTAGGGTGCTTCG
	OsKRN2-CR	CAATGGCAAGCCTTCTGG	CCACCCAGTCCACAACAC

[a] The primers *KRN2*-QRT and *OsKRN2*-CR were also used for confirming the genotypes of *KRN2* and *OsKRN2* overexpression transgenic plants, respectively.

Table S11 (Separate file). Genetic linkage map of the MT-6/B73 RIL population.

Table S12 (Separate file). Summary of predicted off-target sites and their validation via genome-wide resequencing for all gene-editing plants used in this study. The excel file contains two sheets. The first lists the predicted off-target sites. The second summarizes the off-target test for all gene-editing plants used in this study via genome-wide resequencing.